Institute of Solid State Physics
University of Latvia

ANNUAL REPORT 2022

Riga 2023

Annual Report 2022, Institute of Solid State Physics, University of Latvia.
Editor: Dr.habil.phys. A.Šternbergs
Set up at the Institute of Solid State Physics, University of Latvia, Kengaraga Str. 8, LV-1063 Riga, Latvia.

Riga, Institute of Solid State Physics, University of Latvia, 2023, 75 pages

Director: **Dr. phys. A.Anspoks**
Institute of Solid State Physics, University of Latvia
Kengaraga Str. 8, LV-1063 Riga, Latvia
***Tel.:** +371 67187816*
***Fax:** +371 67132778*
ISSP@cfi.lu.lv
http://www.cfi.lu.lv

Contents

Introduction

The Institute of Solid State Physics (ISSP UL) of the University of Latvia is the main materials science institute in Latvia. It was founded in 1978 by an amalgamation of the two largest physics research laboratories in the University of Latvia: Laboratory of Semiconductor Research and Laboratory of Ferro- and Piezoelectric Research. Since 2013, the ISSP UL had the status of a legally and fiscally independent organization of the University.

In the 1990ies, after gaining independence and before joining the EU, the funding of science in Latvia decreased/went in a free plunge, as the former sources disappeared, and new funding channels were not yet established. Under these conditions, many research institutions collapsed, and only a few strongest survived, ISSP UL among them. Four laboratories from the Institute of Physics of the Latvian Academy of Sciences joined ISSP UL in 1995. Twenty scientists of the former Nuclear Research Centre found a shelter at the ISSP UL in 1999 and established the Laboratory of Radiation Physics. In 2004 scientists from the Institute of Physical Energetics joined ISSP UL and established the Laboratory of Organic Materials.

To encourage more students to select material physics and chemistry, in the mid-90ies ISSP UL stepped-up its teaching activities. Several researchers were elected as professors at the University of Latvia. Post-graduate and graduate curricula were prepared. Presently they are offered in solid-state physics, material physics, chemical physics, physics of condensed matter, semiconductor physics, and experimental methods and instruments.

In December 2000, the ISSP UL was awarded the **Centre of Excellence of the European Commission** (Centre of Excellence for Advanced Material Research and Technologies – **CAMART**). Together with the associated financial support of 0.7 M EUR for 3 years duration, this award boosted our research activities and allowed us to extend the network of our research partners and scientists, who came to work at ISSP UL from the leading European research centres. In 2001 the Association EURATOM-University of Latvia was established and the ISSP UL became the coordinator of the Latvian Research Unit. The Institute is involved in theoretical modelling as well as in the experimental characterization of fusion reactor construction and functional materials and has expertise in material erosion and re-deposition diagnostics in Plasma-Facing Components using Laser-Induced Breakdown Spectroscopy. In 2014 EUROfusion consortium agreement was signed, regulating European cooperation in thermonuclear synthesis research. The 34 countries

are working together to tackle the complex challenges facing a practical fusion power plant that produces electricity.

In 2015, ISSP UL was awarded Horizon 2020 Teaming project: "**The Excellence Centre of Advanced Material Research and Technology Transfer – CAMART^2**". 169 proposals were submitted; 31 were selected to develop their Business Plans. The project scored 14.5 from 15 points; it was the only project from Latvia and Baltic countries. It was submitted in cooperation with Swedish partners from the Royal Institute of Technology (KTH) and the Research Institute of Sweden (RISE). During 12 months of Phase 1, a Business Plan for the future Centre of Excellence CAMART^2 was elaborated, demonstrating the long-term science and innovation development strategy. Its vision is to upgrade and further consolidate the ISSP UL as a key centre of excellence for education, science, innovation, and technology transfer in the Baltic countries.

The Business Plan was highly estimated in the second phase of the Horizon 2020 Teaming project, dedicated to the development of the Centre of Excellence during 2017-2023 (Figure 1).

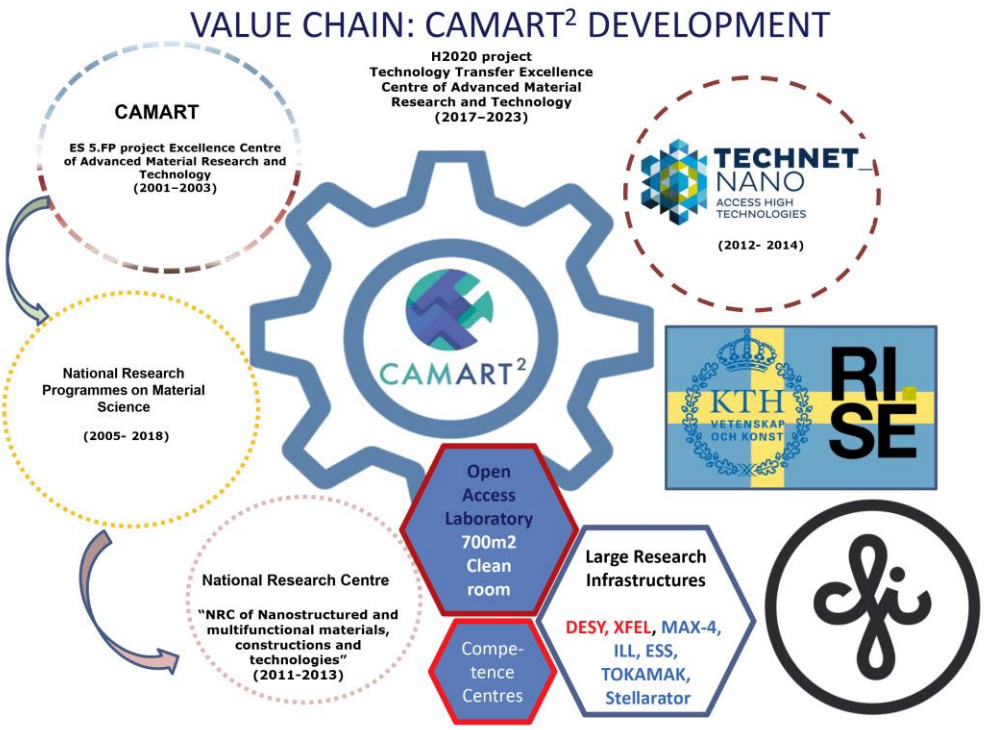

Figure 1: **Value chain: CAMART^2 development.**

ISSP UL has developed a strong research and innovation ecosystem.

680 m^2 of ISO class 7-8 **cleanroom facility** is established, including equipment for:

- basic technological methods: thin-film fabrication and parameter control, chemical synthesis, nano-structuring;
- analytical methods: XRD analysis, electron microscopy (SEM, TEM), X-ray photoelectron spectroscopy (XPS), morphology analysis, optical and EPR spectroscopy, spectral ellipsometry;
- prototyping of photonic and electronic devices. A new dedicated prototyping cleanroom laboratory was newly established.

In prototyping ISSP UL specializes in using methods of optical and e-beam lithography, cleaning and surface preparation, dry etching, bonding and packaging, thermal processes, and wet chemistry.

Presently, ISSP UL is further focusing on education. An overhaul of the University's master's programme in physics is in progress, to make it relevant to the projected industrial needs. Similar upgrades are also planned for the University's doctoral programme.

The ISSP UL's goal is to improve and enhance collaboration with industry in Latvia and abroad. To achieve this, it has set up a platform intended to serve as a single point of contact for scientists and companies. Named "Materize", the platform provides access to the ISSP UL's expertise and resources while also facilitating communication with companies to realise projects based on industry-specific standards. Current case studies being undertaken include a cleanroom-based prototyping facility, organic light-emitting diodes, optical lithography, vacuum deposition of thin films, and composite nanomaterials synthesis.

Every year "Materize" hosts events for idea creation, the Deep Science Hackathons. In 2022, Student Deep Science Hackathon took place November. The Hackathon's goal is to identify high-tech ideas and find teams for their implementation, to create new products and companies that would contribute to the Baltic region's high-tech industry.

The new Research Programme of ISSP UL for the period of 2021-2023-2027 includes the three research priorities of the Institute:

- Science: theory and experimental studies;
- Technology and experimental methods;

- Application: applied research of materials for sensors, scintillators, detectors, materials for photonics and electronics, and materials for energy harvesting and storage.

An important challenge for the Institute is to translate the new knowledge coming from the fundamental research into real innovation potential, which is addressed in Research Programme as new initiatives:

- Organ-on-a-chip and Lab-on-a-chip devices for biomarkers. The project addresses applications in personalized and precision medicine and is based on expertise in easy-to-use microfluidic device design and fabrication capabilities of ISSP UL for creating a novel and impactful biological study test-bed.
- Polymer photonics technology platform. This platform offers standardized polymer photonic device preparation methods to academics and the industry. This system is based on three main parts – computational simulations of photonic devices, photonic material's engineering and formation, photonic element fabrication workflow, and processing of the producible photonic elements.

The Research Programme serves as an "entry-point" for advanced materials-related R&D&I challenges, inquiries, and proposals. It will help launch projects with a scope wider than that of a specific single research domain.

The long-term mission of the ISSP UL Research Programme 2021-2023-2027 and strategic development plan is to raise Institute's scientific capacity and to integrate it better in the European Research Area by heightening the involvement in joint research programs and projects with the EU Member States, especially within the Baltic Sea region.

The mid-term milestone in Research Programme for ISSP UL is January 2025, the date to complete the Teaming project CAMART^2, when it comes to evaluating the planned achievements in quantified Key Performance Indicators (KPI) format, as well as when full sustainability of the Institute must be achieved and demonstrated.

In the year 2022, the domain concept continued to show positive results. 52 projects were implemented. They include 1 Horizon 2020, 5 COST projects, ,4 Investment and Development Agency of Latvia ("LIAA") support Projects 4 EraNet projects, 4 EUROfusion projects, 1 European Regional Development Fund (ERDF) projects, 18 Latvian Council of Science Projects, 10 Postdoctoral projects, 2 EEA and Norway Grants, 1 Latvia-Lithuania-Taiwan mutual project, 1

Latvian-Ukrainian Bilateral Cooperation Program, and 1 National Research Program.

The structure of ISSP UL at the end of 2022 is shown in Figure 2. It promotes research and innovation by creating a service-oriented environment, fostering openness and product-oriented research.

The highest decision-making body of ISSP UL is the **Scientific Council,** consisting of 13 members elected by the employees of the Institute. Presently, Dr.phys. D. Bocharov is the chairperson of the ISSP UL Scientific Council. The Council appoints the director and his/her deputies.

Figure 2: **The organizational structure of ISSP UL in 2022**

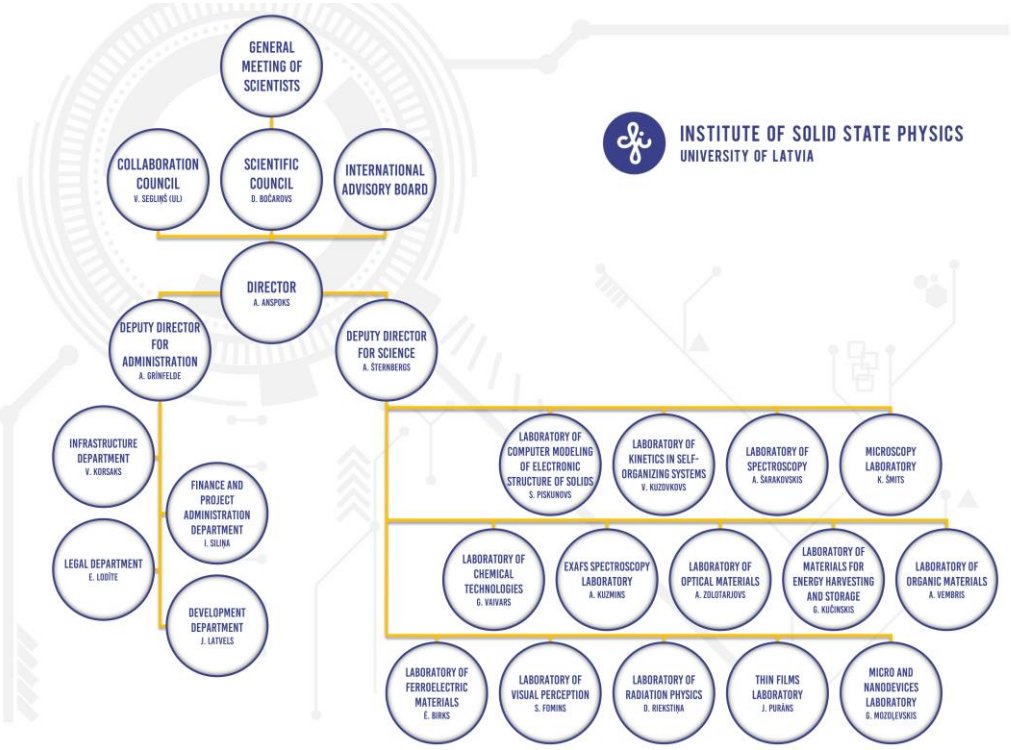

The Scientific Council of the Institute

1. Dmitry Bocharov, Dr.phys., Chair of the Scientific Council
2. Jeļena Butikova, Dr.phys., Vice-Chair of the Scientific Council
3. Andris Anspoks, Dr.phys., Director
4. Līga Grīnberga, Dr.phys.
5. Jurģis Grūbe, Dr.phys.

6. Sergejs Piskunovs, Dr.rer.nat.
7. Boris Polyakov, Dr.phys.
8. Kaspars Pudžs, Dr.phys.
9. Mārtiņš Rutkis, Dr.phys.
10. Anatolijs Šarakovskis, Dr.phys.
11. Andris Šternbergs, Dr.habil.phys.
12. Aivars Vembris, Dr.phys.
13. Virgīnija Vītola, Dr.phys.

To ensure an optimal alignment with global tendencies in material science, the ISSP UL performs consultations with the International Advisory Board (see Table 2) when making strategic decisions. Additionally, the International Advisory Board issues recommendations for the commercialization of scientific results and for improving management. The renewed Advisory board had 2 meetings in 2022 – in July and September.

The International Advisory Board

1. Prof. Juras Banys, Vilnius University, Lithuania
2. Prof. Antonio Bianconi, Rome International Center for Materials Science Superstripes, Italy
3. Prof. Annette Bussmann-Holder, Max-Planck-Institute for Solid State Research, Germany
4. Prof. Ming-Chi Chou, Department of Materials and Optoelectronic Science, National Sun Yat-sen University, Taiwan, R.O.C.
5. Prof. Lars Österlund – Division of Solids State Physics, Dept. Materials Science and Engineering, The Ångström Laboratory, Uppsala University, Sweden;
6. Prof. Marco Kirm, University of Tartu, Estonia
7. Prof. Maija Kuklja, Program director at National Science Foundation, USA
8. Dr. Jiri Kulda, Institut Laue-Langevin, France
9. Prof. Toshio Ogawa, Shizuoka Institute of Science and Technology, Japan
10. Prof. Pauls Stradins, Colorado School of Mines, USA
11. Prof. Andrejs Silins, Latvian Academy of Sciences, Latvia
12. Prof. Tony Donné – Programme Manager (CEO) for the consortium EUROfusion

13. Dr. Nils Nordell – Director, Electrum Laboratory, KTH, Sweden.

The multidisciplinary research (Figure 3) at the ISSP UL is performed by its highly qualified staff. At the end of 2022, 210 employees were working at the Institute. ISSP UL research staff dynamics is shown in Figure 4, indicating an impressive increase in the number of Ph.D. students involved in the implementation of projects during the last two years.

This Annual Report summarizes the research activities of the ISSP UL in 2022. The KPIs of ISSP UL are reported in Table 3 below.

In 2022, a total of 183 papers were published in peer-review journals (2 papers are still in press and will appear in 2023). 88 of them (48%) were published in journals with the SNIP factor >1 (as in 2021). 85% of publications are in journals belonging to the Q1 and Q2 quartiles (compared to 81% in 2021).

It is necessary to separately note the publication in the high-impact journal (IF=39.714) - *Energy and Environmental Science* (DOI: 10.1039/d1ee03982b). This comprehensive study was performed in collaboration with the teams from Riga Technical University and the University of Latvia with a prominent contribution from the ISSP team. It was devoted to a demonstration of amphoteric decoupled electrolysis by using an auxiliary electrode coupled with H_xWO_3 and NiOOH being employed in separate acid and alkaline cells, respectively. The average electrolysis efficiency of the proposed concept is up to 71%, higher than that observed from decoupled electrolysis where both cells are alkaline.

Several metrics as provided by the SCOPUS database were used to evaluate the research output of ISSP and its change during the last seven years (2016-2022). They were calculated using the SciVal research performance assessment tool, which allows analysis of the data from Scopus.

The first two metrics indicate how many ISSP publications are among the most-cited ones within the entire Scopus database or have been published in the most-cited journals indexed by Scopus. The percent of ISSP publications that are among the top 10% of most cited publications worldwide was 16% in 2022 (21% in 2021) (Figure 5). The percent of publications in the top 10% of the most-cited journals indexed by Scopus was maintained at 22% in 2022 (21% in 2021) (Figure 6).

The third metric, Field-Weighted Citation Impact (FWCI), measures how citations received by ISSP publications compare to the world average. An FWCI value of 1.00 indicates that the entity's publications were cited exactly as one would expect based on the global average of similar

publications. The FWCI of ISSP publications for the first time was above one (1.13) in 2021 compared to the world average and remains at 1.05 in 2022, indicating high publication quality (Figure 7).

The fourth metric shows the distribution of ISSP publications across journals, divided into four quartiles according to their Impact Factor. It is important to stress that about 85% (81% in 2021) of all publications in 2022 appeared in journals belonging to the first (Q1) and second (Q2) quartile (Figure 8).

Building the research capacity and development of human capital are among the priorities at ISSP. These are addressed in collaboration with the University of Latvia and other universities through the preparation of the next generation of researchers. The ISSP is a traditional place where many students start and accelerate their research careers to Bachelor's, Master and Ph.D. levels. In 2022, 3 Ph.D., 14 M.Sc., and 8 B.Sc theses were prepared and successfully defended.

The high quality of the research at ISSP UL was recognized by the Latvian Academy of Sciences (LAS). Two studies conducted by the ISSP teams were among the winners of the Science Achievements Competition 2022 in applied science. The first study on "Development of chromogenic materials for smart windows and zero energy buildings" was entirely implemented at ISSP, and the second study on "Development of innovative amphoteric decoupled electrolysis – a simple concept to split water and produce H_2 with high efficiency in a cheap and safe way" was conducted in a collaboration between the Institute of Materials and Surface Engineering of Rīga Technical University, Department of Physical Chemistry of the University of Latvia, and the Institute of Solid State Physics University of Latvia.

Figure 3: Multidisciplinary research at ISSP UL: Publications by Subject Area

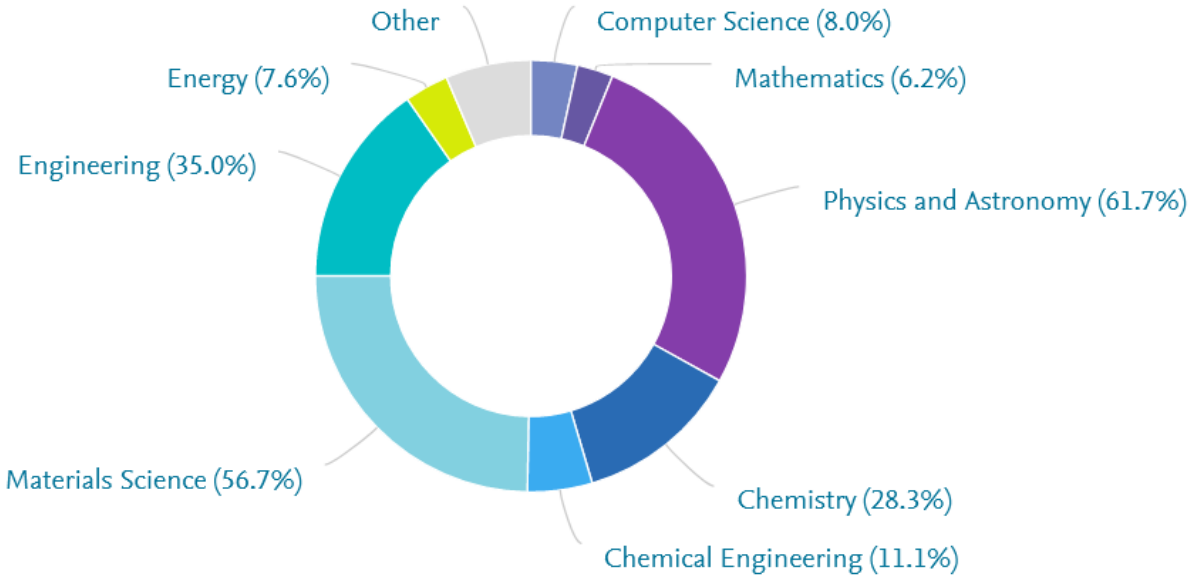

Figure 4: ISSP UL research staff dynamics 2009-2022

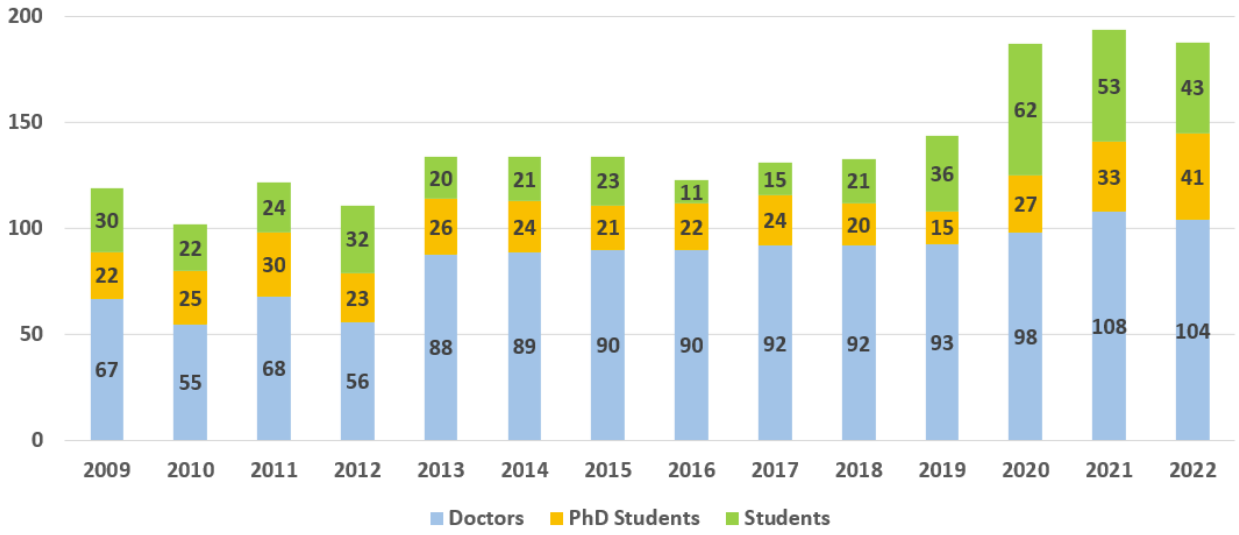

Figure 5: ***Share of the ISSP UL publications belonging to the top 10% of most cited publications worldwide (from Scopus database)***

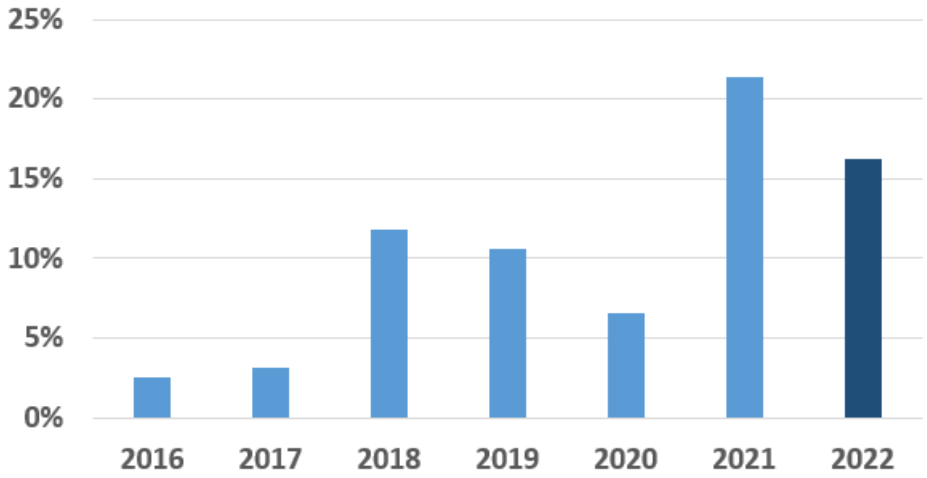

Figure 6: ***Share of the ISSP UL publications belonging to the top 10% of the most-cited journals indexed by Scopus (from Scopus database)***

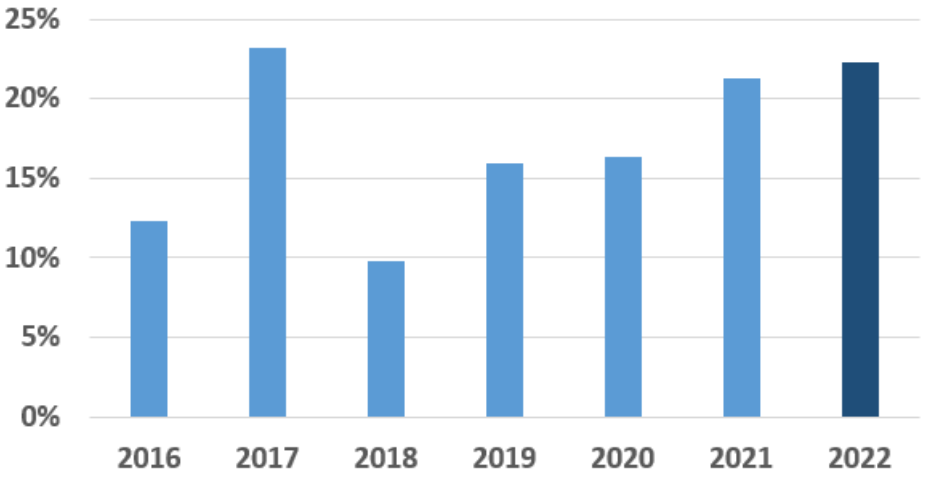

Figure 7: Field-Weighted Citation Impact (FWCI) of ISSP UL publications compared with the world average. A FWCI of 1.00 indicates that the ISSP UL publications have been cited exactly as would be expected based on the global average for similar publications (from Scopus database)

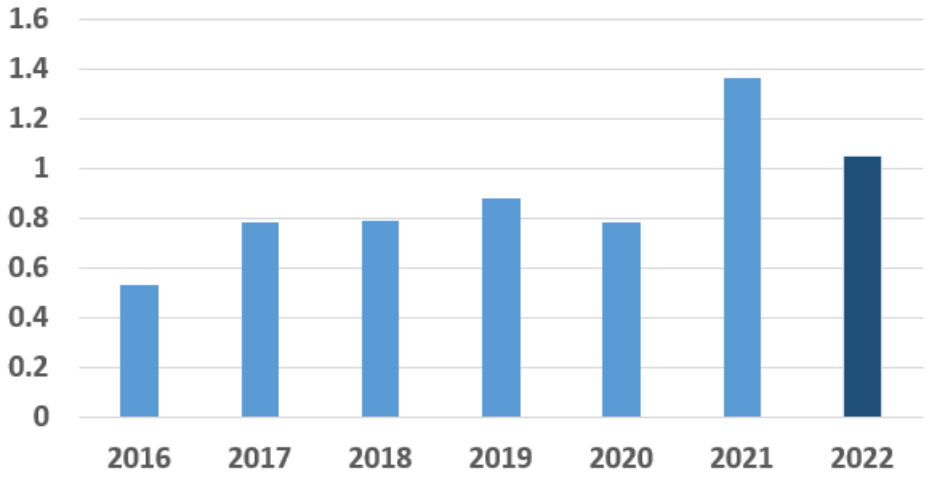

Figure 8: ISSP UL publications by Journal quartile (from Scopus database)

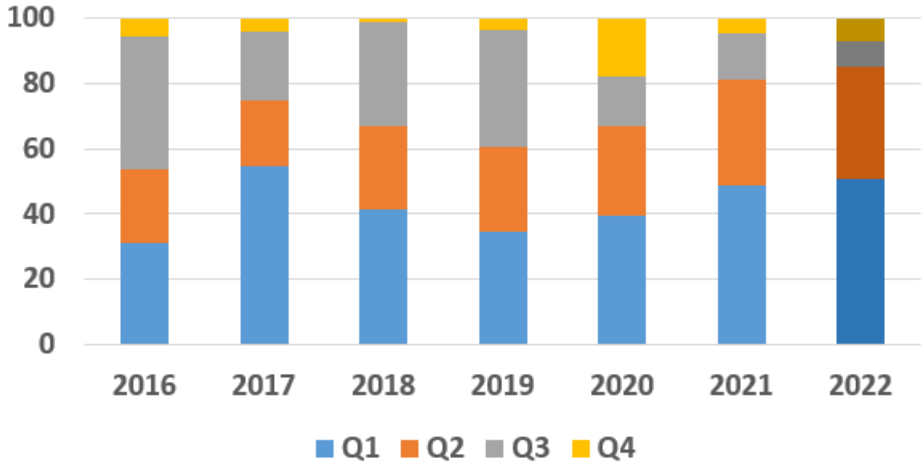

Scientific Highlights

I. Science: Theory and experimental studies

Al-driven peculiarities of local coordination and magnetic properties in single-phase Alx-CrFeCoNi high-entropy alloys

Alevtina Smekhova[a], Alexei Kuzmin[b], Konrad Siemensmeyer[a], Chen Luo[a], Kai Chen[a], Florin Radu[a], Eugen Weschke[a], Uwe Reinholz[c], Ana Guilherme Buzanich[c], Kirill V. Yusenko[c]

[a] *Helmholtz-Zentrum Berlin für Materialien und Energie (HZB), Berlin, D-12489, Germany*
[b] *Institute of Solid State Physics, University of Latvia, Riga, LV-1063, Latvia*
[c] *Bundesanstalt für Materialforschung und - prüfung (BAM), D-12489, Berlin, Germany*

Modern design of superior multi-functional alloys composed of several principal components requires in-depth studies of their local structure for developing desired macroscopic properties. Herein, peculiarities of atomic arrangements on the local scale and electronic states of constituent elements in the single-phase face-centered cubic (fcc)- and body-centered cubic (bcc)-structured high-entropy Alx-CrFeCoNi alloys (x = 0.3 and 3, respectively) are explored by element-specific X-ray absorption spectroscopy in hard and soft X-ray energy ranges. Simulations based on the reverse Monte Carlo approach allow to perform a simultaneous fit of extended X-ray absorption fine structure spectra recorded at K absorption edges of each 3d constituent and to reconstruct the local environment within the first coordination shells of absorbers with high precision. The revealed unimodal and bimodal distributions of all five elements are in agreement with structure-dependent magnetic properties of studied alloys probed by magnetometry. A degree of surface atoms oxidation uncovered by soft X-rays suggests different kinetics of oxide formation for each type of constituents and has to be taken into account. X-ray magnetic circular dichroism technique employed at $L_{2,3}$ absorption edges of transition metals demonstrates reduced magnetic moments of 3d metal constituents in the sub-surface region of in situ cleaned fcc-structured $Al_{0.3}$-CrFeCoNi compared to their bulk values. Extended to nanostructured versions of multicomponent alloys, such studies would bring new insights related to effects of high entropy mixing on low dimensions.

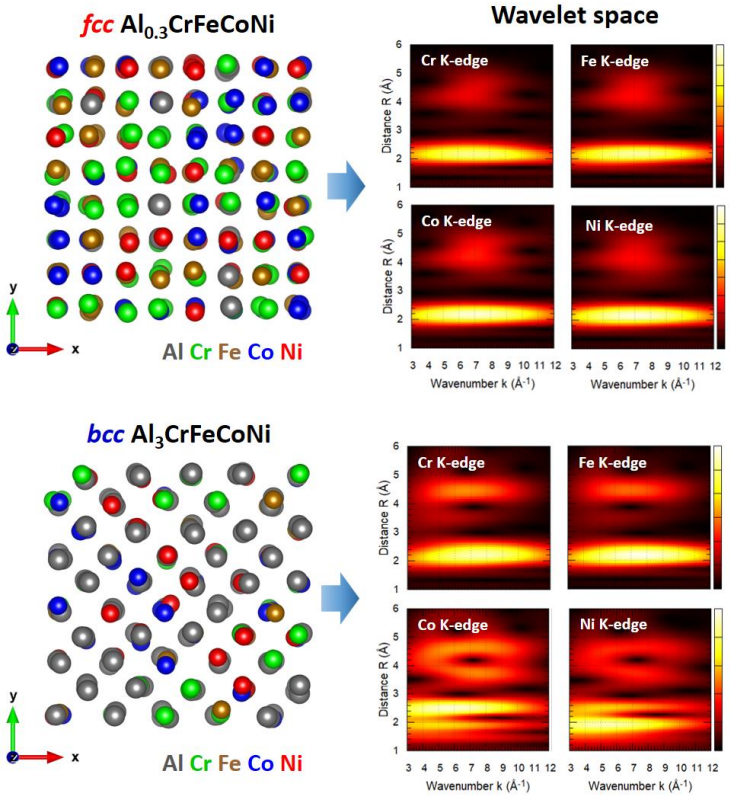

Published in:
A. Smekhova, A. Kuzmin, K. Siemensmeyer, C. Luo, K. Chen, F. Radu, E. Weschke, U. Reinholz, A. Guilherme Buzanich, K. V. Yusenko, Nano Res. 15 (2022) 4845-4858. DOI: 10.1007/s12274-021-3704-5.

Overall direct photocatalytic water-splitting on *C*2*mm*-graphyne: a novel two-dimensional carbon allotrope

Dong-Chun Yang[a,b], Roberts I. Eglitis[c], Zhi-Jun Yi[d], Chun-Sheng Liu[e], Ran Jia[ac]

[a] *Institute of Theoretical Chemistry, College of Chemistry, Jilin University, 130023 Changchun, PR China*
[b] *Institute of Chemistry Chinese Academy of Sciences, 100190 Beijing, PR China*
[c] *Institute of Solid State Physics, University of Latvia, 8 Kengaraga Str., Riga LV1067, Latvia*
[d] *School of Materials and Physics, China University of Mining and Technology, 221116 Xuzhou, PR China*
[e] *College of Electronic Science and Engineering, Nanjing University of Posts and Telecommunications, 210046 Nanjing, PR China*

A novel two-dimensional (2D) carbon allotrope, named *C*2*mm*-graphyne, is predicted with the aid of the first-principles calculations. Its lattice dynamic and thermodynamic stabilities have been confirmed by evaluating its phonon dispersion relation and the trajectory from the ab initio molecular dynamics (AIMD) simulation at 1000 K. The unique network consists of sp–sp^2 hybridized carbons. This 2D carbon allotrope possesses a direct quasi-particle (QP) band gap of 3.06 eV at the Γ point, which is close to the value of rutile. Significantly, some of its extended structures containing B and N dopants possess direct or quasi-direct QP band gaps in the range of 1.37–2.42 eV, which are falling into the visible light region. More exciting, their band arrangements just meet the requirements of photocatalytic water splitting. Furthermore, the HER and the OER are clearly discussed.

Published in:
D.-C. Yang, R.I. Eglitis, Z.-J. Yid, C.-S. Liu, R. Jia, J. Mater. Chem. C 10 (2022) 10843-10852.
DOI: 10.1039/D2TC02345H.

Novel 2D boron nitride with optimal direct band gap: A theoretical prediction

Feng-Yin Li [a], Dong-Chun Yang [a], Liang Qiao [b], Roberts I. Eglitis [c], Ran Jia [a,c], Zhi-Jun Yi [d], Hong-Xing Zhang [a]

[a] *Institute of Theoretical Chemistry, College of Chemistry, Jilin University, 130023 Changchun, PR China*
[b] *School of Science, Changchun University, 130022 Changchun, PR China*
[c] *Institute of Solid State Physics, University of Latvia, 8 Kengaraga Str., Riga LV1067, Latvia*
[d] *School of Materials Science and Physics, China University of Mining and Technology, 221116 Xuzhou, PR China*

A novel structurally stable 2D-boron nitride material, namely di-BN, is predicted using the first-principles simulations. This monolayer BN system is composed of the azo (N–N) and diboron (B–B) groups. Its in-plane stiffness is close to the monolayer h-BN. Usually, the boron nitride materials are semiconductors with large band gaps. However, the monolayer di-BN possesses a moderate direct band gap of 1.622 eV obtained from our HSE06 calculation. Although the GW correction enlarges the band gap to 2.446 eV, this value is still in the range of visible light. The detailed investigation of its band arrangement reveals that this material is able to produce hydrogen molecules in a photocatalytic water-splitting reaction. Furthermore, its charge carrier mobilities are significantly higher than the other popular 2D semiconductors, e.g., MoS_2 and phosphorene. Therefore, this 2D-BN material could have huge application potential in the electronics and solar energy conversion fields.

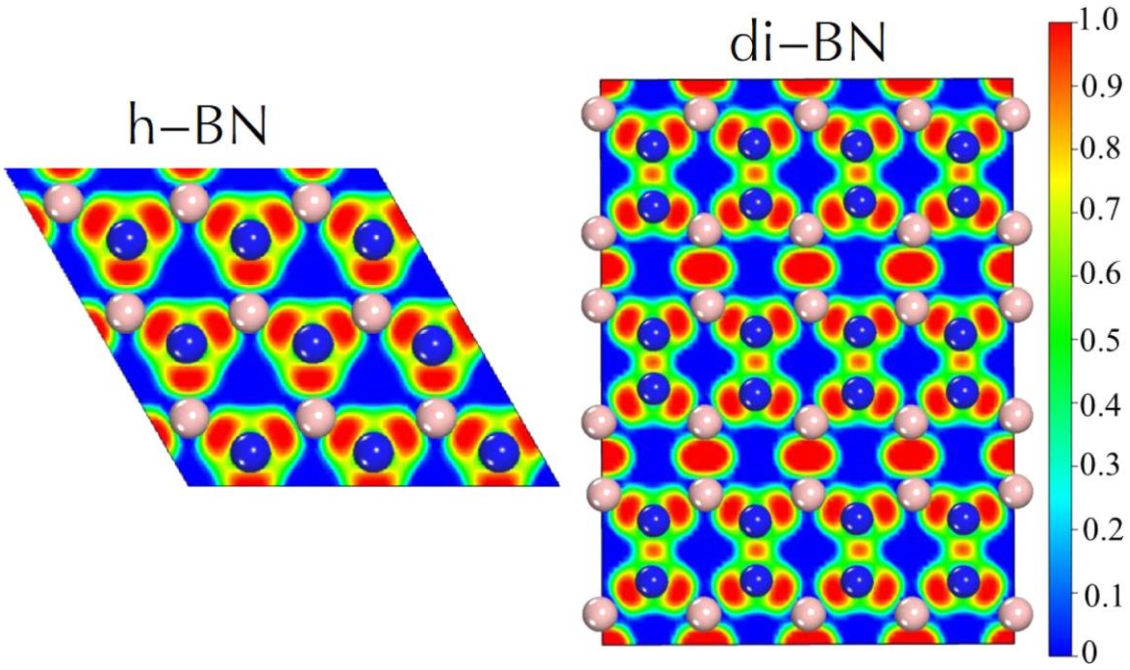

The Electron Localization Function (ELF) maps for the monolayer di-BN and h-BN.

Published in:
F.-Y. Li, D.-C. Yang, L. Qiao, R. I. Eglitis, R. Jia, Z.-J. Yi, H.-X. Zhang, Applied Surface Science 578 (2022) 151929. DOI: 10.1016/j.apsusc.2021.151929.

The adsorption behavior of phenol on the surface of 1D/2D M@MoS_2 (M = Co and Rh) for hydrodeoxidation reaction: Insights from theoretical investigations

Pingxia Wang[a], Xiangyan Geng[a], Lilong Luo[a], Yingtao Liu[a], Roberts I. Eglitis[b], Xin Wang[a]

[a] *State Key Laboratory of High-efficiency Utilization of Coal and Green Chemical Engineering, National Demonstration Center for Experimental Chemistry Education, College of Chemistry and Chemical Engineering, Ningxia University, Yinchuan 750021, China*

[b] *Institute of Solid State Physics, University of Latvia, 8 Kengaraga Str., Riga LV1067, Latvia*

As MoS_2 is a useful catalyst for phenol hydrodeoxidation, it is important to develop MoS_2-based catalysts. However, identifying active sites remains challenging. In the present study, two monatomic catalysts, namely, V_s-Co@MoS_2 and Rh@MoS_2, were prepared, and on which the adsorption sites of phenol were investigated via density functional theory (DFT). By systemically comparing the adsorption configuration, adsorption energy, and adsorption distance, we found that the most stable configuration of phenol on 2D V_s-Co@MoS_2 monatomic catalyst was from η6 adsorption mode (horizontal adsorption; adsorption energy, -1.51 eV; adsorption distance, 1.7 Å), and the adsorption site was the Co-V_s interface that formed by an isolated Co atom and its adjacent S vacancy (V_s) site. The density of state (DOS) analysis indicated the adsorption active sites originated from defect states and orbital hybridization distribution near the Fermi level. As for 1D Rh@MoS_2, the adsorption site was coming from the isolated Rh_1 atom, whose selectivity towards phenol was strengthened by the steric confinement effect of the unique pocket-like structure (Ho-Mo-Rh_1-Mo-OH). It was hoped that this study would provide important ideas for exploring the hydrodeoxygenation mechanism of phenol compounds.

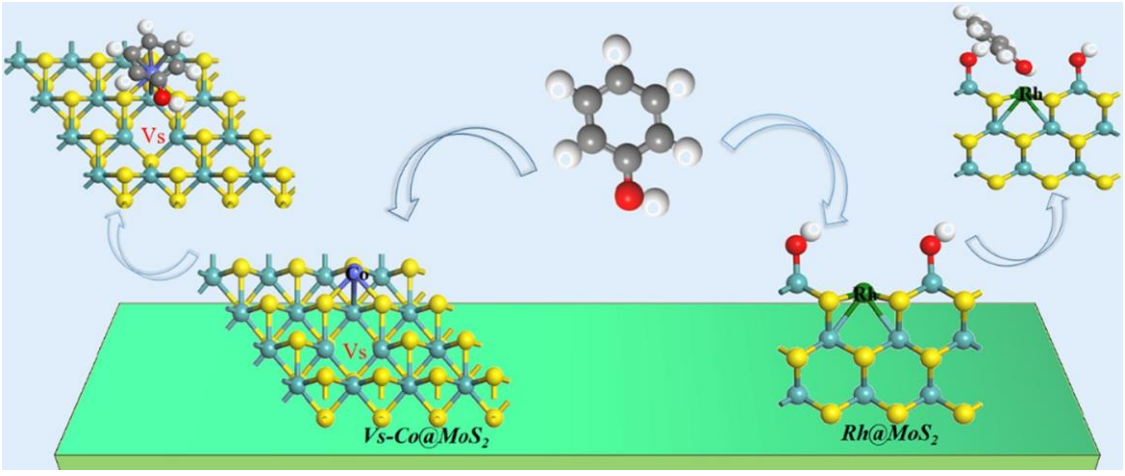

The isolated Co atom and its adjacent V_S site are both active sites for 2D Co@MoS_2, and the Co-V_s interface will lead to the most stable adsorption mode for phenol. For 1D Rh@MoS_2, the adsorption active site for phenol is the Rh_1 atom located at the interior of the HO-Mo-Rh_1-Mo-OH pocket-like Mo edge.

Published in:
P. Wang, X. Geng, L. Luo, Y. Liu, R. I. Eglitis, X. Wang, Applied Surface Science 601 (2022) 154242.
DOI: 10.1016/j.apsusc.2022.154242.

Electrochemical performance of NASICON-structured $Na_{3-x}V_{2-x}Ti_x(PO_4)_3$ ($0.0 < x < 1.0$) as aqueous Na-ion battery positive electrodes

Milda Petrulevičienė[a], Jurgis Pilipavičius[a,b], Jurga Juodkazytė[a], Denis Gryaznov[a,c], Linas Vilčiauskas[a]

[a] *Center for Physical Sciences and Technology (FTMC), Saulėtekio al. 3, LT-10257, Vilnius, Lithuania*
[b] *Institute of Chemistry, Vilnius University, Naugarduko 24, LT-03225, Vilnius, Lithuania*
[c] *Institute of Solid State Physics, University of Latvia, Kengaraga 8, LV-1063 Riga, Latvia*

Phosphate frameworks with NASICON structure are among the most studied and applied Li- and Na-ion battery electrode and electrolyte materials. In this work, the NASICON-structured $Na_{3-x}V_{2-x}Ti_x(PO_4)_3$ with x = 0.0, 0.25, 0.5, 0.75, and 1.0 are successfully prepared by conventional solid-state synthesis and characterized in detail as potential aqueous Na-ion battery positive electrodes with improved charge capacity and cycling stability. Structural analysis using powder X-ray diffractometry indicates that titanium substitutes vanadium at arbitrary concentrations without significant distortion of the NASICON structure. The results show that titanium content in this system directly correlates with its aqueous stability when cycled in a simple 1 M Na_2SO_4 aqueous electrolyte within the vanadium redox potential range. Electrochemical kinetics and charge capacity measurements show $Na_2VTi(PO_4)_3$ as well as $Na_{2.25}V_{1.25}Ti_{0.75}(PO_4)_3$ to be stable positive electrodes in simple aqueous electrolyte solutions. Hybrid density functional theory analysis of V-O chemical bonding suggests that it is stabilized by the presence of titanium in the NASICON structure. In this work, we show that the observed capacity loss in fully symmetric cells is caused by the capacity imbalance between positive and negative electrodes which progresses during cycling but not the stability of the aqueous material per se. This imbalance is caused by several parasitic reactions, the most important being the oxygen reduction reaction catalyzed by Ti(III) species. Careful mitigation and management of this reaction could, in principle, allow for the preparation of truly capacity-balanced cells (i.e. without a need for any electrode overcapacity), and superior cycling stability.

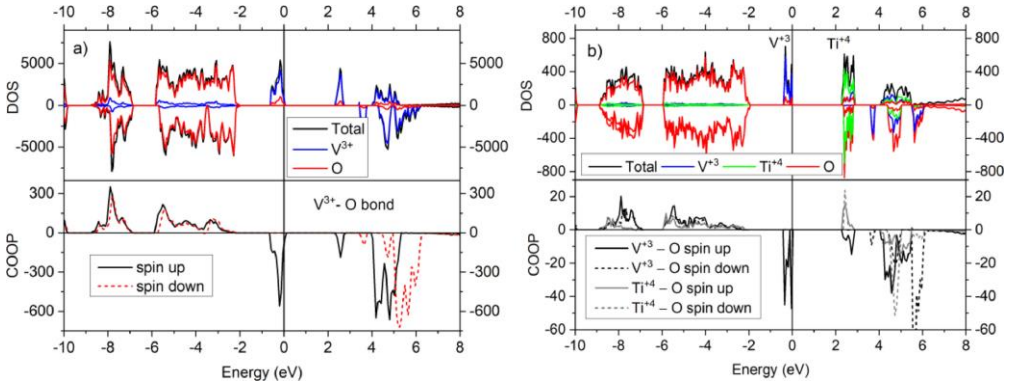

The density of states (DOS) and crystal orbital overlap population (COOP) for the V-O bond in (a) α-$Na_3V_2(PO_4)_3$ and (b) $Na_2VTi(PO_4)_3$. Values of DOS and COOP are given in arbitrary units. Negative DOS values correspond to spin-down electrons. Fermi energy is taken as zero.

Published in:
M. Petrulevičienė, J. Pilipavičius, J. Juodkazytė, D. Gryaznov, L. Vilčiauskas, Electrochimica Acta 424 (2022) 140580. DOI: 10.1016/j.electacta.2022.140580.

Inner relaxations in equiatomic single-phase high-entropy Cantor alloy

Alevtina Smekhova[a], Alexei Kuzmin[b], Konrad Siemensmeyer[a], Radu Abrudan[a], Uwe Reinholz[c], Ana Guilherme Buzanich[c], Mike Schneider[d], Guillaume Laplanche[d], Kirill V. Yusenko[c]

[a] *Helmholtz-Zentrum Berlin für Materialien und Energie (HZB), Berlin, D-12489, Germany*
[b] *Institute of Solid State Physics, University of Latvia, Riga, LV-1063, Latvia*
[c] *Bundesanstalt für Materialforschung und - prüfung (BAM), D-12489, Berlin, Germany*
[d] *Institut für Werkstoffe, Ruhr-Universität Bochum, D-44801 Bochum, Germany*

The superior properties of high-entropy multi-functional materials are strongly connected with their atomic heterogeneity through many different local atomic interactions. The detailed element-specific studies on a local scale can provide insight into the primary arrangements of atoms in multicomponent systems and benefit to unravel the role of individual components in certain macroscopic properties of complex compounds. Herein, multi-edge X-ray absorption spectroscopy combined with reverse Monte Carlo simulations was used to explore a homogeneity of the local crystallographic ordering and specific structure relaxations of each constituent in the equiatomic single-phase face-centered cubic CrMnFeCoNi high-entropy alloy at room temperature.

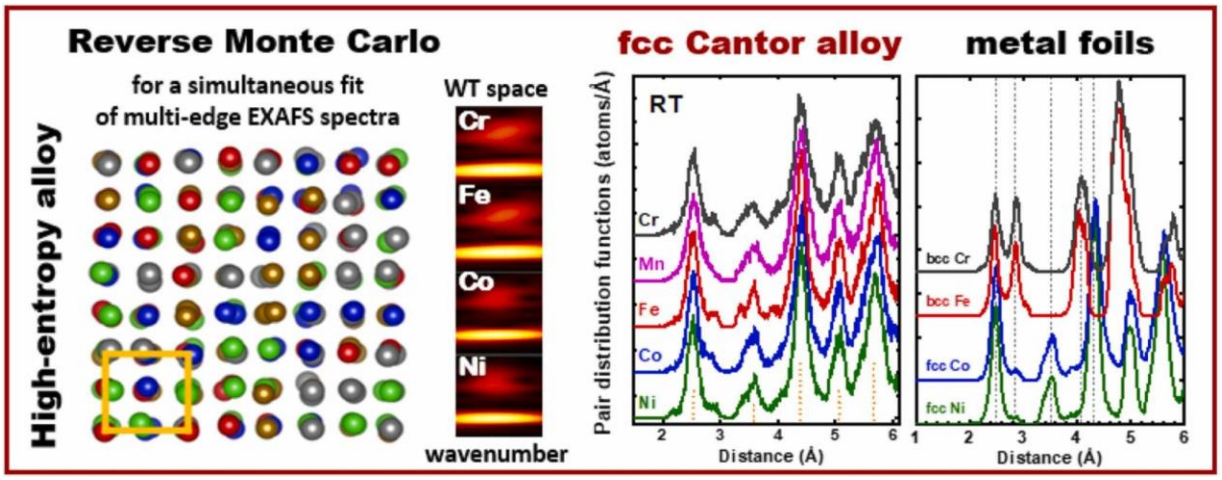

Within the considered fitting approach, all five elements of the alloy were found to be distributed at the nodes of the fcc lattice without any signatures of the additional phases at the atomic scale and exhibit very close statistically averaged interatomic distances (2.54–2.55 Å) with their nearest-neighbors. Enlarged structural displacements were found solely for Cr atoms. The macroscopic magnetic properties probed by conventional magnetometry demonstrate no opening of the hysteresis loops at 5 K and illustrate a complex character of the long-range magnetic order after field-assisted cooling in ±5 T. The observed magnetic behavior is assigned to effects related to structural relaxations of Cr. Besides, the advantages and limitations of the reverse Monte Carlo approach to studies of multicomponent systems like high-entropy alloys are highlighted.

Published in:
A. Smekhova, A. Kuzmin, K. Siemensmeyer, R. Abrudan, U. Reinholz, A. G. Buzanich, M. Schneider, G. Laplanche, K. V. Yusenko, J. Alloys Compd. 920 (2022) 165999. DOI: 10.1016/j.jallcom.2022.165999.

Influence of stress on electronic and optical properties of rocksalt and wurtzite MgO–ZnO nanocomposites with varying concentrations of magnesium and zinc

Yin-Pai Lin[a], Sergei Piskunov[a], Laima Trinkler[a], Mitch Ming-Chi Chou[b], Liuwen Chang[b]

[a] *Institute of Solid State Physics, University of Latvia, 8 Kengaraga Str., Riga LV-1063, Latvia*
[b] *Center of Crystal Research, Department of Materials and Optoelectronic Science, National Sun Yat-Sen University, 70 Lienhai Rd., Kaohsiung 80424, Taiwan*

The structural, electronic, and optical properties of stressed MgO–ZnO nanocomposite alloys with concentrations of Zn and Mg varying from 0.125 to 0.875 were studied using ab initio simulations. Two crystal structures are considered for the initial MgO–ZnO alloys: the rocksalt $Mg_{1-x}Zn_xO$ and wurtzite $Zn_{1-x}Mg_xO$ phases. For rocksalt $Mg_{1-x}Zn_xO$, the optimized structures are stable at pressures below 10 GPa. The larger the Mg concentration and pressure, the wider the Eg of the rocksalt phase. In contrast, the optimal geometries of wurtzite $Zn_{1-x}Mg_xO$ reveal a diversity of possibilities, including rocksalt, wurtzite, and mixed phases. These effects lead to the fact that the optical properties of wurtzite $Zn_{1-x}Mg_xO$ not only demonstrate the properties of the wurtzite phase but also indicate the optical features of the rocksalt phase. In addition, mixed phases of $Zn_{1-x}Mg_xO$ simultaneously provide the characteristics of both wurtzite and rocksalt phases with the same structures in different dielectric matrices.

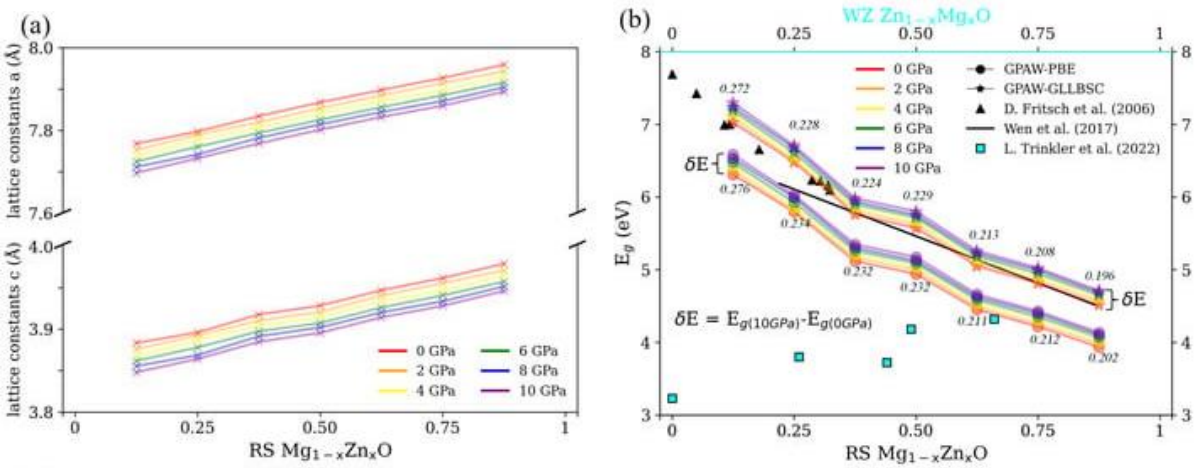

(a) The lattice constants and (b) band gap (Eg) of rocksalt (RS) $Mg_{1-x}Zn_xO$ for x = 0.125, 0.25, 0.375, 0.5, 0.625, 0.75, and 0.875 as well as the pressures ranging from 0 to 10 GPa. In Subfigure (b), the black triangles and cyan squares are the experimental *Eg* of the RS ZMO alloys and WZ ZMO epilayers, respectively. The black line is the fitted result of *Eg* ranging from x = 0.22 to 0.87 according to RS $Mg_{1-x}Zn_xO$ = 4.17 + 2.58(1 − x) eV. The circle and star symbols are the theoretical *Eg* of the PBE and GLLBSC functionals, respectively. The colors red, orange, yellow, green, blue, and purple correspond to 0, 2, 4, 6, 8, and 10 GPa. The difference in the theoretical *Eg* (δ*E*) between 10 and 0 GPa is marked. The top label of cyan color corresponds to the expression of wurtzite (WZ) $Zn_{1-x}Mg_xO$ for the experimental concentration in Subfigure (b).

Published in:
Y.-P. Lin, S. Piskunov, L. Trinkler, M. M.-C. Chou, L. Chang, Nanomaterials 12 (2022) 3408.
DOI: 10.3390/nano12193408.

Revealing the local structure of $CuMo_{1-x}W_xO_4$ solid solutions by multi-edge X-ray absorption spectroscopy

Inga Pudza[a], Andris Anspoks[a], Giuliana Aquilanti[b], Alexei Kuzmin[a,c]

[a] *Institute of Solid State Physics, University of Latvia, Riga, LV-1063, Latvia*
[b] *Elettra – Sincrotrone Trieste S.C.p.A., Ss 14, Km 163.5, Basovizza I-34149, Trieste, Italy*
c International Research Organization for Advanced Science and Technology (IROAST), Kumamoto University, 2-39-1 Kurokami, Chuo-ku, Kumamoto 860-8555, Japan

The effect of tungsten substitution with molybdenum on the structure of $CuMo_{1-x}W_xO_4$ (x = 0.20, 0.30, 0.50, 0.75) solid solutions was studied by multi-edge X-ray absorption spectroscopy. The simultaneous analysis of EXAFS spectra measured at several (Cu K-edge, Mo K-edge and W L_3-edge) absorption edges was performed by the reverse Monte Carlo method taking into account multiple-scattering effects. The degree of distortion of the coordination shells and its dependence on the composition were estimated from partial radial distribution functions (RDFs) and bond angle distribution functions (BADFs). The analysis of partial RDFs suggests that the structure of solid solutions is mainly determined by the tungsten-related sublattice, while molybdenum atoms adapt to a locally distorted environment. As a result, the coordination of both tungsten and molybdenum atoms remains octahedral as in $CuWO_4$ for all the studied compositions. For both Mo and W atoms, the distorted octahedra consist of three short and three long metal–oxygen bonds, and the group of the nearest three oxygen atoms has narrow distribution

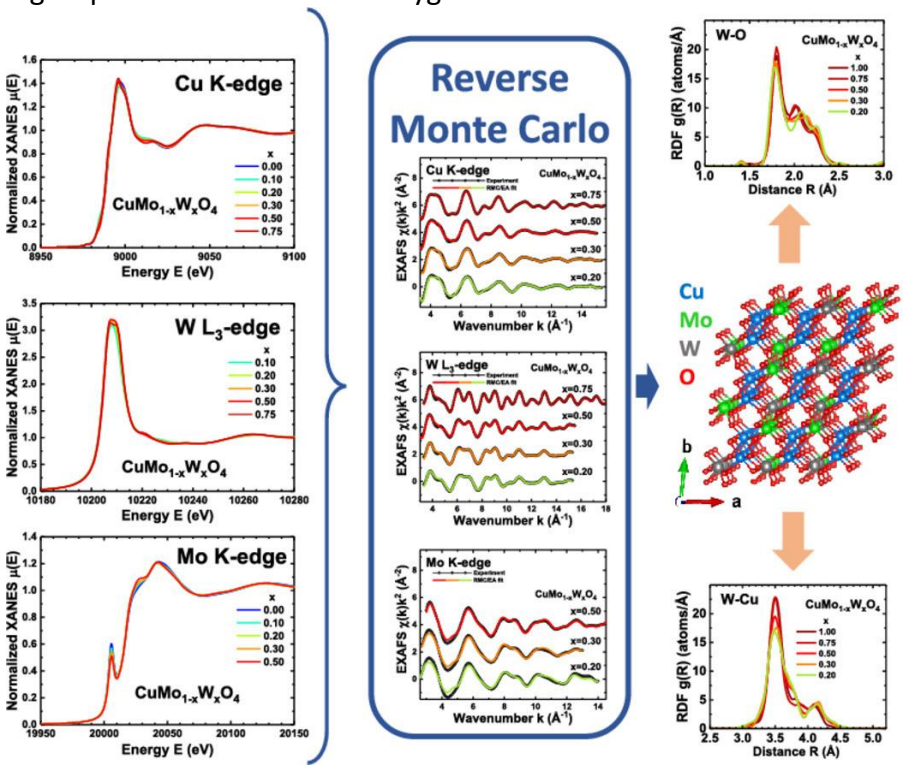

Published in:
I. Pudza, A. Anspoks, G. Aquilanti, A. Kuzmin, Mater. Res. Bull. 153 (2022) 111910.
DOI: 10.1016/j.materresbull.2022.111910.

II. Technology and experimental methods

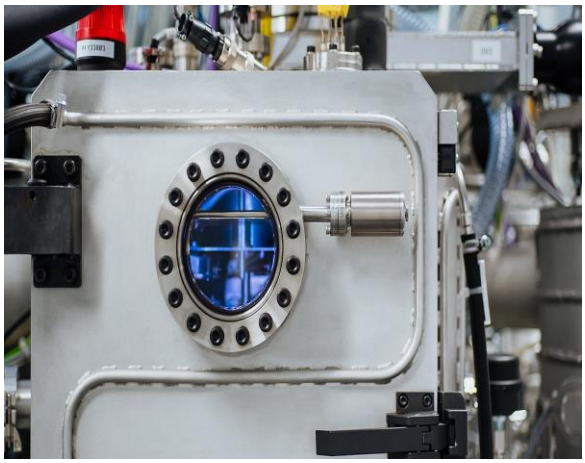

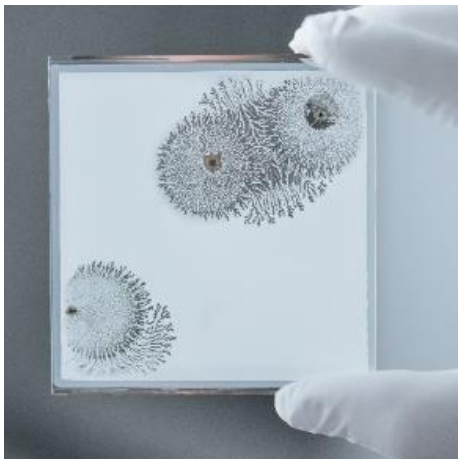

Membrane-less amphoteric decoupled water electrolysis using WO_3 and $Ni(OH)_2$ auxiliary electrodes

Martins Vanags[a], Guntis Kulikovskis[a], Juris Kostjukovs[b], Laimonis Jekabsons[c], Anatolijs Sarakovskis[c], K. Smits[c], Liga Bikse[c], Andris Šutka[a]

[a] *Institute of Materials and Surface Engineering, Faculty of Materials Science and Applied Chemistry, Riga Technical University, P. Valdena Street 3, Riga LV-1048, Latvia*
[b] *Department of Physical Chemistry, University of Latvia, LV1004 Jelgavas Street 1, Riga, Latvia*
[c] *Institute of Solid State Physics, University of Latvia, Kengaraga Street 8, Riga LV-1063, Latvia*

Energy storage and delivery play a crucial role in the effective management of renewable power sources such as solar and wind. Hydrogen energy is proposed to be one of the major substitutes to fill the gap between the production plant and the consumer. The energy from renewable power sources is used to generate hydrogen, which is later converted to electricity and water. Hydrogen generation in water electrolysis from renewable energy is a sustainable process. However, the need for membrane separation of hydrogen from oxygen in single-cell water electrolysis is detrimental. Moreover, the hydrogen production rate in conventional single-cell electrolysers is strictly limited by the rate of oxygen evolution. Recently decoupled water electrolysis has been proposed where hydrogen and oxygen are generated in spatially separated alkaline cells. Here we demonstrate amphoteric decoupled electrolysis by using an auxiliary electrode (AE) coupled with H_xWO_3 and NiOOH being employed in separate acid and alkaline cells, respectively. The average electrolysis efficiency of the proposed concept is up to 71%, higher than that observed from decoupled electrolysis where both cells are alkaline.

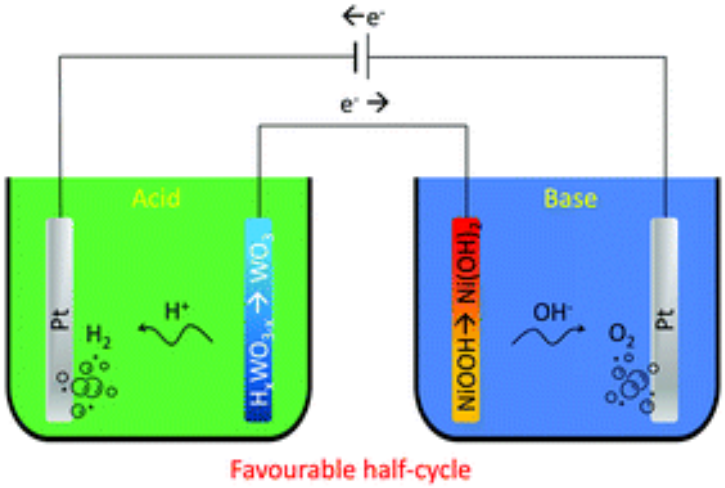

Published in:
M. Vanags, G. Kulikovskis, J. Kostjukovs, L. Jekabsons, A. Sarakovskis, K. Smits, L. Bikse, A. Šutka, Energy Environ. Sci. 15 (2022) 2021-2028. DOI: 10.1039/d1ee03982b.

Different strategies for GaN-MoS_2 and GaN-WS_2 core–shell nanowire growth

Edgars Butanovs[a,b], Kevon Kadiwala[a], Aleksejs Gopejenko[a], Dmitry Bocharov[a], Sergei Piskunov [a], Boris Polyakov[a]

[a] *Institute of Solid State Physics, University of Latvia, Riga, LV-1063, Latvia*
[b] *Institute of Technology, University of Tartu, Nooruse 1, 50411 Tartu, Estonia*

One-dimensional (1D) nanostructures – nanowires (NWs) – exhibit attractive properties for integration in different types of functional devices. Their properties can be enhanced even further or tuned for a specific application by combining different promising materials, such as layered van der Waals materials and conventional semiconductors, into 1D-1D core–shell heterostructures. In this work, we demonstrated the growth of GaN-MoS_2 and GaN-WS_2 core–shell NWs via two different methods: (1) a two-step process of sputter-deposition of a sacrificial transition metal oxide coating on GaN NWs followed by sulfurization; (2) pulsed laser deposition of few-layer MoS_2 or WS_2 on GaN NWs from the respective material targets. As-prepared nanostructures were characterized via scanning and transmission electron microscopies, X-ray diffraction, micro-Raman spectroscopy, and X-ray photoelectron spectroscopy. High crystalline quality core–shell NW heterostructures with few-layer MoS_2 and WS_2 shells can be prepared via both routes. The experimental results were supported by theoretical electronic structure calculations, which demonstrated the potential of the synthesised core–shell NW heterostructures as photocatalysts for efficient hydrogen production from water.

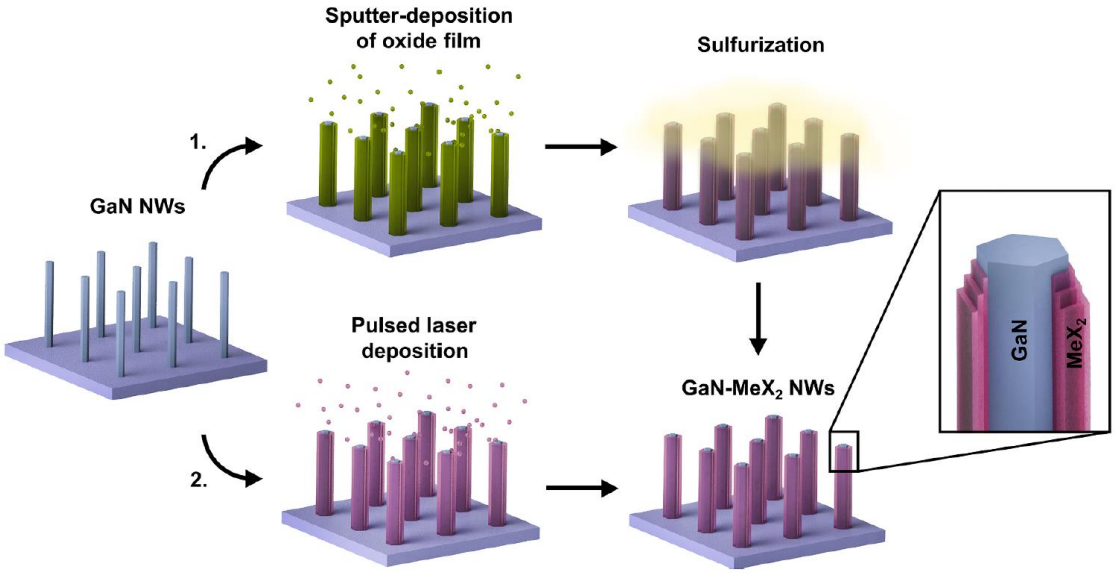

A schematic of both demonstrated GaN-MeX_2 core–shell NW preparation methods on Si/SiO_2 substrates: (1) two-step method, which includes sulfurization of pre-deposited metal oxide coating; and (2) direct deposition of MoS_2 or WS_2 with pulsed laser deposition.

Published in:
E. Butanovs, A. Kuzmin, A. Zolotarjovs, S. Vlassov, B. Polyakov, Applied Surface Science 590 (2022) 153106.
DOI: 10.1016/j.apsusc.2022.153106.

Sol-gel assisted molten-salt synthesis of novel single phase $Y_{3-2x}Ca_{2x}Ta_xAl_{5-x}O_{12}$:1%Eu garnet structure phosphors

Monika Skruodiene[a], Ruta Juodvalkyte[b], Greta Inkrataite[b], Andrius Pakalniskis[b], Rimantas Ramanauskas[c], Anatolijs Sarakovskis[a], Ramunas Skaudzius[b]

[a] *Institute of Solid State Physics, University of Latvia, 8 Kengaraga str., LV-1063 Riga, Latvia*
[b] *Institute of Chemistry, Faculty of Chemistry and Geosciences, Vilnius University, Naugarduko 24, LT-03225 Vilnius, Lithuania*
[c] *State Research Institute Center for Physical Sciences and Technology, Sauletekio av. 3, LT-10257 Vilnius, Lithuania*

Strong absorption and emission are the key features of any phosphor. The results obtained during this study demonstrate the difficulty of the incorporation of tantalum ions into the garnet structure and reveal that only the combination of the Sol-Gel synthesis method together with the Molten-Salt technique enables to obtain of the single-phase cubic garnet structure. Note that, the Sol-Gel synthesis assisted by further processing by the Molten-Salt technique can be a potentially new way of material preparation reported in the literature. This work also proves that this combination of synthesis methods is much more capable of incorporating ions with large ionic radii into the garnet structure as compared to the traditional Sol-Gel method. Moreover, samples synthesized using this new technique exhibit 30% higher emission intensities as compared to the ones prepared by the original Sol-Gel method, while also reducing the needed sintering temperature by 200 °C. To the best of our knowledge, the modification of yttrium aluminum garnet ($Y_3Al_5O_{12}$, YAG) by co-doping it with Ca^{2+} and Ta^{5+} ions by Sol-Gel-assisted Molten-Salt route has been investigated for the first time.

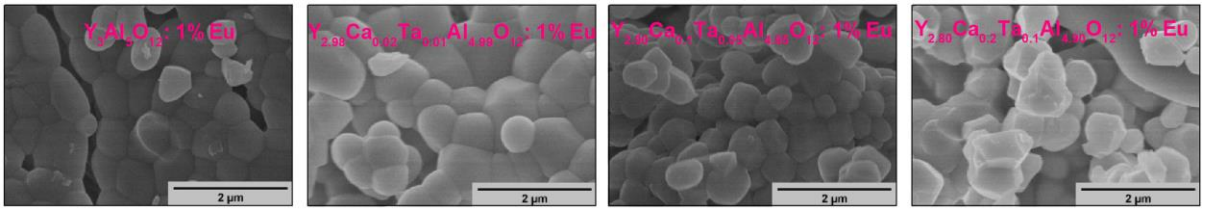

SEM images of different powder samples, synthesized via the Sol-Gel route, annealed at 1500 °C in air.

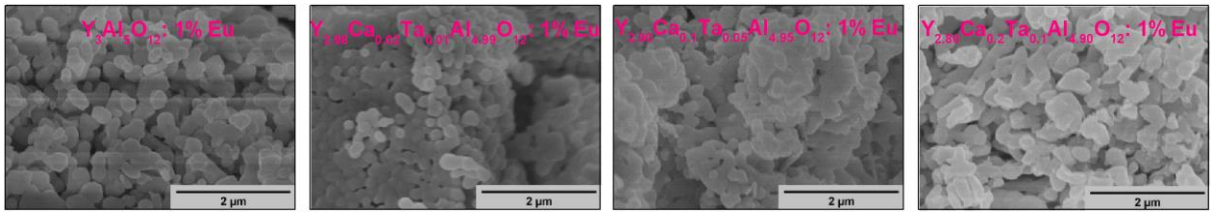

SEM images of different powder samples, synthesized *via* the Molten-Salt route, annealed at 1300 °C in KCl, in air.

Published in:
M. Skruodiene, R. Juodvalkyte, G. Inkrataite, A. Pakalniskis, R. Ramanauskas, A. Sarakovskis, R. Skaudzius, J. Alloys Compd. 890 (2022) 161889. DOI: 10.1016/j.jallcom.2021.161889.

Characterization of wurtzite $Zn_{1-x}Mg_xO$ epilayers grown on $ScAlMgO_4$ substrate by methods of optical spectroscopy

Laima Trinkler[a], Ilze Aulika[a], Guna Krieke[a], Dace Nilova[a], Rihards Ruska[a], Jelena Butikova[a], Baiba Berzina[a], Mitch Ming-Chi Chou[b,c], Liuwen Chang[b,c], Meng-Chieh Wen[b,c], Tao Yan[d], Ramunas Nedzinskas[e]

[a] *Institute of Solid State Physics, University of Latvia, Kengaraga St.8, Riga LV-1063, Latvia*
[b] *Department of Materials and Optoelectronic Science, National Sun Yat-sen University, Kaohsiung 80424, Taiwan*
[c] *Center of Crystal Research, National Sun Yat-sen University, Kaohsiung 80424, Taiwan*
[d] *Key Laboratory of Optoelectronic Materials Chemistry and Physics, Fujian Institute of Research on the Structure of Matter, Chinese Academy of Sciences, Fuzhou, People's Republic of China*
[e] *Center for Physical Sciences and Technology, Vilnius, Saulėtekio ave. 3, Vilnius 10257, Lithuania*

Wurtzite $Zn_{1-x}Mg_xO$ epilayers (x = 0, 0.26, 0.44, 0.49, 0.66) grown by the plasma-assisted molecular beam epitaxy on $ScAlMgO_4$ substrate were characterized using the methods of optical spectroscopy: spectroscopic ellipsometry (SE), optical absorption (OA), and photoluminescence (PL). The complex dielectric function in the spectral range of 210–1690 nm, band gap width, exciton absorption, and emission parameters, and film quality were studied and discussed. Individual characterization of samples was provided by combining SE and OA measurement results. The observed increase of the band gap up to 4.35 eV with the rise of the MgO content allowed the recommendation of the wurtzite $Zn_{1-x}MgxO$ epilayers as material for UV sensors. The origin of defects hampering the practical application of the materials was discussed.

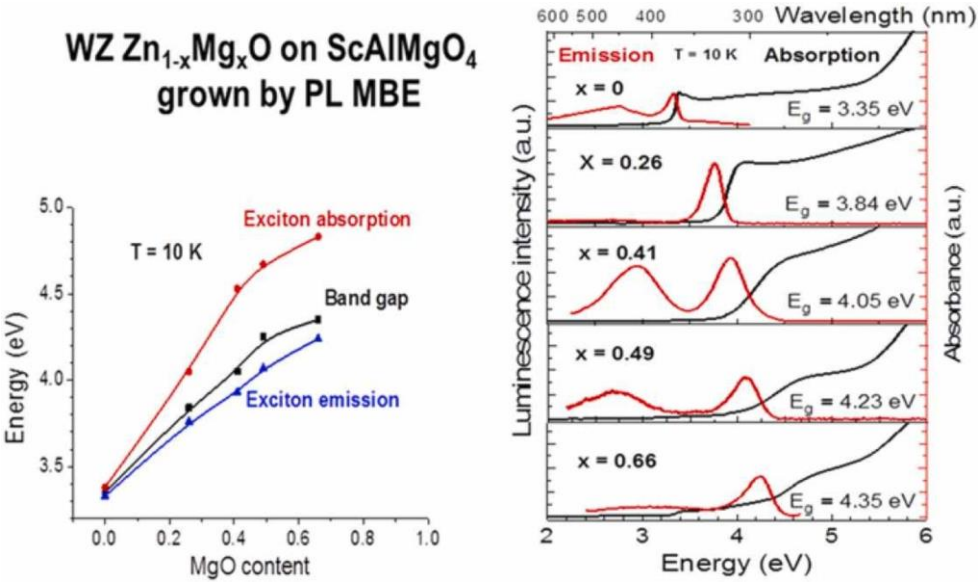

Published in:
L. Trinkler, I. Aulika, G. Krieke, D. Nilova, R. Ruska, J. Butikova, B. Berzina, M. M.-C. Chou, L. Chang, M.-C. Wen, T. Yan, R. Nedzinskas, J. Alloys Compd. 912 (2022) 165178*. DOI: 10.1016/j.jallcom.2022.165178.*

The role of Al_2O_3 interlayer in the synthesis of $ZnS/Al_2O_3/MoS_2$ core-shell nanowires

Edgars Butanovs[a,c], Alexei Kuzmin[a], Aleksejs Zolotarjovs[a], Sergei Vlassov[b], Boris Polyakov[a]

[a] *Institute of Solid State Physics, University of Latvia, Riga, LV-1063, Latvia*
[b] *Institute of Physics, University of Tartu, W. Ostwaldi Str. 1, 50412 Tartu, Estonia*
[c] *Institute of Technology, University of Tartu, Nooruse 1, 50411 Tartu, Estonia*

During the synthesis of heterostructured nanomaterials, unwanted structural and morphological changes in nanostructures may occur, especially when multiple sequential growth steps are involved. In this study, we describe a synthesis strategy of heterostructured $ZnS/Al_2O_3/MoS_2$ core-shell nanowires (NWs), and explore the role of the Al_2O_3 interlayer during synthesis. Core-shell NWs were produced via a four-step route: (1) synthesis of ZnO NWs on a silicon wafer, (2) deposition of thin Al_2O_3 layer by ALD, (3) magnetron deposition of MoO_3 layer, and (4) annealing of the sample in the sulphur atmosphere.

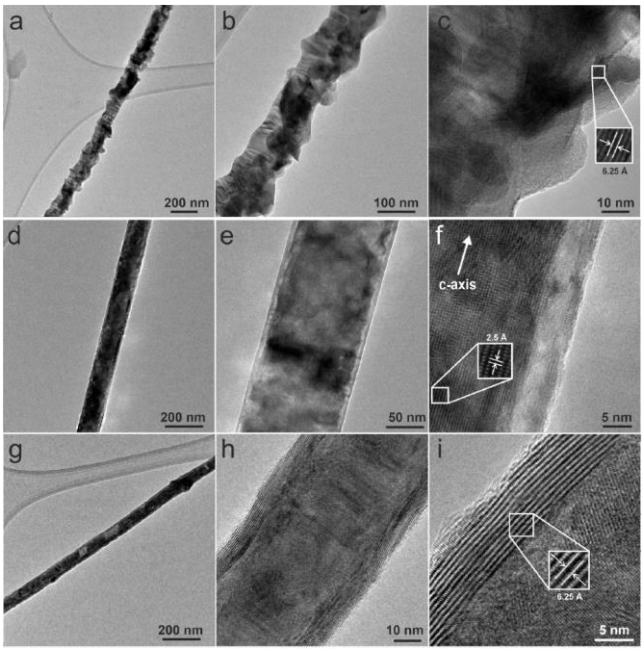

TEM images of ZnS/MoS_2 (a–c), ZnO/Al_2O_3 (d–f), and $ZnS/Al_2O_3/MoS_2$ (g–i) NWs annealed at 750 °C.

During sulphurization, ZnO is converted into ZnS, and MoO_3 into MoS_2, while the Al_2O_3 interlayer preserves the smooth surface of an NW required for the growth of a continuous MoS_2 shell. The resulting $ZnS/Al_2O_3/MoS_2$ core-shell NWs were characterized by transmission electron microscopy, X-ray diffraction and photoelectron spectroscopy, Raman spectroscopy, and optical photoluminescence spectroscopy. A reported strategy can be used for the synthesis of other core-shell NWs with a transition metal dichalcogenides (TMDs) shell to protect the NW core material that may otherwise be altered or damaged by the reactive chalcogenides at high temperatures.

Published in:
E. Butanovs, A. Kuzmin, A. Zolotarjovs, S. Vlassov, B. Polyakov, J. Alloys Compd. 918 (2022) 165648.
DOI: 10.1016/j.jallcom.2022.165648.

Pulsed electric fields alter expression of NF-κB promoter-controlled gene

Justina Kavaliauskaitė[a,b], Auksė Kazlauskaitė[a,b], Juozas Rimantas Lazutka[b], Gatis Mozolevskis[c], Arūnas Stirkė[a,c]

[a] *Laboratory of Bioelectrics, Center for Physical Sciences and Technology, Sauletekio Ave. 3, LT-10257 Vilnius, Lithuania*
[b] *Department of Botany and Genetics, Institute of Biosciences, Life Sciences Center, Vilnius University, Sauletekio Ave. 7, LT-10222 Vilnius, Lithuania*
[c] *Laboratory of Prototyping of Electronic and Photonic Devices, Institute of Solid State Physics, University of Latvia, Kengaraga Str. 8, LV-1063 Riga, Latvia*

The possibility to artificially adjust and fine-tune gene expression is one of the key milestones in bioengineering, synthetic biology, and advanced medicine. Since the effects of proteins or other transgene products depend on the dosage, controlled gene expression is required for any applications, where even slight fluctuations of the transgene product impact its function or other critical cell parameters. In this context, physical techniques demonstrate optimistic perspectives, and pulsed electric field technology is a potential candidate for a noninvasive, biophysical gene regulator, exploiting an easily adjustable pulse generating device. We exposed mammalian cells, transfected with a NF-κB pathway-controlled transcription system, to a range of microsecond-duration pulsed electric field parameters. To prevent toxicity, we used protocols that would generate relatively mild physical stimulation. The present study, for the first time, proves the principle that microsecond-duration pulsed electric fields can alter single-gene expression in plasmid context in mammalian cells without significant damage to cell integrity or viability. Gene expression might be upregulated or downregulated depending on the cell line and parameters applied. This noninvasive, ligand-, cofactor-, nanoparticle-free approach enables easily controlled direct electrostimulation of the construct carrying the gene of interest; the discovery may contribute towards the path of simplification of the complexity of physical systems in gene regulation and create further synergies between electronics, synthetic biology, and medicine.

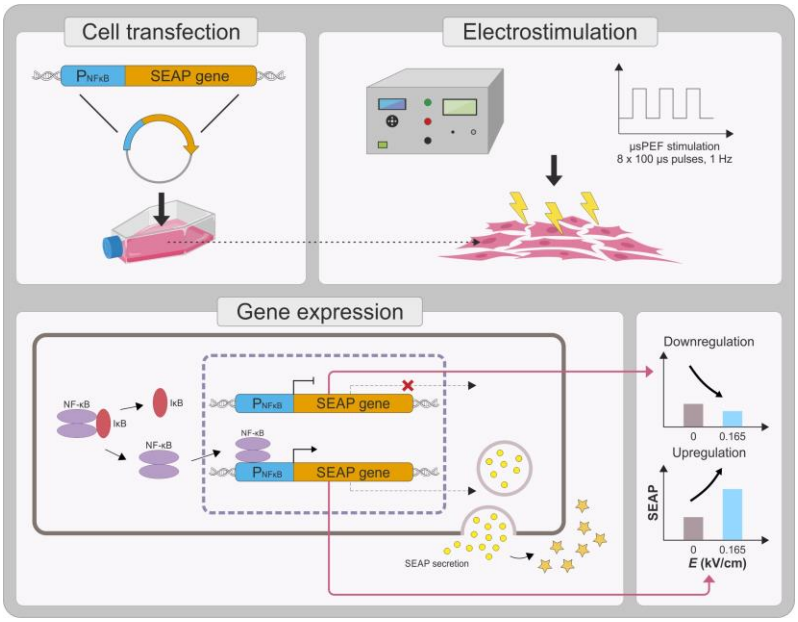

Published in:
J. Kavaliauskaitė, A. Kazlauskaitė, J. Rimantas Lazutka, G. Mozolevskis, A. Stirkė, Int. J. Mol. Sci. 23 (2022) 451. DOI: 10.3390/ijms23010451.

Magnetotransport studies of encapsulated topological insulator Bi_2Se_3 nanoribbons

Gunta Kunakova[a], Edijs Kauranens[a], Kiryl Niherysh[a,b], Mikhael Bechelany[c], Krisjanis Smits[d], Gatis Mozolevskis[d], Thilo Bauch[e], Floriana Lombardi[e], Donats Erts[a]

[a] *Institute of Chemical Physics, University of Latvia, 19 Raina Blvd., LV-1586 Riga, Latvia*
[b] *Research and Development Department, Integrated Micro- and Nanosystems, Belarusian State University of Informatics and Radioelectronics, P. Brovki Str. 6, 220013 Minsk, Belarus*
[c] *Institut Européen des Membranes, IEM, UMR 5635, University of Montpellier, ENSCM, CNRS, 34095 Montpellier, France*
[d] *Institute of Solid State Physics, University of Latvia, Kengaraga 8, LV-1063 Riga, Latvia*
[e] *Quantum Device Physics Laboratory, Department of Microtechnology and Nanoscience, Chalmers University of Technology, SE-41296 Goteborg, Sweden*

The majority of proposed exotic applications employing 3D topological insulators require high-quality materials with reduced dimensions. Catalyst-free, PVD-grown Bi_2Se_3 nanoribbons are particularly promising for these applications due to the extraordinarily high mobility of their surface Dirac states, and low bulk carrier densities. However, these materials are prone to the formation of surface accumulation layers; therefore, the implementation of surface encapsulation layers and the choice of appropriate dielectrics for building gate-tunable devices are important. In this study, all-around ZnO-encapsulated nanoribbons are investigated. Gate-dependent magnetotransport measurements show improved charge transport characteristics as reduced nanoribbon/substrate interface carrier densities compared to the values obtained for the as-grown nanoribbons on SiO_2 substrates.

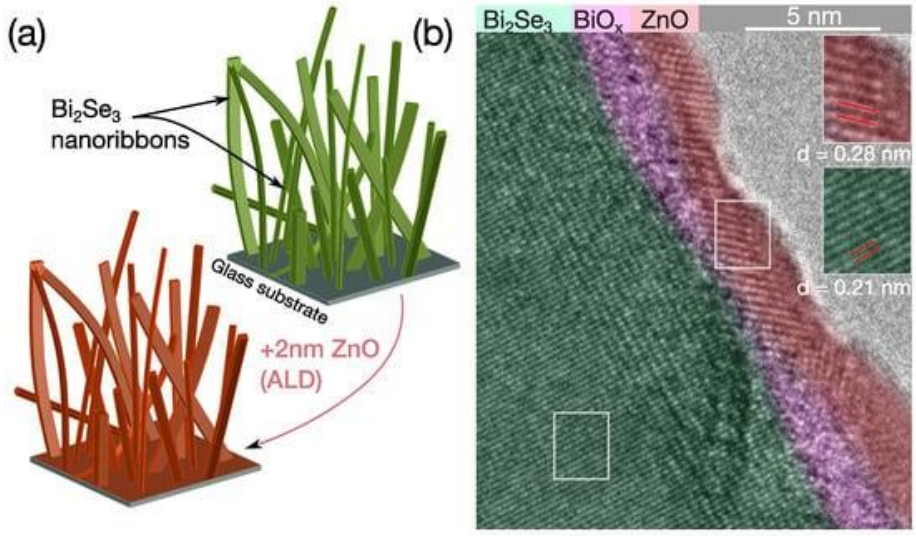

(a) Schematic representation of catalyst-free PVD-synthesized free-standing Bi_2Se_3 nanoribbons on a glass substrate; (b) false-colored HR-TEM image of a Bi_2Se_3 nanoribbon after encapsulation with a thin layer of ZnO.

Published in:
G. Kunakova, E. Kauranens, K. Niherysh, M. Bechelany, K. Smits, G. Mozolevskis, T. Bauche, F. Lombardie, D. Erts, Nanomaterials 12 (2022) 768. DOI: 10.3390/nano12050768.

Evaluation of radiation stability of electron beam irradiated Nafion® and sulfonated poly(ether ether ketone) membranes

E. Pajuste[a,b], I. Reinholds[c,g], G. Vaivars[a,d], A. Antuzevičs[d], L. Avotiņa[a], E. Sprūģis[a,d], R. Mikko[e], K. Heikki[e], R.M. Meri[f], R. Kaparkalējs[a]

[a] *Institute of Chemical Physics, University of Latvia, Jelgavas iela 1, Riga, Latvia*
[b] *Faculty of Chemistry, University of Latvia, Jelgavas iela 1, Riga, Latvia*
[c] *Baltic Scientific Instruments, Ganibu dambis 26, Riga, Latvia*
[d] *Institute of Solid State Physics, University of Latvia, Kengaraga iela 8, Riga, Latvia*
[e] *Department of Physics, University of Jyväskylä, Survontie 9 C, Jyväskylä, Finland*
[f] *Institute of Polymer Materials, Faculty of Materials Science and Applied Chemistry, Riga Technical University, Riga, Latvia*
[g] *Institute of Food Safety, Animal Health and Environment "BIOR", Lejupes iela 3, Riga, Latvia*

Proton exchange membranes (PEM), which have been commonly used in fuel cells have raised interest for their application in harsh environments involving ionizing radiation. Therefore, radiation stability and the ability to sustain their functionality under the radiation environment are of great interest. Within this study, electron beam irradiation in a dose range from 50 to 500 kGy was used to evaluate the effects of radiation on the physico-chemical and mechanical properties of two types of PEM: commercial Nafion®117 and sulfonated poly(ether-ether-ketone) (SPEEK) with a high degree of sulfonation (DS = 0.75±0.5).

SPEEK membrane presented higher mechanical and thermal stability compared to that of Nafion® at doses up to 250 kGy, which was evidenced by infrared and electron paramagnetic resonance spectroscopy, thermal analysis, and ion chromatography methods. Tensile tests at room temperature and dynamical mechanical analysis of irradiated membranes revealed improved strength, and storage modulus at room and elevated temperatures (80°C) for irradiated SPEEK as compared to pristine PEM. For comparison, Nafion® exhibited notable deterioration of mechanical properties including elongation at the break due to the predominant oxidation and chain scission already at doses exceeding 50 kGy. The study indicated that SPEEK could be a perspective replacement for traditional PEM for application in fuel cells exposed to ionising radiation.

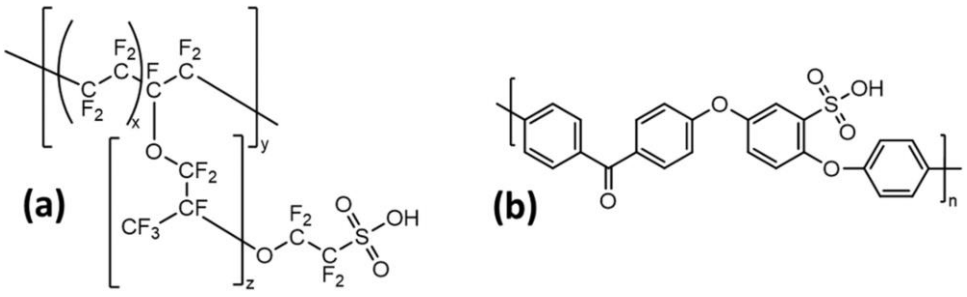

The general chemical structures of Nafion® (a) and SPEEK (b) polymers.

Published in:
E. Pajuste, I. Reinholds, G. Vaivars, A. Antuzevičs, L. Avotiņa, E. Sprūģis, R. Mikko, K. Heikki, R.M. Meri, R. Kaparkalējs, Polymer Degradation and Stability 200 (2022) 109970.
DOI: 10.1016/j.polymdegradstab.2022.109970.

III. Application: applied research of materials for sensors, scintillators, detectors, materials for photonics and electronics, and materials for energy harvesting and storage

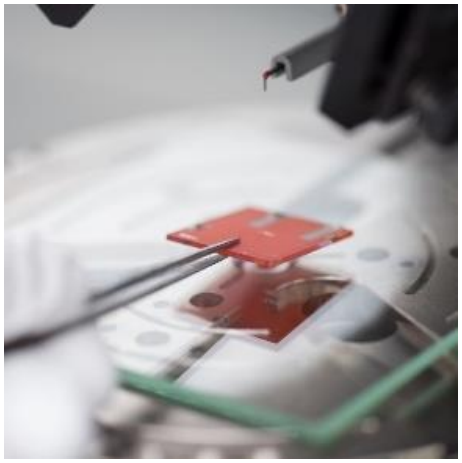

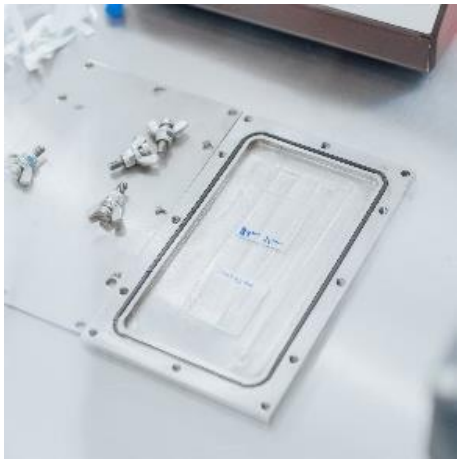

Smooth polymers charge negatively: Controlling contact electrification polarity in polymers

Osvalds Verners[a], Linards Lapčinskis[a], Līva Ģērmane[b], Aarne Kasikov[c], Martin Timusk[c], Kaspars Pudzs[d], Amanda V. Ellis[e], Peter C. Sherrell[e], Andris Šutka[a]

[a] *Institute of Materials and Surface Engineering, Faculty of Materials Science and Applied Chemistry, Riga Technical University, Riga LV-1048, Latvia*
[b] *Institute of Technical Physics, Faculty of Materials Science and Applied Chemistry, Riga Technical University, Riga LV-1048, Latvia*
[c] *Institute of Physics, University of Tartu, W. Ostwaldi 1, 50411 Tartu, Estonia*
[d] *Institute of Solid State Physics, University of Latvia, Kengaraga 8, Riga LV-1063, Latvia*
[e] *Department of Chemical Engineering, Faculty of Engineering and Information Technology, The University of Melbourne, Parkville 3010, Australia*

Contact electrification is a powerful tool to harvest energy from mechanical motion. However, current models of contact electrification at polymer | polymer interfaces only explain charge transfer for the contact between chemically dissimilar polymers. Recently, strong contact electrification between chemically identical polymer surfaces has been observed. Understanding contact electrification between chemically identical polymers is a key issue in developing a holistic model for polymer triboelectrification. Herein, we present a combined experimental and computational approach to develop a model of contact electrification between chemically identical polymers. The model developed describes how the relative surface roughness influences surface charge. The chemically identical polymer surfaces show an increase in the surface charge when the difference in surface roughness is increased. Further, the roughest surface was found to present a positive surface charge, and the smoother surface had a negative charge. These observations were justified through the modelling of a consistently lower strain on rougher surfaces during contact separation. Molecular dynamics simulations demonstrated the relationship between this strain with bond-scission and charged material transfer. It was found that a negatively charged fragment has a higher statistical probability to be transferred due to smaller scission/desorption energies. This comparison of surface roughness can be extended to dissimilar polymer interfaces and will enable the engineering of highly efficient triboelectric nanogenerator (TENG) devices in the future.

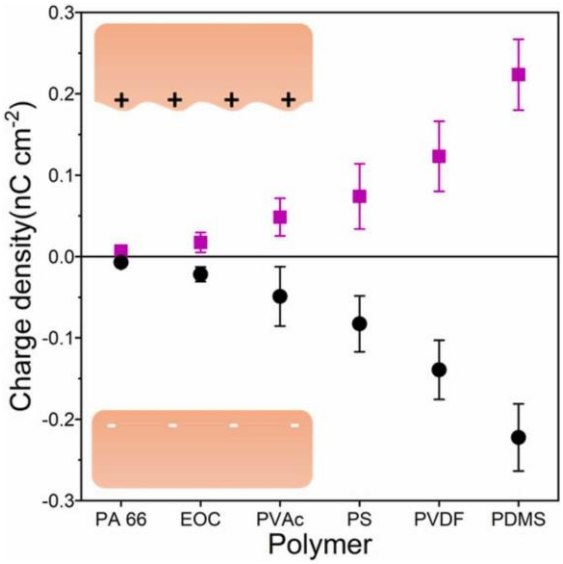

Published in:
O. Verners, L. Lapčinskis, L. Ģermane, A. Kasikov, M. Timusk, K. Pudzs, A. V. Ellis, P. C. Sherrell, A. Šutka, Nano Energy 104 (2022) 107914. DOI: 10.1016/j.nanoen.2022.107914.

Unveiling the role of carbonate in nickel-based plasmonic core@shell hybrid nanostructure for photocatalytic water splitting

Parisa Talebi[a], Andrey A. Kistanov[a], Ekta Rani[a], Harishchandra Singh[a], Vladimir Pankratov[b], Viktorija Pankratova[b,a], Graham King[c], Marko Huttula[a], Wei Cao[a]

[a] *Nano and Molecular Systems Research Unit, University of Oulu, FIN-90014, Finland*
[b] *Institute of Solid-State Physics, University of Latvia, 8 Kengaraga street, 1063 Riga, Latvia*
[c] *Canadian Light Source, 44 Innovation Blvd., Saskatoon, Saskatchewan S7N 2V3, Canada*

Though carbonates are known for several decades, their role in sun-light-driven photocatalysis is still hidden. Herein, carbonate-boosted solar water splitting in nickel-based plasmonic hybrid nanostructures is disclosed for the first time via in-situ experiments and density-functional theory (DFT)-based calculations. Ni@NiO/$NiCO_3$ core@shell (shell consisting of crystalline NiO and amorphous $NiCO_3$) nanostructure with varying sizes and compositions are studied for hydrogen production. The visible light absorption at ~470 nm excludes the possibility of NiO as an active photocatalyst, emphasizing plasmon-driven H_2 evolution. Under white light irradiation, a higher hydrogen yield of ~80 µmol/g/h for vacuum annealed sample over pristine (~50 µmol/g/h) complements the spectroscopic data and DFT results, uncovering amorphous $NiCO_3$ as an active site for H_2 absorption due to its unique electronic structure. This conclusion also supports the time-resolved photoluminescence results, indicating that the plasmonic electrons originating from Ni are transferred to $NiCO_3$ via NiO. The H_2 evolution rate can further be enhanced and tuned by the incorporation of NiO between Ni and $NiCO_3$.

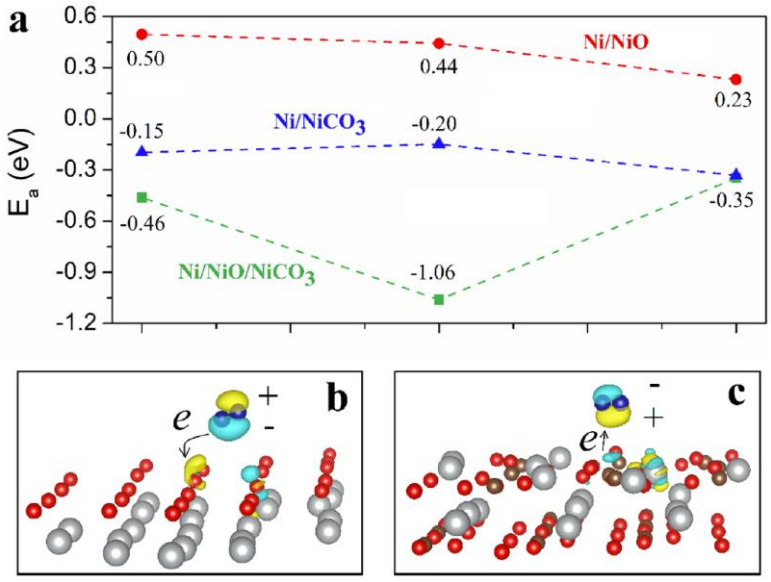

(a) Absorption energy of hydrogen at different absorption sites on Ni-NiO-$NiCO_3$, Ni-NiO, and Ni-$NiCO_3$. Charge density difference isosurface plot for hydrogen on (b) Ni-NiO and (c) Ni-NiO-$NiCO_3$. The yellow/blue color denotes the accumulation/depletion of electrons.

Published in:
P. Talebi, A. A. Kistanov, E. Rani, H. Singh, V. Pankratov, V. Pankratova, G. King, M. Huttula, W. Cao, Applied Energy 322 (2022) 119461. DOI: 10.1016/j.apenergy.2022.119461.

Liquid-assisted grinding/compression: a facile mechanosynthetic route for the production of high-performing Co–N–C electrocatalyst materials

Akmal Kosimov[a], Gulnara Yusibova[a], Jaan Aruväli[b], Päärn Paiste[b], Maike Käärik[a], Jaan Leis[a], Arvo Kikas[c], Vambola Kisand[c], Krišjānis Šmits[d], Nadezda Kongi[a]

[a] *Institute of Chemistry, University of Tartu, Tartu 50411, Estonia*
[b] *Institute of Ecology and Earth Sciences, University of Tartu, Tartu 50411, Estonia*
[c] *Institute of Physics, University of Tartu, Tartu 50411, Estonia*
[d] *Institute of Solid-State Physics, University of Latvia, 8 Kengaraga street, 1063 Riga, Latvia*

Worldwide implementation of energy conversion devices such as metal–air batteries and fuel cells needs an innovative approach for the sustainable design of noble metal-free electrocatalysts. A key factor to be considered is the industry-scale production method, which should be cost and energy-effective, and environmentally friendly. A novel solid-phase-based methodology is introduced herein as a new approach for the mechanosynthesis of M–N–C-type catalysts. This method employs low-cost commercially available materials, is time and energy-efficient, results in no solvent/toxic waste, and does not require a complex post-synthetic treatment. The liquid-assisted grinding/compression approach yielded a series of meso- and microporous Co–N–C catalysts, with excellent bifunctional activity towards oxygen evolution and reduction reactions. In-depth physical characterization confirmed that all NaCl-supported catalysts possess cross-linked sheet-like mesoporous carbon structures with high exposure of catalytically active sites. This study provides a new avenue for the large-scale production of high-performance and low-cost M–N–C materials via energy-effective and environmentally sustainable synthetic protocols.

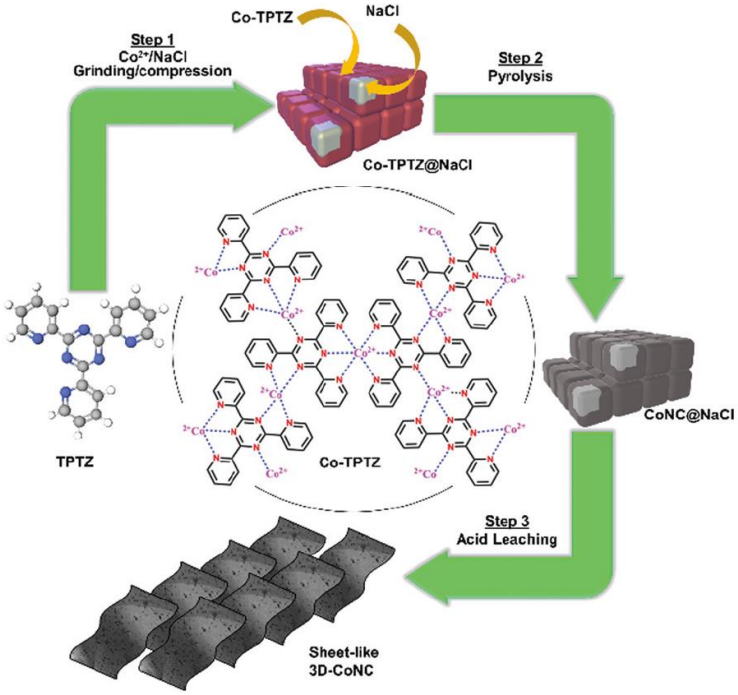

Schematic diagram of green mechanochemical approach toward synthesis of Co–N–C-type catalysts.

Published in:
A. Kosimov, G. Yusibova, J. Aruväli, P. Paiste, M. Käärik, J. Leis, A. Kikas, V. Kisand, K. Šmits, N. Kongi, Green Chemistry 24 (2022) 305–314. DOI: 10.1039/d1gc03433b.

Thiazoline Carbene–Cu(I)–Amide complexes: Efficient White Electroluminescence from Combined Monomer and Excimer Emission

Armands Ruduss[a], Baiba Turovska[b], Sergey Belyakov[b], Kitija A. Stucere[c], Aivars Vembris[c], Glib Baryshnikov[d], Hans Ågren[e], Jhao-Cheng Lu[f], Wei-Han Lin[f], Chih-Hao Chang[b], Kaspars Traskovskis[a]

[a] *Faculty of Materials Science and Applied Chemistry, Riga Technical University, P. Valdena Str. 3, LV-1048, Riga, Latvia*
[b] *Latvian Institute of Organic Synthesis, Aizkraukles Str. 21, Riga LV-1006, Latvia*
[c] *Institute of Solid-State Physics, University of Latvia, 8 Kengaraga street, 1063 Riga, Latvia*
[d] *Laboratory of Organic Electronics, Department of Science and Technology, Linköping University, SE-60174 Norrköping, Sweden*
[e] *Department of Physics and Astronomy, Uppsala University, SE-751 20 Uppsala, Sweden*
[f] *Department of Electrical Engineering, Yuan Ze University, Chungli 32003, Taiwan*

Luminescent carbene–metal–amide complexes bearing group 11 metals (Cu, Ag, Au) have recently attracted great attention due to their exceptional emission efficiency and high radiative decay rates (k_r). These materials provide a less costly alternative to organic light-emitting diode (OLED) emitters based on more scarce metals, such as Ir and Pt. Herein, a series of eight Cu(I) complexes bearing as yet unexplored 1,3-thiazoline carbenes have been investigated and analyzed with respect to their light emission properties and OLED application. For the first time among the class of copper-based organometallic compounds the formation of efficient electroluminescent excimers is demonstrated. The prevalence of electroluminescence (EL) from either the monomer (bluish green) or the excimer (orange-red) can be adjusted in vacuum-deposited emissive layers by altering the extent of steric encumbrance of the emitter or its concentration. Optimized conditions in terms of the emitter structure and mass fraction allowed a simultaneous EL from the monomer and excimer, which laid the basis for a preparation of a single-emitter white OLED (WOLED) with external quantum efficiency of 16.5% and a maximum luminance of over 40000 cd m^{-2}. Wide overlapping emission bands of the monomer and excimer ensure a device color rendering index (CRI) of above 80. In such a way the prospects of copper complexes as cost-effective materials for lighting devices are demonstrated, offering expense reduction through a cheaper emissive component and a simplified device architecture.

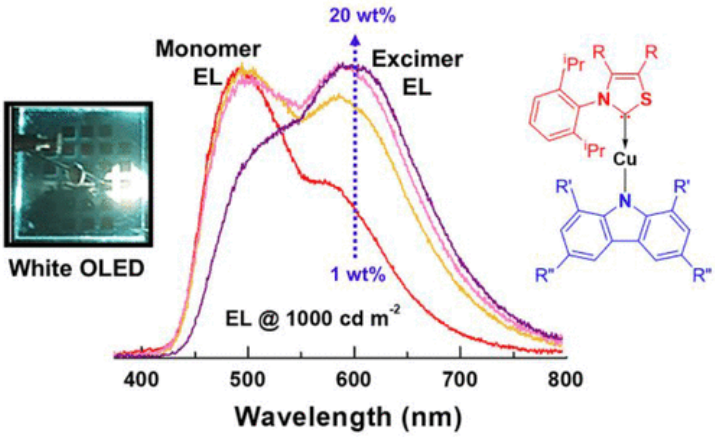

Published in:
A. Ruduss, B. Turovska, S. Belyakov, K. A. Stucere, A. Vembris, G. Baryshnikov, H. Ågren, J.-C. Lu, W.-H. Lin, C.-H. Chang, K. Traskovskis, ACS Appl. Mater. Interfaces 14 (2022) 15478–15493. DOI: 10.1021/acsami.2c00847.

Arrhenius plots for Li-ion battery ageing as a function of temperature, C-rate, and ageing state – An experimental study

Gints Kucinskis[a,b], Maral Bozorgchenani[a], Max Feinauer[a], Michael Kasper[a], Margret Wohlfahrt-Mehrens[a], Thomas Waldmann[a]

[a] *ZSW – Zentrum für Sonnenenergie- und Wasserstoff-Forschung, Baden-Württemberg, Helmholtzstrasse 8, D-89081 Ulm, Germany*
[b] *Institute of Solid-State Physics, University of Latvia, 8 Kengaraga street, 1063 Riga, Latvia*

We present an extensive analysis of Li-ion battery ageing via Arrhenius plots. The V-shaped Arrhenius plots show minima at an optimum temperature corresponding to the longest cycle-life. The V-shape of the Arrhenius plots signifies the crossover between the two dominating ageing mechanisms – solid electrolyte interphase (SEI) growth in the high-temperature range and lithium deposition in the low-temperature range. Subjects of our investigations are commercial 5 Ah high energy 21,700-type cells with $LiNi_{0.90}Co_{0.05}Al_{0.05}O_2$ + $LiNiO_2$ (NCA + LNO) cathode and Si/graphite anode (~3% Si) and 0.1 Ah lab-made pouch cells with $LiNi_{1/3}Mn_{1/3}Co_{1/3}O_2$ (NMC111) cathode and a graphite anode.

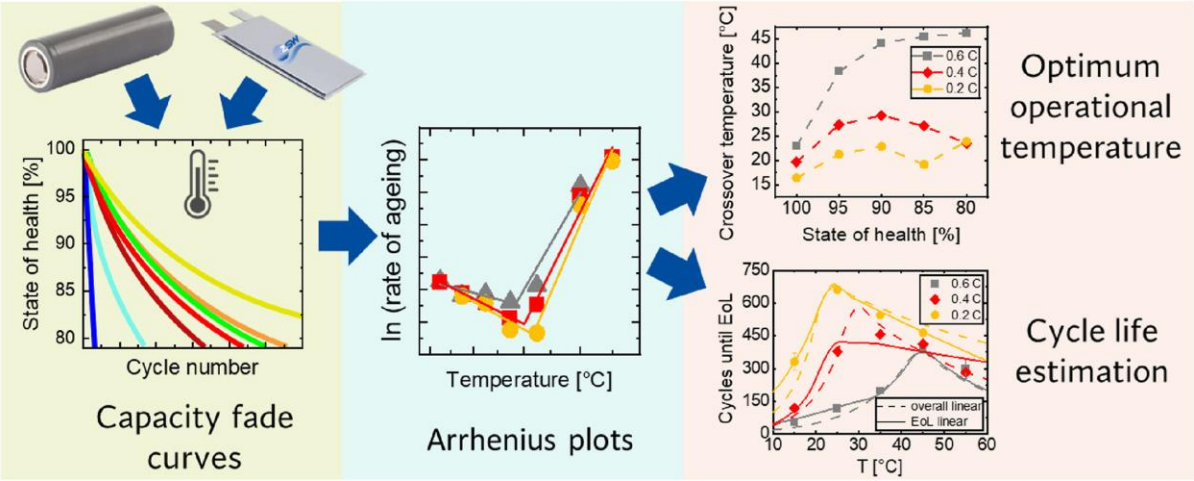

The results of the Arrhenius plots are analysed in the context of C-rate, cell ageing, and electrode properties. We find that the crossover between the dominating ageing mechanism and hence the optimum operating temperature of the Li-ion cells depend on C-rate, anode coating thickness/particle sizes, the state of health, and the shape of the capacity fade curve. Considering the change of the dominant ageing mechanism can help designing battery systems with longer service life. Additionally, we show a lifetime estimation for temperature-dependent cycling of batteries emphasizing the merit of Arrhenius plots in the context of battery cell ageing.

Published in:
G. Kucinskis, M. Bozorgchenani, M. Feinauer, M. Kasper, M. Wohlfahrt-Mehrens, T. Waldmann, Journal of Power Sources 549 (2022) 232129. DOI: 10.1016/j.jpowsour.2022.232129.

Bio-Inspired Macromolecular Ordering of Elastomers for Enhanced Contact Electrification and Triboelectric Energy Harvesting

Andris Šutka[a], Linards Lapčinskis[a], Osvalds Verners[a], Līva Ģērmane[b], Krisjanis Smits[c], Arturs Pludons[d], Sergejs Gaidukovs[d], Ilze Jerāne, Martins Zubkins[c], Kaspars Pudzs[c], Peter C. Sherrell[e], Juris Blums[b]

[a] *Institute of Materials and Surface Engineering, Faculty of Materials Science and Applied Chemistry, Riga Technical University, Riga LV-1048, Latvia*
[b] *Institute of Technical Physics, Faculty of Materials Science and Applied Chemistry, Riga Technical University, Riga LV-1048, Latvia*
[c] *Institute of Solid State Physics, University of Latvia, Kengaraga 8, Riga LV-1063, Latvia*
[d] *Institute of Polymer Materials, Faculty of Materials Science and Applied Chemistry, Riga Technical University, P. Valdena str. 3/7, Riga, LV-1048 Latvia*
[e] *Department of Chemical Engineering, Faculty of Engineering and Information Technology, The University of Melbourne, Parkville 3010, Australia*

Triboelectrification of polymers enables mechanical energy harvesting in triboelectric generators, droplet generators, and ferroelectrets. Herein, triboelectric polymers, inspired by the ordering in spider-silk, with strongly enhanced contact electrification are presented. The ordering in polyether block amide (PEBA) is induced by the addition of inorganic goethite (α-FeOOH) nanowires that form H-bonds with the elastomeric matrix. The addition of as little as 0.1 vol% of α-FeOOH into PEBA increases the surface charge by more than order of magnitude (from 0.069 to 0.93 nC cm^{-2}). The H-bonds between α-FeOOH and PEBA promote the formation of inclusions with higher degree of macromolecular ordering, analogous to the structure of spider silk. The formation of these inclusions is proven via nanoindentation hardness measurements and correlated with H-bond-induced chemical changes by Fourier transform infrared spectroscopy and direct scanning calorimetry. Theoretical studies reveal that the irregularity in hardness provides stress accumulation on the polymer surface during contact-separation. Subsequent molecular dynamic studies demonstrate that stress accumulation promotes the mass-transfer mechanism of contact electrification. The proposed macromolecular structure design provides a new paradigm for developing materials for applications in mechanical energy harvesting.

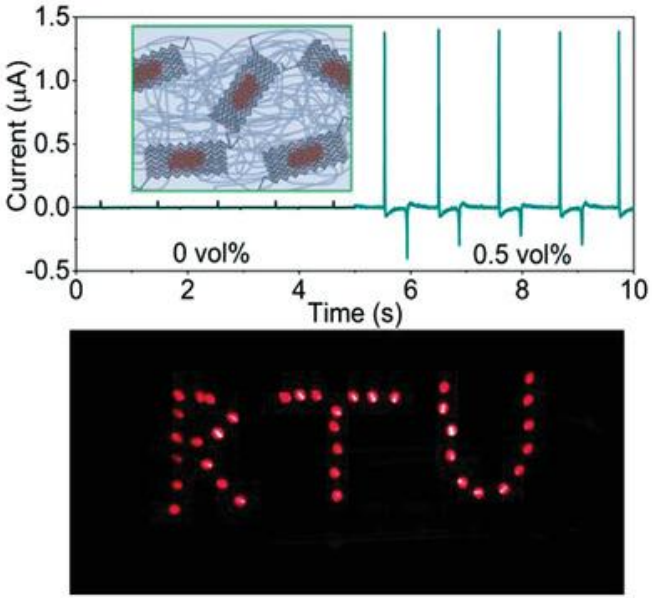

Published in:
A. Šutka, L. Lapčinskis, O. Verners, L. Ģērmane, K. Smits, A. Pludons, S. Gaidukovs, I. Jerāne, M. Zubkins, K. Pudzs, P. C. Sherrell, J. Blums, Adv. Mater. Technol. 7 (2022) 2200162. DOI: 10.1002/admt.202200162.

Sb_2S_3 solar cells with a cost-effective and dopant-free fluorene-based enamine as a hole transport material

Nimish Juneja[a], Sreekanth Mandati[a], Atanas Katerski[a], Nicolae Spalatu[a], Sarune Daskeviciute-Geguziene[b], Aivars Vembris[c], Smagul Karazhanov [d], Vytautas Getautis[b], Malle Krunks[a], Ilona Oja Acik[a]

[a] *Laboratory of Thin Film Chemical Technologies, Department of Materials and Environmental Technology, Tallinn University of Technology, Ehitajate tee 5, 19086 Tallinn, Estonia*
[b] *Department of Organic Chemistry, Kaunas University of Technology, Kaunas LT-50254, Lithuania*
[c] *Institute of Solid State Physics, University of Latvia, Kengaraga Str. 8, Riga, Latvia*
[d] *Institute for Energy Technology (IFE), P. O Box 40, No 2027, Kjeller, Norway*

Antimony sulphide (Sb_2S_3) is a promising candidate for semi-transparent and tandem solar cells owing to its suitable optoelectronic properties. However, the applications of Sb_2S_3 solar cells are rather limited by their low power conversion efficiencies (PCEs) and the use of expensive hole transport materials (HTMs). Furthermore, HTMs like P3HT exhibit parasitic absorption and hinder the overall transparency of the devices. To circumvent these problems, V1236, a fluorene-based enamine is explored for the first time for Sb_2S_3 solar cells, which is significantly cheaper, transparent, and does not require high-temperature activation like P3HT. Solar cells are fabricated in the glass/FTO/TiO_2/Sb_2S_3/HTM/Au configuration wherein TiO_2 and Sb_2S_3 are deposited using ultrasonic spray pyrolysis and HTMs are spin-coated. The concentration of V1236 is systematically varied and its impact on the Sb2S3 device performance is investigated. The J_{SC} of the solar cells with V1236 is about 17% higher which is attributed to the better valence band edge alignment compared to P3HT. The EQE measurements show no parasitic absorption with V1236 while the optical studies show a larger bandgap for V1236 (2.6 eV) over P3HT (1.8 eV), indicating negligible loss of transparency. Furthermore, the overall transparency is increased by 20% for V1236 devices in comparison to P3HT devices while yielding better PCEs, demonstrating the efficacy of novel V1236 as an HTM for semi-transparent Sb_2S_3 solar cells.

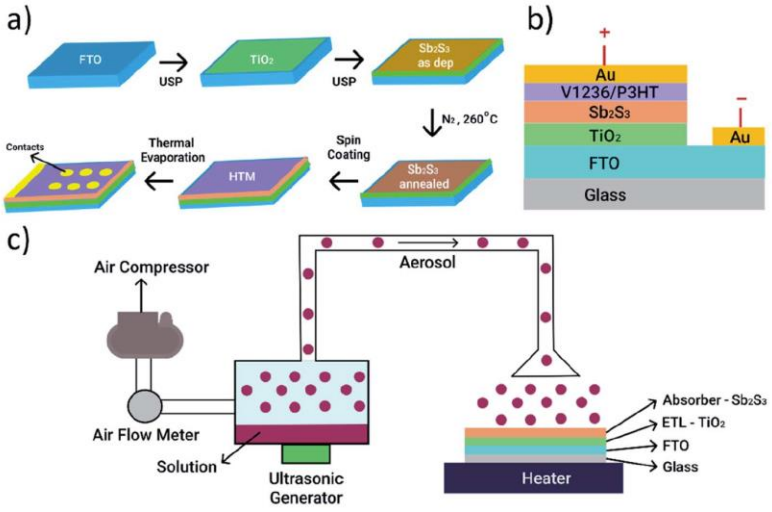

(a) Schematic of the procedure adopted for the fabrication of Sb_2S_3 solar cells, (b) Sb_2S_3 solar cell configuration and (c) schematic of ultrasonic spray pyrolysis (USP) deposition.

Published in:
N. Juneja, S. Mandati, A. Katerski, N. Spalatu, S. Daskeviciute-Geguziene, A. Vembris, S.I Karazhanov, V. Getautis, M. Krunks, I.O. Acik, Sustainable Energy Fuels 6 (2022) 3220-3229. DOI: 10.1039/D2SE00356B.

Synthesis and properties of bismuth selenide-based nanolaminates for application in thermoelectrics

Jana Andzane[a], Andrei Felsharuk[a], Krisjanis Buks[a], Anatolijs Sarakovskis[b], Kiryl Niherysh[a], Jevgenijs Gabrusenoks[b], Donats Erts[a]

[a] *Institute of Chemical Physics, University of Latvia, Raina blvd. 19, Riga, LV-1586 Latvia*
[b] *Institute of Solid State Physics, University of Latvia, Kengaraga str. 8, Riga, LV-1063 Latvia*

In this study, a simple and cost-effective physical vapor deposition method is applied for the deposition of single Bi_2Se_3, $Bi_{1.925}Sn_{0.075}Se_3$, $Bi_2Se_{2.975}Te_{0.025}$ ultrathin films of average thickness 10–12 nm, and the fabrication of n-type 5-layer nanolaminates. The nanolaminates are composed of alternating doped and undoped ultrathin films. Electrical and thermoelectric properties (Seebeck coefficient, resistivity, electron thermal conductivity, charge carrier concentration, and mobility) of nanolaminates as well as single ultrathin undoped and doped films are studied at room temperature under ambient conditions. Both types of nanolaminates show a 75–125% increase of the Seebeck coefficient accompanied by a 65–85% reduction of the electron thermal conductivity in comparison with the nanostructured bulk materials of similar chemical compositions. The mechanisms underlying such improvement of properties of studied nanolaminates in comparison with the nanostructured bulk counterparts are discussed.

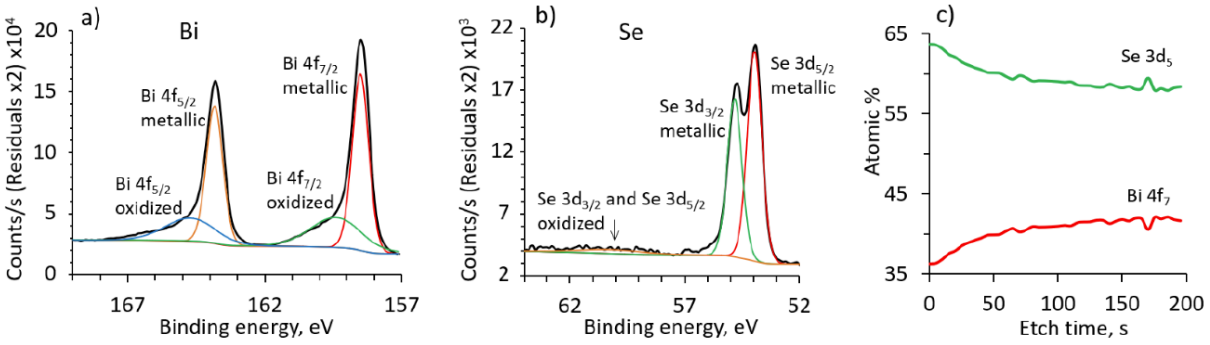

(a, b) Representative deconvoluted XPS spectra of $Bi_{1.925}Sn_{0.075}Se_3$ ultrathin film; (c) depth profile of a $Bi_2Se_3/Bi_{1.925}Sn_{0.075}Se_3$ double layer.

Published in:
J. Andzane, A. Felsharuk, K. Buks, A. Sarakovskis, K. Niherysh, J. Gabrusenoks, D. Erts, Adv. Mater. Interfaces 9 (2022) 2200385. DOI: 10.1002/admi.202200385.

Highly efficient flexible n-type thermoelectric films formed by encapsulation of Bi_2Se_3-MWCNT hybrid networks in polyvinyl alcohol

Krisjanis Buks[a], Jana Andzane[a], Lasma Bugovecka[a], Mikhail V. Katkov[b], Krisjanis Smits[c], Olesja Starkova[d], Juris Katkevics[a], Agris Bērziņš[e], Loreta Brauna[a], Vanda Voikiva[a], Donats Erts[a]

[a] *Institute of Chemical Physics, University of Latvia, Raina blvd. 19, Riga, LV-1586 Latvia*
[b] *3D Strong Ltd., Instituta str. 36-17, Ulbroka, LV-2130 Latvia*
[c] *Institute of Solid State Physics, University of Latvia, Kengaraga str. 8, Riga, LV-1063 Latvia*
[d] *Institute for Mechanics of Materials, University of Latvia, Jelgavas str. 3, Riga, LV-1004 Latvia*
[e] *Faculty of Chemistry, University of Latvia, Jelgavas str. 1, Riga, LV-1004 Latvia*

The use of organic–inorganic nanocomposites has shown the greatest potential for engineering efficient flexible thermoelectric devices. In this work, a novel approach of encapsulation of as-grown bismuth selenide-multiwalled carbon nanotubes (Bi_2Se_3-MWCNT) hybrid network in polyvinyl alcohol for fabrication of n-type flexible thermoelectric films is demonstrated as a successful alternative to the mechanically mixed counterparts. The developed stable flexible n-type thermoelectric material has a Seebeck coefficient and power factor at room temperature as high as −85 μV K^{-1} and 0.4 μW m^{-1} K^{-2}, and figure-of-merit, exceeding the value shown by the mixed counterpart by ≈2 orders of magnitude, while requiring 3–4 times less inorganic material in comparison with mixed composites. Charge carrier transport mechanisms and contribution of Bi_2Se_3 and MWCNT components of not encapsulated and encapsulated hybrid networks to the total Seebeck coefficient, electrical conductance, and power factor are studied. In addition, the fabricated flexible thermoelectric films show good environmental stability at relative humidity levels up to 60%, as well as great mechanical and electrical stability with the increase of resistance within 0.5% and deviations of the Seebeck coefficient within 2% from the initial value during the 100 repetitive bending cycles.

Published in:
K. Buks, J. Andzane, L. Bugovecka, M. V. Katkov, K. Smits, O. Starkova, J. Katkevics, A. Bērziņš, L. Brauna, V. Voikiva, D. Erts, Adv. Mater. Interfaces 9 (2022) 2200318. DOI: 10.1002/admi.202200318.

Tuneable persistent luminescence of novel $Mg_3Y_2Ge_3O_{12}$ garnet,

Guna Krieke[a], Guna Doke[a], Andris Antuzevics[a], Inga Pudza[a], Alexei Kuzmin[a], Edmund Welter[b]

[a] *Institute of Solid State Physics, University of Latvia, Riga, LV-1063, Latvia*
[b] *Deutsches Elektronen-Synchrotron – A Research Centre of the Helmholtz Association, Notkestrasse 85, D-22607 Hamburg, Germany*

In this work, novel garnet persistent luminescence phosphor $Mg_3Y_2Ge_3O_{12}$: Tb^{3+} (MYG: Tb^{3+}) with bright blue to green tuneable emission is reported.

MYG: Tb^{3+} samples with Tb3+ content ranging from 0 % to 100 % were analysed. X-ray absorption spectroscopy analysis showed that Tb^{3+} ions incorporate in the garnet structure by replacing Y^{3+} ions. Optimal dopant content was determined to achieve bright afterglow lasting more than ten hours. Tuneability of persistent luminescence was attributed to the deviations in populations of $^5D_4$ and $^5D_3$ emitting states of Tb^{3+} due to multiphonon relaxation and cross-relaxation processes. Photoluminescence, thermostimulated luminescence (TSL) and electron paramagnetic resonance (EPR) methods were used to determine the dominant persistent luminescence processes in the investigated material.

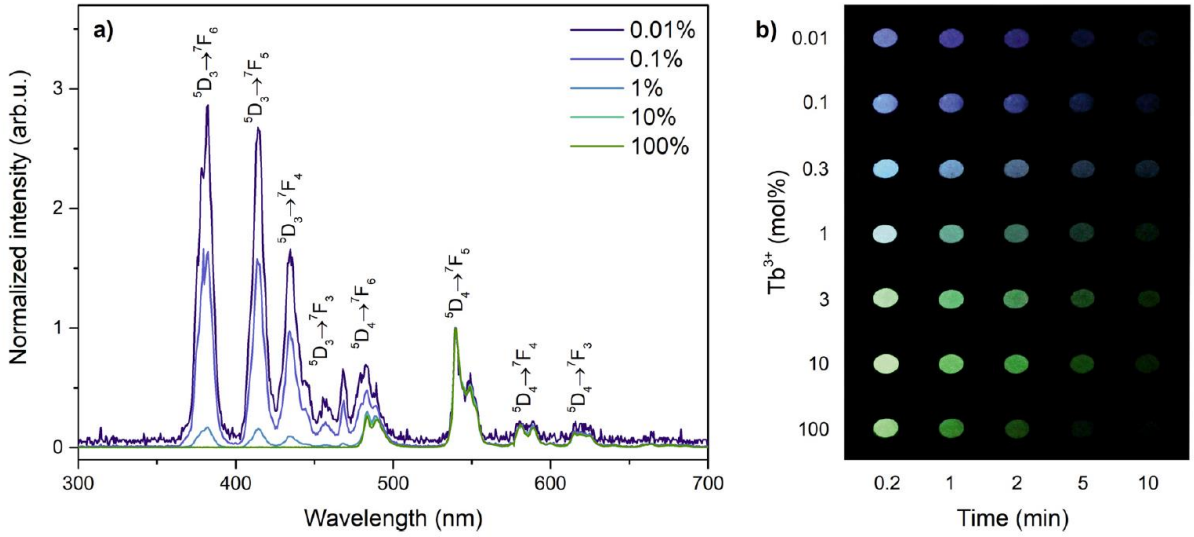

a) Afterglow spectra detected 5 s after irradiation with 263 nm and b) photographs taken 0.2–10 min after irradiation of MYG: Tb^{3+} samples containing 0–100 % Tb^{3+}.

The analysis of intrinsic defects in the material using EPR spectroscopy showed the presence of three distinct paramagnetic V-type centres and at least one F-type centre. The role of Tb^{3+} as a charge trap was discussed. MYG: Tb^{3+} exhibited luminescence tuneability by doping and temperature, which is promising for advanced anti-counterfeiting applications.

Published in:
G. Krieke, G. Doke, A. Antuzevics, I.Pudza, A. Kuzmin, E. Welter, J. Alloys Compd. 922 (2022) 166312.
DOI: 10.1016/j.jallcom.2022.166312.

Novel broadband near-infrared emitting long afterglow phosphor $MgGeO_3:Cr^{3+}$

Guna Doke, Andris Antuzevics, Guna Krieke, Aija Kalnina, Anatolijs Sarakovskis

Institute of Solid State Physics, University of Latvia, Kengaraga str. 8, Riga, LV-1063 Latvia

In this study, we report broadband near-infrared persistent luminescence of a novel $MgGeO_3:Cr^{3+}$ material. The luminescence can be excited by ultraviolet radiation and detected for more than 16 h. Optical and electron paramagnetic resonance spectroscopy experiments suggest that the observed bands appear as a result of interaction between Cr^{3+} luminescence centre and oxygen-impurity complexes and oxygen vacancy-related trapping states. Thermally stimulated luminescence (TSL) analysis revealed that the states are closely overlapping and lie relatively deep in the band gap with the activation energy exceeding 0.9 eV. The experimental data strongly suggest that the main detrapping route for the trapped charge carriers in the $MgGeO_3:Cr^{3+}$ material is athermal tunnelling directly to the luminescence centres.

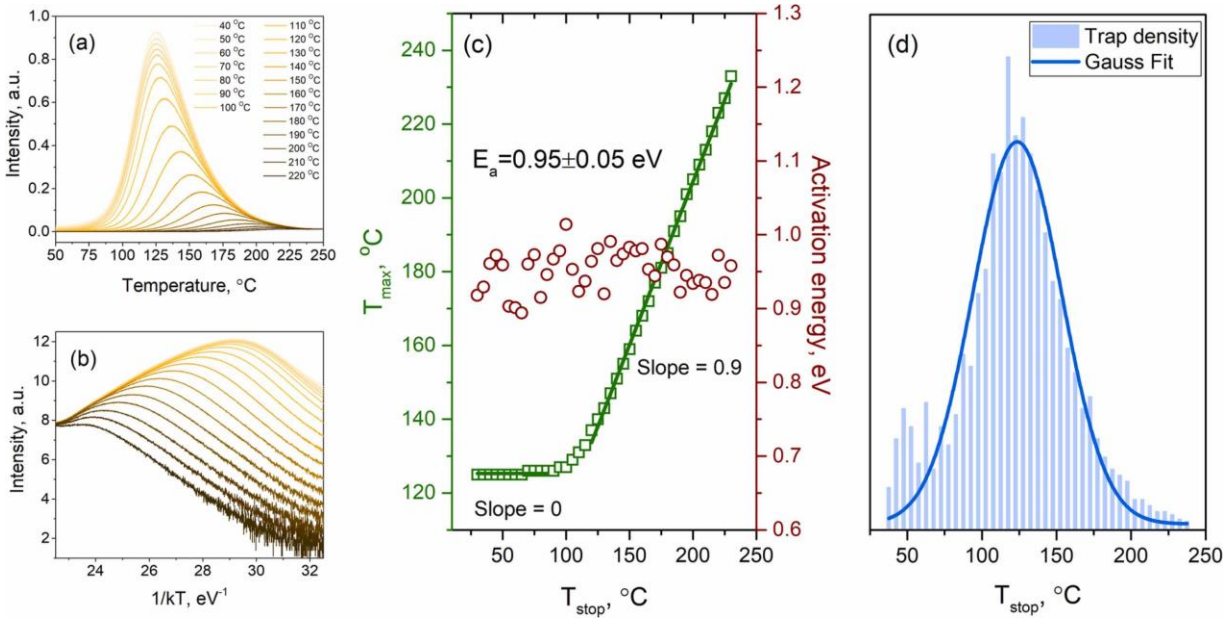

TSL glow curves of the MGO: 0.25 mol% Cr^{3+} sample measured after preheating to T_{stop} from 40 °C to 220 °C (a); initial rise analysis (IRA) of the data obtained from $T_{max} - T_{stop}$ experiment (b) $T_{max} - T_{stop}$ plot and E_a values obtained by IRA (c) and the calculated trap density distribution (d). The sample was charged with 263 nm for 60 s.

Published in:
G. Doke, A. Antuzevics, G. Krieke, A. Kalnina, A. Sarakovskis, J. Alloys Compd. 918 (2022) 165768.
DOI: 10.1002/admi.202200318.

Electrochemical performance of $Na_2FeP_2O_7$/C cathode for sodium-ion batteries in electrolyte with fluoroethylene carbonate additive

Gints Kucinskis, Inara Nesterova, Anatolijs Sarakovskis, Liga Bikse, Julija Hodakovska, Gunars Bajars

Institute of Solid State Physics, University of Latvia, LV-1063 Riga, Latvia

Solution synthesis was used to prepare pristine $Na_2FeP_2O_7$ and $Na_2FeP_2O_7$/C composite cathode materials for sodium-ion batteries, using glucose as a carbon source. While the pristine $Na_2FeP_2O_7$ displays capacity of only 45 mAh/g due to the relatively large grain size, the addition of carbon increases the capacity to up to 92 mAh/g (95% of the theoretical 97 mAh/g capacity) with excellent rate capability, as 44 mAh/g capacity is still retained even at 20 C (1.94 A/g) current. The optimal content of carbon was found to be 4.8%. The initial capacity of 81 mAh/g is fully retained after 500 cycles at 1 C, indicating excellent cycle life. Measurements were carried out in 1 M $NaClO_4$ salt in propylene carbonate as electrolyte and show that the addition of 5 wt% fluoroethylene carbonate solid electrolyte interphase stabilizing additive greatly benefits the rate and cycling performance of $Na_2FeP_2O_7$/C as measured in half-cells.

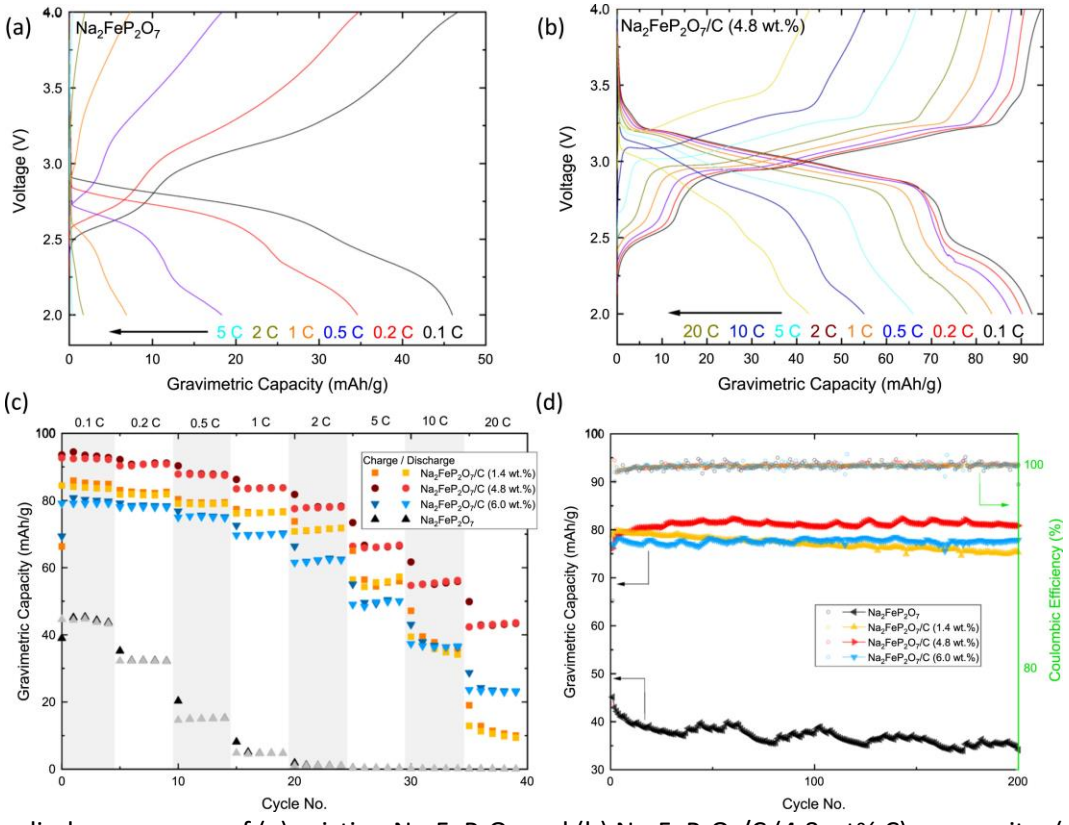

Charge-discharge curves of (a) pristine $Na_2FeP_2O_7$ and (b) $Na_2FeP_2O_7$/C (4.8 wt% C) composite; (c) rate capability of pristine and $Na_2FeP_2O_7$ and $Na_2FeP_2O_7$/C composites and (d) cycle performance of pristine $Na_2FeP_2O_7$ and $Na_2FeP_2O_7$/C composites.

Published in:
G. Kucinskis, I. Nesterova, A. Sarakovskis, L. Bikse, J. Hodakovska, G. Bajars, J. Alloys Compd. 895 (2022) 162656. DOI: 10.1016/j.jallcom.2021.162656.

Photocatalytic activity of TiO_2 coatings obtained at room temperature on a polymethyl methacrylate substrate

Mairis Iesalnieks[a], Raivis Eglītis[a], Tālis Juhna[b], Krišjānis Šmits[c], Andris Šutka[a]

[a] *Institute of Materials and Surface Engineering, Faculty of Materials Science and Applied Chemistry, Riga Technical University, P. Valdena Street 3/7, LV1048 Riga, Latvia*
[b] *Water Research and Environmental Biotechnology Laboratory, Faculty of Civil Engineering, Riga Technical University, Kipsalas Street 6a, LV1048 Riga, Latvia*
[c] *Institute of Solid-State Physics, University of Latvia, Kengaraga Street 8, LV1063 Riga, Latvia*

Titanium dioxide (TiO_2) coatings have a wide range of applications. Anatase exhibits hydrophilic, antimicrobial, and photocatalytic properties for the degradation of organic pollutants or water splitting. The main challenge is to obtain durable anatase nanoparticle coatings on plastic substrates by using straightforward approaches. In the present study, we revealed the preparation of a transparent TiO_2 coating on polymethylmethacrylate (PMMA), widely used for organic optical fibres as well as other polymer substrates such as polypropylene (PP), polystyrene (PS), and polycarbonate (PC). The films were spin-coated at room temperature without annealing; therefore, our approach can be used for thermo-sensitive substrates. The deposition was successful due to the use of stripped ultra-small (<4 nm) TiO_2 particles. Coatings were studied for the photocatalytic degradation of organic pollutants such as MB, methyl orange (MO), and rhodamine B (RB) under UV light. The TiO_2 coating on PMMA degraded over 80% of RB in 300 min under a 365 nm, 100 W mercury lamp, showing a degradation rate constant of 6×10^{-3} min^{-1}. The coatings were stable and showed no significant decrease in degradation activity even after five cycles.

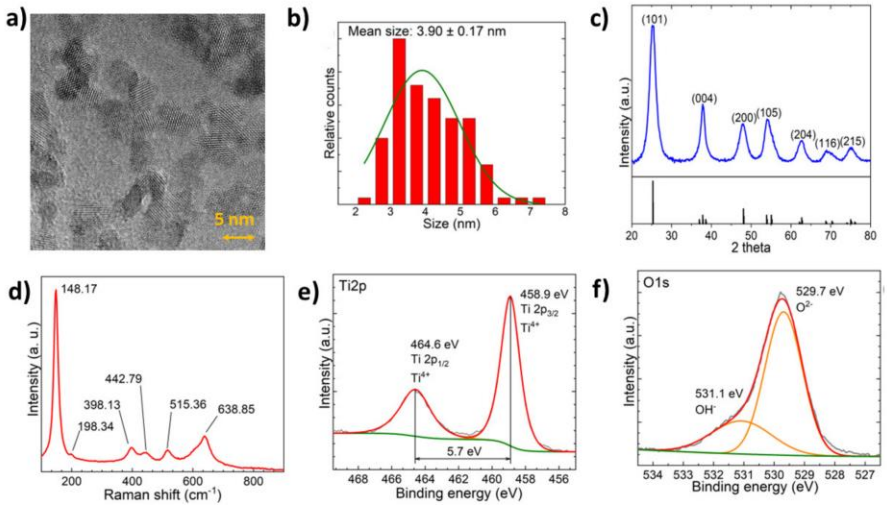

(a) TEM micrograph of the synthesised nanoparticles at 450,000× magnification. (b) Size distribution histogram for synthesised nanoparticles. (c) XRD diffractogram with JCPDS 21-1272 XRD data. (d) Raman spectra of TiO_2 nanoparticles. (e) High-resolution XPS of the Ti 2p peak with peak fitting. (f) High-resolution XPS of the O 1s peak with peak fitting.

Published in:
M. Iesalnieks, R. Eglītis, T. Juhna, K. Šmits, A. Šutka, Int. J. Mol. Sci. 23 (2022) 12936.
DOI: 10.3390/ijms232112936.

Enhanced electrochemical properties of $Na_{0.67}MnO_2$ cathode for Na-ion batteries prepared with novel tetrabutylammonium alginate binder

Gints Kucinskis[a], Beate Kruze[a], Prasad Korde[a,b], Anatolijs Sarakovskis[a], Arturs Viksna[c], Julija Hodakovska[a], Gunars Bajars[a]

[a] *Institute of Solid State Physics, University of Latvia, LV-1063 Riga, Latvia*
[b] *Department of Chemical Engineering, Division of Applied Electrochemistry, KTH Royal Institute of Technology, SE-10044 Stockholm, Sweden*
[c] *Department of Analytical Chemistry, Faculty of Chemistry, University of Latvia, LV-1004 Riga, Latvia*

Both the binder and solid–electrolyte interface play an important role in improving the cycling stability of electrodes for Na-ion batteries. In this study, a novel tetrabutylammonium (TBA) alginate binder is used to prepare a $Na_{0.67}MnO_2$ electrode for sodium-ion batteries with improved

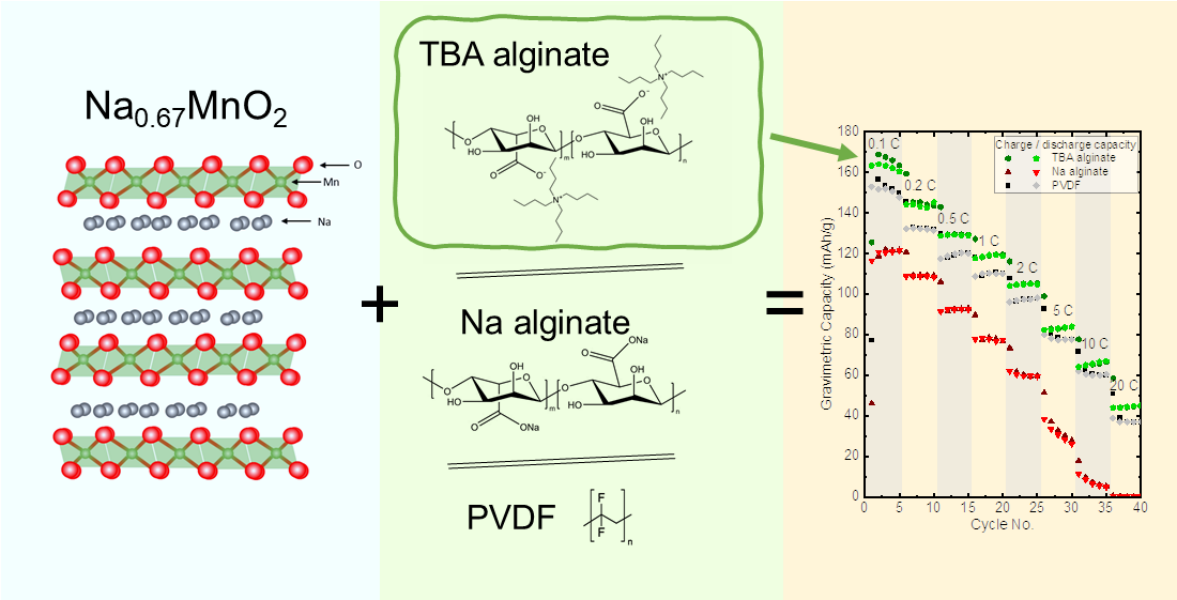

electrochemical performance.

The ageing of the electrodes is characterized. TBA alginate-based electrodes are compared to polyvinylidene fluoride- (PVDF) and Na alginate-based electrodes and show favorable electrochemical performance, with gravimetric capacity values of up to 164 mAh/g, which is 6% higher than measured for the electrode prepared with PVDF binder. TBA alginate-based electrodes also display good rate capability and improved cyclability. The solid–electrolyte interface of TBA alginate-based electrodes is similar to that of PVDF-based electrodes. As the only salt of alginic acid soluble in non-aqueous solvents, TBA alginate emerges as a good alternative to PVDF binder in battery applications where the water-based processing of electrode slurries is not feasible, such as the demonstrated case with $Na_{0.67}MnO_2$.

Published in:
G. Kucinskis, B. Kruze, P. Korde, A. Sarakovskis, A. Viksna, J. Hodakovska, G. Bajars, Batteries 8 (2022) 6. DOI: 10.3390/batteries8010006.

Bi_2Se_3 nanostructured thin films as perspective anodes for aqueous rechargeable lithium-ion batteries

Vitalijs Lazarenko[a], Yelyzaveta Rublova[a], Raimonds Meija[a], Jana Andzane[a], Vanda Voikiva[a], Artis Kons[a], Anatolijs Sarakovskis[b], Arturs Viksna[c], Donats Erts[a,c]

[a] *Institute of Chemical Physics, University of Latvia, Raina Blvd. 19, LV-1586 Riga, Latvia*
[b] *Institute of Solid State Physics, University of Latvia, Kengaraga Street 8, LV-1063 Riga, Latvia*
[c] *Faculty of Chemistry, University of Latvia, Raina Blvd. 19, LV-1586 Riga, Latvia*

In recent years, aqueous rechargeable lithium-ion batteries (ARLIBs) have attracted attention as an alternative technology for electrical storage. One of the perspective battery anode materials for application in ARLIBs is Bi_2Se_3, which has already shown good perspectives in the application of conventional lithium-ion batteries (LIBs) that use organic electrolytes.

In this study, the electrochemical properties of Bi_2Se_3 thin films with two different layers on the electrode surface — the solid electrolyte interphase (SEI) and the Bi_2Se_3 layer — were investigated. The results of this work show that the formation of the SEI layer on the surface of Bi_2Se_3 thin films ensures high diffusivity of Li+, high electrochemical stability, and high capacity up to 100 cycles, demonstrating the perspectives of Bi_2Se_3 as anode material for ARLIBs.

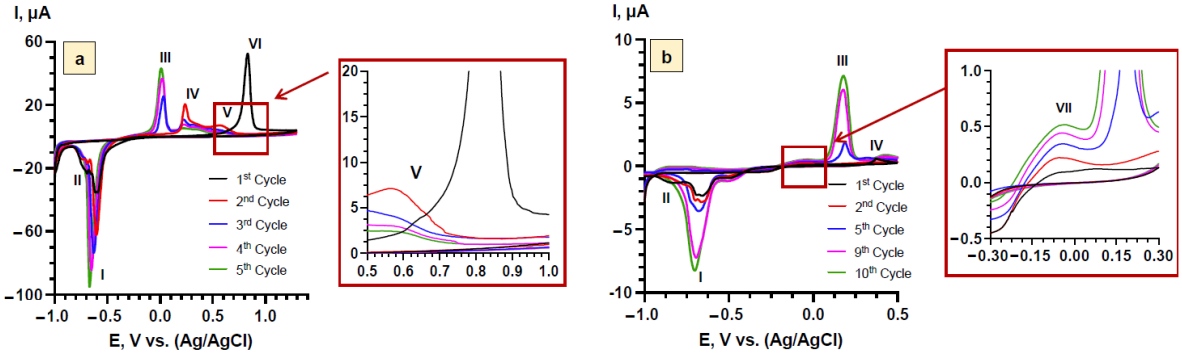

Cyclic voltammograms of Bi_2Se_3 thin films in 5 M $LiNO_3$ at the scan rates 0.25 mV s^{-1}: (a) samples with SEI layer (-1.0 V ÷ 1.3 V vs. Ag/AgCl), (b) samples with Bi_2Se_3 layer (-1.0 V ÷ 0.5 V vs. Ag/AgCl).

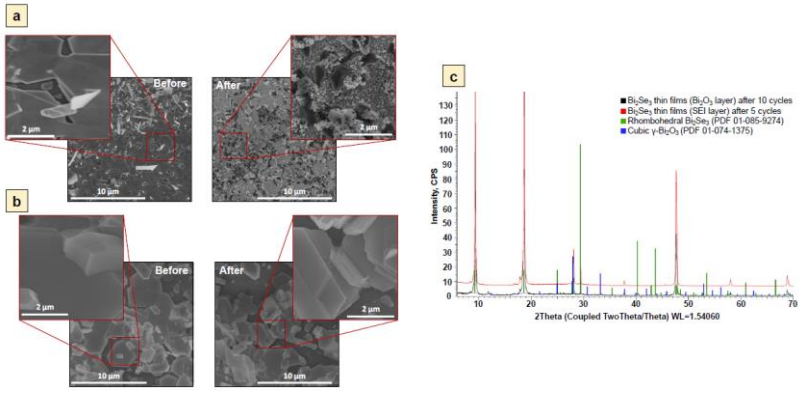

Scanning electron microscope images of Bi_2Se_3 thin films in 5 M $LiNO_3$ before and after cyclic voltammetry measurements for: (a) SEI layer after 5 cycles (-1.0 V ¸ 1.3 V), (b) Bi_2O_3 layer after 10 cycles (-1.0 V ¸ 0.5 V), (**c**) XRD pattern of samples with SEI layer after 5 cycles (-1.0 V ¸1.3 V) and Bi_2O_3 layer after 10 cycles (-1.0 V ¸ 0.5 V).

Published in:
V. Lazarenko, Y. Rublova, R. Meija, J. Andzane, V. Voikiva, A. Kons, A. Sarakovskis, A. Viksna, D. Erts, Batteries 8 (2022) 144. DOI: 10.3390/batteries8100144.

Impact of helium ion implantation dose and annealing on dense near-surface layers of NV centers

Andris Berzins[a], Hugo Grube[a], Einars Sprugis[b], Guntars Vaivars[b], Ilja Fescenko[a]

[a] *Laser Center, University of Latvia, LV-1004 Riga, Latvia*
[b] *Institute of Solid State Physics, University of Latvia, 8 Kengaraga Str., Riga LV-1063, Latvia*

The implantation of diamonds with helium ions has become a common method to create hundreds-nanometers-thick near-surface layers of NV centers for high-sensitivity sensing and imaging applications; however, optimal implantation dose and annealing temperature are still a matter of discussion. In this study, we irradiated HPHT diamonds with an initial nitrogen concentration of 100 ppm using different implantation doses of helium ions to create 200-nm thick NV layers. We compare a previously considered optimal implantation dose of ~10^{12} He^+/cm^2 to double and triple doses by measuring fluorescence intensity, contrast, and linewidth of magnetic resonances, as well as longitudinal and transversal relaxation times T_1 and T_2. From these direct measurements, we also estimate concentrations of P1 and NV centers. In addition, we compare the three diamond samples that underwent three consequent annealing steps to quantify the impact of processing at 1100 °C, which follows initial annealing at 800 °C. By tripling the implantation dose, we have increased the magnetic sensitivity of our sensors by 28 ± 5%. By projecting our results to higher implantation doses, we demonstrate that it is possible to achieve a further improvement of up to 70%. At the same time, additional annealing steps at 1100 °C improve the sensitivity only by 6.6 ± 2.7%.

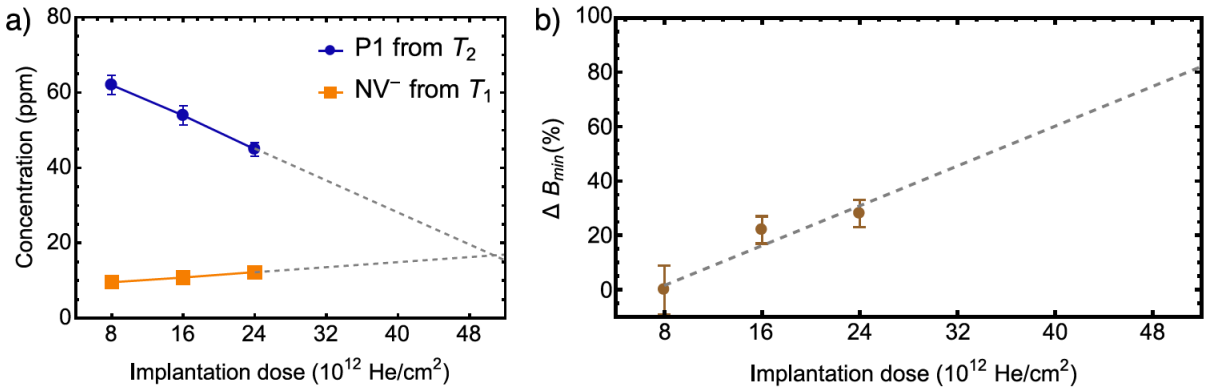

Projected values: (a) Linear extrapolations of P1 and NV^- concentrations to higher implantation doses. The optimal dose is expected at 0.5×10^{14} He^+/cm^2 where the P1 concentration is equal to the NV^- concentration. (b) The linear extrapolation to higher implantation doses of relative improvement of sensitivity (minimum detectable magnetic field B_{min}).

Published in:
A. Berzins, H. Grube, E. Sprugis, G. Vaivars, I. Fescenko, Nanomaterials 12 (2022) 2234.
DOI: 10.3390/nano12132234.

Study of the effect of two phases in Li_4SiO_4–Li_2SiO_3 ceramics on the strength and thermophysical parameters

Artem Kozlovskiy[a,b], Dmitriy I. Shlimas[a,b], Maxim V. Zdorovets[a,b], Aleksandra Moskina[c], Vladimir Pankratov[c], Anatoli I. Popov[a,c]

[a] *Engineering Profile Laboratory, L.N. Gumilyov Eurasian National University, Nur-Sultan 010000, Kazakhstan*
[b] *Laboratory of Solid State Physics, The Institute of Nuclear Physics of Republic of Kazakhstan, Almaty 050032, Kazakhstan*
[c] *Institute of Solid State Physics, University of Latvia, LV-1063 Riga, Latvia*

The study was devoted to the effect of Li_2SiO_3/Li_4SiO_4 phase formation in lithium-containing ceramics on the strength and thermophysical characteristics of lithium-containing ceramics, which have great prospects for use as blanket materials for tritium propagation. During the phase composition analysis of the studied ceramics using the X-ray diffraction method, it was found that an increase in the lithium component during synthesis leads to the formation of an additional orthorhombic Li_2SiO_3 phase, and the main phase in ceramics is the monoclinic Li_4SiO_4 phase. An analysis of the morphological features of the synthesized ceramics showed that an increase in the Li_2SiO_3 impurity phase leads to ceramic densification and the formation of impurity grains near grain boundaries and joints. During the determination of the strength characteristics of the studied ceramics, a positive effect of an increase in the Li_2SiO_3 impurity phase and dimensional factors on the strengthening and increase in the resistance to external influences during the compression of ceramics was established. During tests for resistance to long-term thermal heating, it was found that for two-phase ceramics, the decrease in strength and thermophysical characteristics after 500 h of annealing was less than 5%, which indicates a high resistance and stability of these ceramics in comparison with single-phase orthosilicate ceramics.

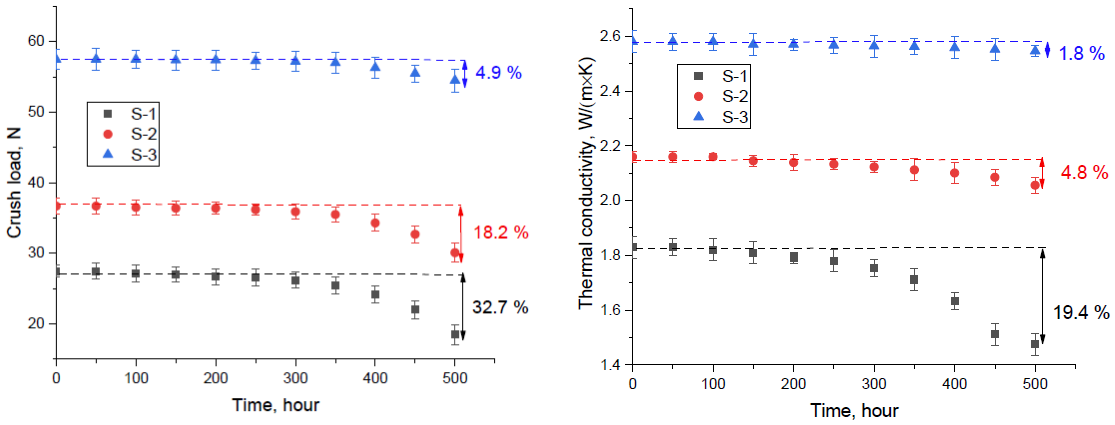

a) Results of the stability of crack resistance during long-term thermal heating; (b) the results of the change in the thermal conductivity coefficient depending on the time of thermal tests.

Published in:
A. Kozlovskiy, D.I. Shlimas, M.V. Zdorovets, A. Moskina, V. Pankratov, A.I. Popov, Nanomaterials 12 (2022) 3682. DOI: 10.3390/nano12203682.

Carbene-metal complexes as molecular scaffolds for construction of through-space thermally activated delayed fluorescence emitters

Armands Ruduss[a], Baiba Turovska[b], Sergey Belyakov[b], Kitija A. Stucere[c], Aivars Vembris[c], Kaspars Traskovskis[a]

[a] *Faculty of Materials Science and Applied Chemistry, Riga Technical University, P. Valdena Str. 3, LV-1048, Riga, Latvia*
[b] *Latvian Institute of Organic Synthesis, Aizkraukles Str. 21, Riga LV-1006, Latvia*
[c] *Institute of Solid State Physics, University of Latvia, Kengaraga Str. 8, LV-1063 Riga, Latvia*

The through-space charge transfer (CT) process is observed in Cu(I) carbene–metal–amide complexes, where conventional imidazole or imidazoline N-heterocyclic (NHC) carbene fragments act as inert linkers and CT proceeds between a metal-bound carbazole donor and a distantly situated carbene-bound phenylsulfonyl acceptor. The resulting electron transfer gives a rise to efficient thermally activated delayed fluorescence (TADF), characterized with high photoluminescence quantum yields (Φ_{PL} up to 90%) and radiative rates (k_r) up to 3.32 × 105 s^{-1}. The TADF process is aided by fast reverse intersystem crossing (rISC) rates of up to 2.56 × 107 s^{-1}. Such emitters can be considered as hybrids of two existing TADF emitter design strategies, combining low singlet–triplet energy gaps (ΔE_{ST}) met in all-organic exciplex-like emitters (0.0062–0.0075 eV) and small, but non-negligible spin–orbital coupling (SOC) provided by a Cu atom, like in TADF-active organometallic complexes.

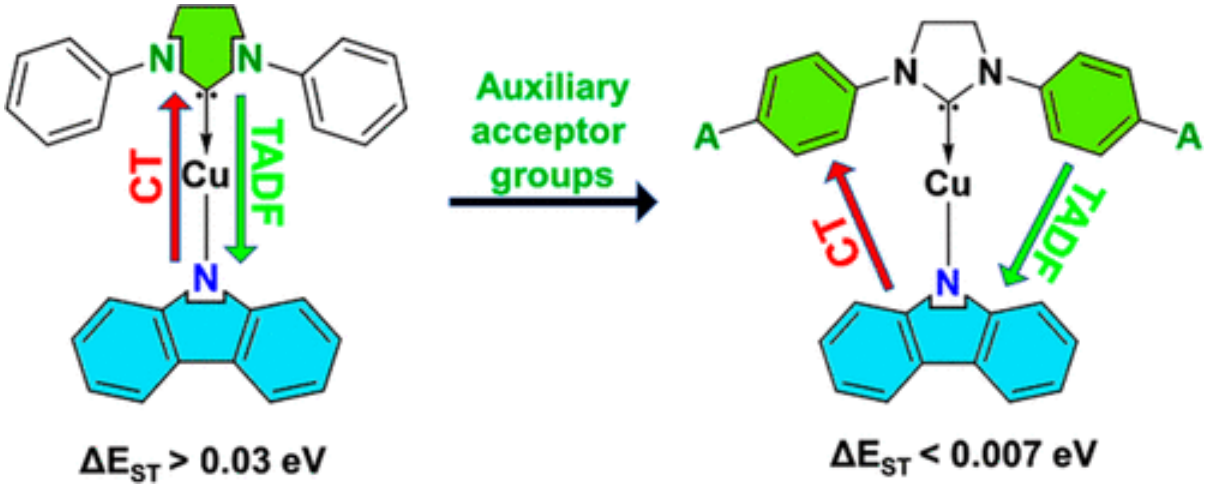

Published in:
A. Ruduss, B. Turovska, S. Belyakov, K.A. Stucere, A. Vembris, K. Traskovskis, Inorg. Chem. 61 (2022) 2174–2185. DOI: 10.1021/acs.inorgchem.1c03371.

Utilization of amorphous phase forming trityl groups and Ar-Ar^F interactions in the synthesis of NLO active azochromophores

Lauma Laipniece[a], Valdis Kampars[a], Sergey Belyakov[a,b], Arturs Bundulis[c], Andrejs Tokmakovs[c], Martins Rutkis[c]

[a] *Faculty of Materials Science and Applied Chemistry, Riga Technical University, P. Valdena 3/7, Riga, LV-1048, Latvia*
[b] *Latvian Institute of Organic Synthesis, Aizkraukles 21, Riga, LV-1006, Latvia*
[c] *Institute of Solid State Physics, University of Latvia, Kengaraga 8, Riga, LV-1063, Latvia*

New NLO active organic molecular glasses were synthesized based on push-pull azobenzene, which was dendronized with 3,5-bis[2-(trityloxy)ethoxy]benzoic acid and pentafluorophenyl groups were added to enhance thermal and NLO properties via Ar-Ar^F interactions. The configuration, where pentafluorophenyl groups containing dendronizing fragment was attached to the donor part of azochromophore, was very promising in our recent research, therefore trityl groups containing dendron was added to the acceptor part to rise the glass transition temperature of the amorphous compound. The effect of one or two pentafluorophenyl groups was investigated and about three times better NLO parameters were obtained when using one pentafluorophenyl group, as it has a greater possibility of NLO properties enchanting Ar-Ar^F interactions with neighboring molecules. A new convergent method was used to synthesize azobenzene core dendrimer fully functionalized with trityl end groups. Thermal, optical, and NLO properties were compared to previously reported results of dendrimer samples containing both hydroxyl and trityl groups. A full set of trityl end groups resulted in decreased NLO parameters and stability of poled order. Glass transition temperatures of all synthesized molecular glasses were 63–83 °C, and thermal destruction temperatures of all synthesized compounds were at least 250 °C. NLO coefficient d_{33} values were 14–73 pm·V^{-1}.

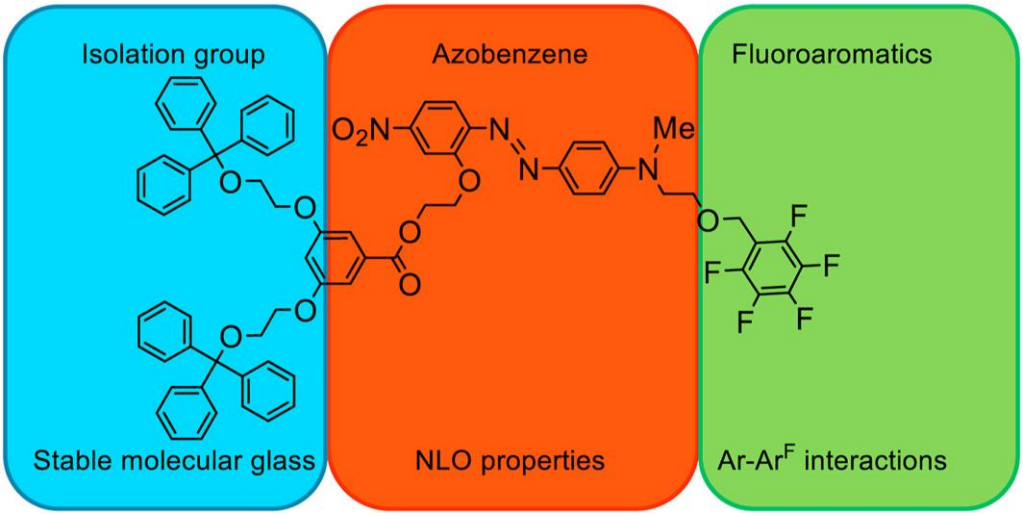

Published in:
L. Laipniece, V. Kampars, S. Belyakov, A. Bundulis, A. Tokmakovs, M. Rutkis, Dyes and Pigments 204 (2022) 110395. DOI: 10.1016/j.dyepig.2022.110395.

Bis(N-naphthyl-N-phenylamino)benzophenones as exciton-modulating materials for white TADF OLEDs with separated charge and exciton recombination zones

Malek Mahmoudi[a], Jonas Keruckas[a], Dmytro Volyniuk[a], Viktorija Andrulevičienė[a], Rasa Keruckienė[a], Edgaras Narbutaitis[a], Yu-Chiang Chao[b], Martins Rutkis[c], Juozas V. Grazulevicius[a]

[a] *Department of Polymer Chemistry and Technology, Kaunas University of Technology, Baršausko Str. 59, LT-51423, Kaunas, Lithuania*
[b] *Department of Physics, National Taiwan Normal University, 88, Sec.4, Ting-Chou Rd., Taipei, 116, Taiwan*
[c] *Institute of Solid State Physics, University of Latvia, 8 Kengaraga St., Riga, LV-1063, Latvia*

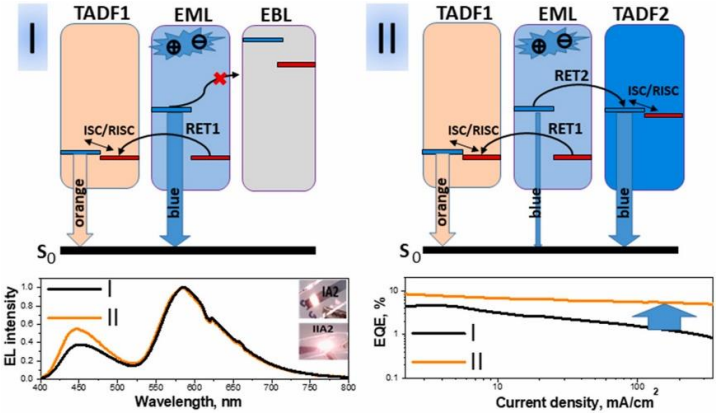

Organic semiconductors were employed as exciton modulators, blue emitters, hole-transporting materials, and hosts with resonant-appropriate singlet and triplet energies for efficient and stable white organic light-emitting diodes (OLEDs). Two 4,4'-bis(N-naphthyl-N-phenylamino)benzophenones were synthesized using isomeric N-naphthyl-N-phenylamines as the donors and benzophenone as the acceptor moiety. The molecular design of new compounds allowed to obtain the required combination of properties, i.e. blue prompt fluorescence in the solid state with singlet energies close to those of the selected blue emitter exhibiting thermally activated delayed fluorescence (TADF), low triplet energies of 2.32 and 2.45 eV which are close to those of orange TADF emitter, good charge injecting properties (ionization potentials of 5.68 and 5.79 eV), a good charge transporting properties with hole mobilities exceeding 10−4 cm^2 $(V\ s)^{-1}$ and high thermal stability with five percent weight loss temperatures up to 428 °C. The blue-emitting compounds were used as exciton modulators between the known blue and orange TADF emitters for the fabrication of white OLEDs exploiting spatial exciton allocation strategy. In the frame of this strategy, resonant energy transfers: NPABP emitters → blue TADF and NPABP emitters → orange TADF emitters were investigated using different device structures towards efficient white electroluminescence. About twice higher external quantum efficiency was obtained for devices with two resonant energy transfers in comparison to that of the reference devices with one resonant energy transfer proving the efficiency of spatial exciton allocation strategy for white TADF OLEDs. The best quality of white electroluminescence is characterized by CIE coordinates of (0.32, 0.31), colour temperature of 4490 K and colour rendering index of 80. Similar stability of blue and orange emission bands in white electroluminescence spectra was achieved due to the separation of charge and exciton recombination zones in the device structure.

Published in:
M. Mahmoudi, J. Keruckas, D. Volyniuk, V. Andrulevičienė, R. Keruckienė, E. Narbutaitis, Y.-C. Chao, M. Rutkis, J. V. Grazulevicius, Dyes and Pigments 197 (2022) 109868. DOI: 10.1016/j.dyepig.2021.109868.

Dicyanomethylene-functionalized s-indacene-based D-π-A-π-D dyes exhibiting large near-infrared two-photon absorption cross-section

Arnis Zagata[a], Kaspars Traskovskis[a], Sergey Belyakov[b], Igors Mihailovs[c], Arturs Bundulis[c], Martins Rutkis[c]

[a] *Faculty of Materials Science and Applied Chemistry, Riga Technical University, P. Valdena Str. 3, LV-1048, Riga, Latvia*
[b] *Latvian Institute of Organic Synthesis, Aizkraukles Str. 21, Riga, LV-1006, Latvia*
[c] *Institute of Solid State Physics, University of Latvia, Kengaraga Str. 8, LV-1063, Riga, Latvia*

A series of centrosymmetric chromophores with D-π-A-π-D molecular architecture has been synthesized and characterized with respect to their third-order nonlinear optical (NLO) properties. The investigated compounds feature novel central electron acceptor fragments composed of derivatives of s-indacene-1,3,5,7(2H,6H)-tetraone (Janus dione), in which the carbonyls have been substituted by either two or four dicyanomethylene groups. Due to the increased electron acceptor strength, up to twofold increase in two-photon absorption (2 PA) cross-section is observed for the dyes in comparison to the structural analogues based on the parent compound. The best performing dye exhibits intensive 2 PA absorption band in 1000–1300 nm range with a peak cross-section value of 11,000 GM. Optical limiting was successfully demonstrated using the compound, marking the presented chemical design as a promising direction for optical power-limiting applications in the important near-infrared (NIR) spectral region.

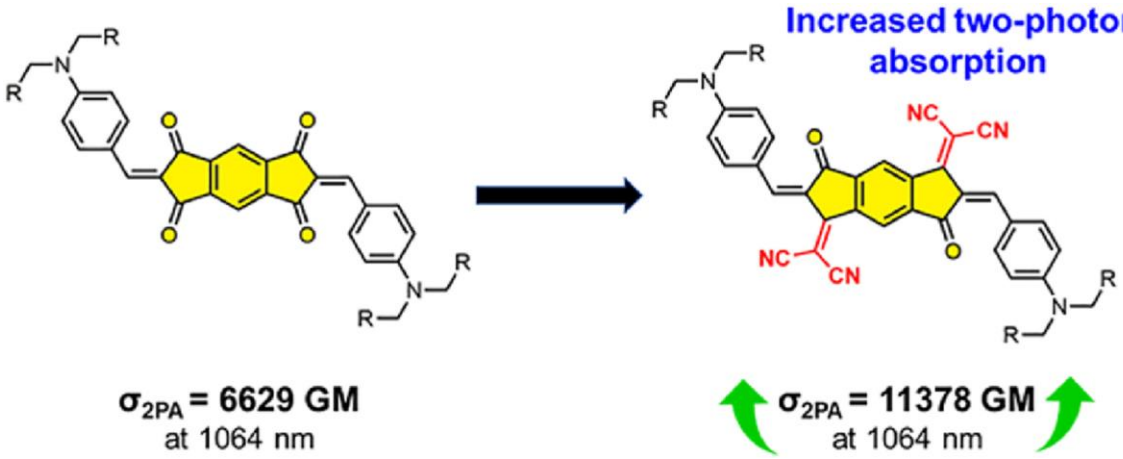

Published in:
A. Zagata, K. Traskovskis, S. Belyakov, I. Mihailovs, A. Bundulis, M. Rutkis, Dyes and Pigments 208 (2022) 110864. DOI: 10.1016/j.dyepig.2022.110864.

Synthesis, structural and luminescent properties of Mn-doped calcium pyrophosphate ($Ca_2P_2O_7$) polymorphs

Diana Griesiute[a], Edita Garskaite[b], Andris Antuzevics[c], Vytautas Klimavicius[d], Vytautas Balevicius[d], Aleksej Zarkov[a], Arturas Katelnikovas[a], Dick Sandberg[b], Aivaras Kareiva[a]

[a] *Institute of Chemistry, Vilnius University, Naugarduko 24, 03225 Vilnius, Lithuania*
[b] *Wood Science and Engineering, Department of Engineering Sciences and Mathematics, Luleå University of Technology, Forskargatan 1, 931 87 Skellefteå, Sweden*
[c] *Institute of Solid State Physics, University of Latvia, Kengaraga 8, Riga 1063, Latvia*
[d] *Institute of Chemical Physics, Vilnius University, Sauletekio 3, 10257 Vilnius, Lithuania*

In the present work, three different Mn^{2+}-doped calcium pyrophosphate (CPP, $Ca_2P_2O_7$) polymorphs were synthesized by wet co-precipitation method followed by annealing at different temperatures. The crystal structure and purity were studied by powder X-ray diffraction (XRD), Fourier-transform infrared (FTIR), solid-state nuclear magnetic resonance (SS-NMR), and electron paramagnetic resonance (EPR) spectroscopies. Scanning electron microscopy (SEM) was used to investigate the morphological features of the synthesized products. Optical properties were investigated using photoluminescence measurements. Excitation spectra, emission spectra, and photoluminescence decay curves of the samples were studied. All Mn-doped polymorphs exhibited a broadband emission ranging from approximately 500 to 730 nm. The emission maximum was host-dependent and centered at around 580, 570, and 595 nm for γ-, β-, and α-CPP, respectively.

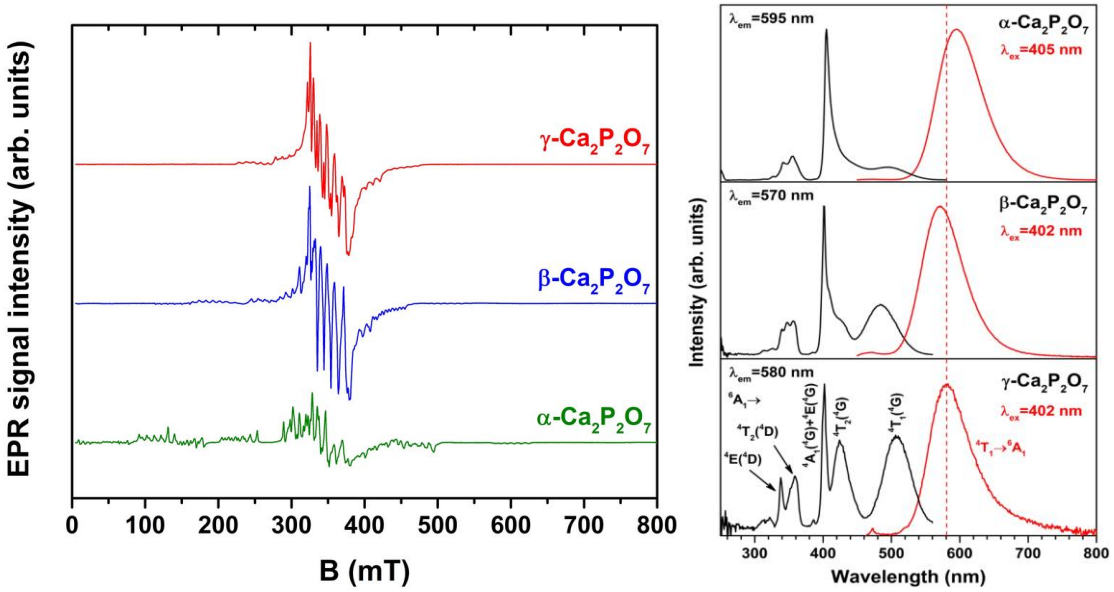

Left: Experimental X-band EPR spectra of calcium phosphate samples.
Right: Excitation and emission spectra of Mn-doped CPP polymorphs.

Published in:
D. Griesiute, E. Garskaite, A. Antuzevics, V. Klimavicius, V. Balevicius, A. Zarkov, A. Katelnikovas, D. Sandberg, A. Kareiva, Scientific Reports 12 (2022) 7116. DOI: 10.1038/s41598-022-11337-y.

Antiviral efficacy of cerium oxide nanoparticles

Alexandra Nefedova[a], Kai Rausalu[b], Eva Zusinaite[b], Alexander Vanetsev[a], Merilin Rosenberg[c,d], Kairi Koppel[c], Stevin Lilla[a], Meeri Visnapuu[a], Krisjanis Smits[e], Vambola Kisand[a], Tanel Tätte[a], Angela Ivask[c]

[a] *Institute of Physics, University of Tartu, W. Ostwaldi Street 1, 50411 Tartu, Estonia*
[b] *Institute of Technology, University of Tartu, Nooruse Street 1, 50411 Tartu, Estonia*
[c] *Institute of Molecular and Cell Biology, University of Tartu, Riia Street 23, 51010 Tartu, Estonia*
[d] *Department of Chemistry and Biotechnology, Tallinn University of Technology, Akadeemia Street 15, 12618 Tallinn, Estonia*
[e] *Institute of Solid State Physics, University of Latvia, Kengaraga Street 8, Riga 1063, Latvia*

Nanomaterials are prospective candidates for the elimination of viruses due to their multimodal mechanisms of action. Here, we tested the antiviral potential of a largely unexplored nanoparticle of cerium dioxide (CeO_2). Two nano-CeO_2 with opposing surface charge, (+) and (−), were assessed for their capability to decrease the plaque forming units (PFU) of four enveloped and two non-enveloped viruses during 1-h exposure. Statistically significant antiviral activity towards enveloped coronavirus SARS-CoV-2 and influenza virus was registered already at 20 mg Ce/l. For the other two enveloped viruses, transmissible gastroenteritis virus and bacteriophage ϕ6, antiviral activity was evidenced at 200 mg Ce/l. As expected, the sensitivity of non-enveloped viruses towards nano-CeO_2 was significantly lower. EMCV picornavirus showed no decrease in PFU until the highest tested concentration, 2000 mg Ce/l and MS2 bacteriophage showed a slight non-monotonic response to high concentrations of nano-CeO2(−). Parallel testing of the antiviral activity of Ce^{3+} ions and SiO_2 nanoparticles allows concluding that nano-CeO_2 activity was neither due to released Ce-ions nor the nonspecific effects of nanoparticles. Moreover, we evidenced higher antiviral efficacy of nano-CeO_2 compared with Ag nanoparticles. This result along with low antibacterial activity and non-existent cytotoxicity of nano-CeO_2 allow us to propose CeO_2 nanoparticles for specific antiviral applications.

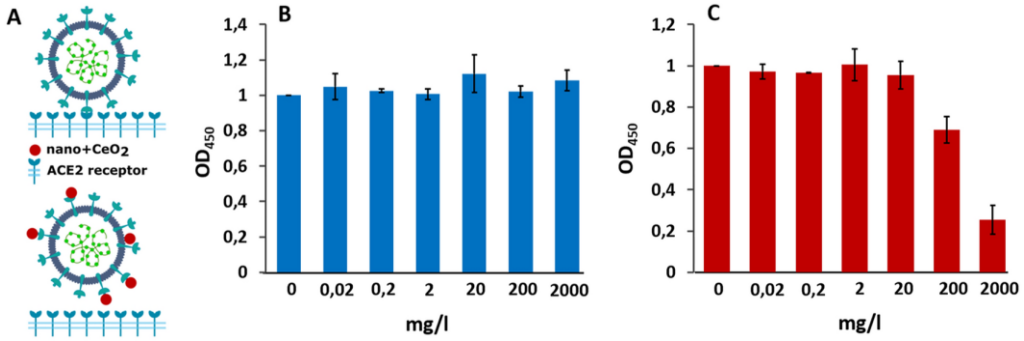

Schematics of the experiment (A), where the upper part shows SARS-CoV-2 binding to ACE2 receptor without nanoparticles and lower part demonstrates the theoretical inhibition of SARS-CoV2 binding to ACE2 receptor by of CeO_2 nanoparticles. (B) Shows the effect of nano-CeO_2(+) and (C) the effect of nano-CeO_2(−) particles on binding of SARS-CoV-2 onto ACE2 receptor in an ELISA assay, measured as optical density (OD450).

Published in:
A. Nefedova, K. Rausalu, E. Zusinaite, A. Vanetsev, M. Rosenberg, K. Koppel, S. Lilla, M. Visnapuu, K. Smits, V. Kisand, T. Tätte, A. Ivask, Scientific Reports 12 (2022) 18746. DOI: 10.1038/s41598-022-11337-y.

Publications
with the authorship of ISSP UL in
Web of Science and Scopus Databases

[1] S. Al Saedi, A. Burkhanov, K. Bormanis, Repolarization processes in lead-free KNN ceramics, Ferroelectrics 591 (2022) 1–6.

[2] D. Ananchenko, S. Nikiforov, K. Sobyanin, S. Konev, A. Dauletbekova, G. Akhmetova-Abdik, A. Akilbekov, A. Popov, Paramagnetic defects and thermoluminescence in irradiated nanostructured monoclinic zirconium dioxide, Materials 15 (2022) 8624.

[3] J. Andzane, A. Felsharuk, K. Buks, A. Sarakovskis, K. Niherysh, J. Gabrusenoks, D. Erts, Synthesis and properties of bismuth selenide based nanolaminates for application in thermoelectrics, Advanced Materials Interfaces 9 (2022) 2200385.

[4] L. Ansone-bertina, V. Ozols, L. Arbidans, L. Dobkevica, K. Sarsuns, E. Vanags, M. Klavins, Metal–organic frameworks (MOFs) containing adsorbents for carbon capture, Energies 15 (2022) 3473.

[5] A. Antuzevics, G. Krieke, G. Doke, B. Berzina, The origin of bright cyan persistent luminescence in $Ca_2SnO_4:La^{3+}$, Materialia 21 (2022) 101374.

[6] A. Antuzevics, A. Zarins, A. Ansone, J. Cipa, G. Kizane, J. Leys, R. Knitter, Thermal properties of paramagnetic radiation-induced defects in lithium orthosilicate containing breeder material, Journal of Nuclear Materials 565 (2022) 153713.

[7] I. Aulika, M. Zubkins, J. Butikova, J. Purans, Enhanced reflectivity change and phase shift of polarized light: double parameter multilayer sensor, Physica Status Solidi (A) Applications and Materials Science 219 (2022) 2100424.

[8] G. Bakradze, A. Kuzmin, Octahedral tilting in homologous perovskite series $CaMoO_3$-$SrMoO_3$-$BaMoO_3$ probed by temperature-dependent EXAFS spectroscopy, Materials 15 (2022) 7619.

[9] G. Bakradze, A. Kalinko, A. Kuzmin, Chemical-state analyses of Ni, Zn, and W ions in $NiWO_4$–$ZnWO_4$ solid solutions by X-ray photoelectron spectroscopy, Journal of Physics and Chemistry of Solids 161 (2022) 110425.

[10] B. Berzina, R. Ruska, J. Cipa, L. Trinkler, A. Sarakovskis, J. Grabis, Steins, Luminescence of AlN:Eu ceramics: Properties and mechanisms, Optical Materials 127 (2022) 112217.

[11] A. Berzins, H. Grube, E. Sprugis, G. Vaivars, I. Fescenko, Impact of helium ion implantation dose and annealing on dense near-surface layers of NV centers, Nanomaterials 12 (2022) 2234.

[12] E. Blumbergs, V. Serga, A. Shishkin, D. Goljandin, A. Shishko,V. Zemcenkovs, K. Markus, J. Baronins, V. Pankratov, Selective disintegration–milling to obtain metal-rich particle fractions from E-waste, Metals 12 (2022) 1468.

[13] D. Bocharov, A. Chesnokov, G. Chikvaidze, J. Gabrusenoks, R. Ignatans, R. Kalendarev, M. Krack, K. Kundzins, A. Kuzmin, N. Mironova-Ulmane, I. Pudza, L. Puust, I. Sildos, E. Vasil'chenko, M. Zubkins, J. Purans, A comprehensive study of structure and properties of nanocrystalline zinc peroxide, Journal of Physics and Chemistry of Solids 160 (2022) 110318.

[14] M. Bozorgchenani, G. Kucinskis, M. Wohlfahrt-Mehrens, T. Waldmann, Experimental confirmation of C-rate dependent minima shifts in arrhenius plots of Li-ion battery aging, Journal of the Electrochem- ical Society 169 (2022) 030509.

[15] M. Brik, A. Srivastava, A. Popov, A few common misconceptions in the interpretation of experimental spectroscopic data, Optical Materials 127 (2022) 112276.

[16] K. Buks, J. Andzane, L. Bugovecka, M. Katkov, K. Smits, O. Starkova, J. Katkevics, A. Bērziņš, L. Brauna, V. Voikiva, D. Erts, Highly efficient flexible n-Type thermoelectric films formed by encapsulation of Bi_2Se_3-MWCNT hybrid networks in polyvinyl alcohol, Advanced Materials Interfaces 9 (2022) 2200318.

[17] A. Burkhanov, S. Al Saedi, K. Bormanis, Photoelectric properties of KNN ceramics, Ferroelectrics 591 (2022) 26–32.

[18] E. Butanovs, K. Kadiwala, A. Gopejenko, D. Bocharov, S. Piskunov, B. Polyakov, Different strategies for GaN-MoS_2 and GaN-WS_2 core–shell nanowire growth, Applied Surface Science 590 (2022) 153106.

[19] E. Butanovs, L. Dipane, A. Zolotarjovs, S. Vlassov, B. Polyakov, Preparation of functional Ga_2S_3 and Ga_2Se_3 shells around Ga_2O_3 nanowires via sulfurization or selenization, Optical Materials 131 (2022) 112675.

[20] E. Butanovs, A. Kuzmin, A. Zolotarjovs, S. Vlassov, B. Polyakov, The role of Al_2O_3 interlayer in the synthesis of ZnS/Al_2O_3/MoS_2 core-shell nanowires, Journal of Alloys and Compounds 918 (2022) 165648.

[21] X. Chen, G. Nusinovich, O. Dumbrajs, H. Xiao, X. Han, D. Xia, T. Peng, Mode excitation in gyrotrons with triode-type electron guns, IEEE Transactions on Electron Devices 69 (2022) 785–791.

[22] K. Cherednichenko, V. Mukhanov, A. Kalinko, V. Solozhenko, High-pressure synthesis of boron-rich chalcogenides $B_{12}S$ and $B_{12}Se$, Journal of Alloys and Compounds 898 (2022) 162874.

[23] A. Dauletbekova, A. Akylbekova, G. Sarsekhan, A. Usseinov, Z. Baimukhanov, A. Kozlovskiy, L. Vlasukova, F. Komarov, A. Popov, A. Akilbekov, Ion-track template synthesis and characterization of $ZnSeO_3$ nanocrystals, Crystals 12 (2022) 817.

[24] L. Dimitrocenko, G. Strikis, B. Polyakov, L. Bikse, S. Oras, E. Butan- ovs, The Effect of a Nucleation Layer on Morphology and Grain Size in MOCVD-Grown β-Ga_2O_3 Thin Films on C-Plane Sapphire, Materials 15 (2022) 8362.

[25] G. Doke, A. Antuzevics, G. Krieke, A. Kalnina, A. Sarakovskis, Novel broadband near-infrared emitting long afterglow phosphor $MgGeO_3:Cr^{3+}$, Journal of Alloys and Compounds 918 (2022) 165768.

[26] G. Doke, A. Kalnina, J. Cipa, M. Springis, A. Sarakovskis, Optical properties of near infrared persistent phosphor $CaZnGe_2O_6$: Cr^{3+}, M^{3+} (M^{3+} = B^{3+}; Al^{3+}; Ga^{3+}), Solid State Communications 354 (2022) 114894.

[27] M. Dunce, E. Birks, L. Bikse, R. Ignatans, A. Fuith, H. Kabelka, E. Nitiss, M. Kundzins, A. Sternberg, Novel approach in analyzing phase transitions in $Na_{0.5}Bi_{0.5}TiO_3$-Comparison with $0.95Na_{0.5}Bi_{0.5}TiO_3$-$0.05CaTiO_3$, Journal of Applied Physics 131 (2022) 224101.

[28] M. Dunce, E. Birks, M. Antonova, L. Bikse, K. Kundzins, O. Freimanis, M. Livins, S. Dutkevica, A. Sternberg, Composition and microstructure of $Na_{0.5}Bi_{0.5}TiO_3$ ceramics with excess Bi, Journal of the American Ceramic Society 105 (2022) 3874–3884.

[29] O. Eberlins, E. Birks, M. Antonova, M. Kundzins, M. Livins, A. Sternberg, Electrocaloric Effect in (1x)($0.8Na_{0.5}Bi_{0.5}TiO_3$-$0.2BaTiO_3$)x$CaTiO_3$ Solid Solutions at High Electric Fields, Crystals 12 (2022) 134.

[30] R. Eglitis, A. Popov, J. Purans, D. Bocharov, Y. Mastrikov, R. Jia, S. Kruchinin, Ab initio computations of $BaZrO_3$, $CaTiO_3$, $SrTiO_3$ perovskite as well as WO_3 and ReO_3(001) surfaces, Low Temperature Physics 48 (2022) 811–818.

[31] R. I. Eglitis, S. Piskunov, A. I. Popov, J. Purans, D. Bocharov, R. Jia, Systematic trends in hybrid-DFT computations of $BaTiO_3/SrTiO_3$, $PbTiO_3/SrTiO_3$ and $PbZrO_3/SrZrO_3$ (001) hetero structures, Condensed Matter 7 (2022) 70.

[32] R. Eglitis, J. Purans, A. Popov, D. Bocharov, A. Chekhovska, R. Jia, Ab Initio Computations of O and AO as well as ReO_2, WO_2 and BO_2-Terminated ReO_3, WO_3, $BaTiO_3$, $SrTiO_3$ and $BaZrO_3$ (001) Surfaces, Symmetry 14 (2022) 1050.

[33] R. Eglitis, E. Kotomin, A. Popov, S. Kruchinin, R. Jia, Comparative ab initio calculations of $SrTiO_3$, $BaTiO_3$, $PbTiO_3$, and $SrZrO_3$(001) and (111) surfaces as well as oxygen vacancies, Low Temperature Physics 48 (2022) 80–88.

[34] E. Einbergs, A. Zolotarjovs, I. Bite, V. Vītola, A. Spustaka, G. Tunēns, A. Arnautov, A mechanoluminescence based approach to spatial mechanical stress visualisation of additively manufactured (3D printed) parts, Materialia 24 (2022) 101516.

[35] E. Einbergs, A. Zolotarjovs, Programmable material testing device for mechanoluminescence measurements, HardwareX 12 (2022) e00349.

[36] K. El-Kelany, F. Pascale, A. Platonenko, A. Ferrari, R. Dovesi, Quantum mechanical simulation of various phases of KVF_3 perovskite, Journal of Physics Condensed Matter 34 (2022) 285401.

[37] E. Elsts, A. Supe, S. Spolitis, K. Zakis, S. Olonkins, A. Udalcovs, R. Murnieks, U. Senkans, D. Prigunovs, L. Gegere, K. Draguns, I. Lukosevics, O. Ozolins, J. Grube, V. Bobrovs, Fibre optical coupler simulation by COMSOL multiphysics software, Latvian Journal of Physics and Technical Sciences 59 (2022) 3–14.

[38] D. Erts, J. Katkevics, M. Sjomkane, J. Andzane, A. Sarakovskis, K. Smits, A. Viksna, Y. Rublova, R. Meija, EIS characterization of aging and humidity-related behavior of Bi_2Se_3 films of different morphologies, Nano-Structures and Nano-Objects 30 (2022) 100847.

[39] R. Ganeev, V. Kim, I. Shuklov, V. Popov, N. Lavrentyev, V. Ponomarenko, A. Mardini, D. Dyomkin, T. Milenkovič, A. Bundulis, J. Grube, A. Sarakovskis, Third harmonic generation in the thin films containing quantum dots and exfoliated nanoparticles, Applied Physics B: Lasers and Optics 128 (2022) 202.

[40] T. Garmysheva, A. Nepomnyashchikh, A. Shalaev, E. Kaneva, A. Paklin, K. Chernenko, A. Kozlova, V. Pankratov, R. Shendrik, Luminescence of ODC(II) in quartz and cristobalite glasses, Journal of Non-Crystalline Solids 575 (2022) 121199.

[41] V. Gerbreders, M. Krasovska, I. Mihailova, E. Sledevskis, A. Ogurcovs, E. Tamanis, V. Auksmuksts, A. Bulanovs, V. Mizers, Morphology influence on wettability and wetting dynamics of ZnO nanostructure arrays, Latvian Journal of Physics and Technical Sciences 59 (2022) 30–43.

[42] P. Gismondi, A. Kuzmin, C. Unsworth, S. Rangan, S. Khalid, D. Saha, Understanding the adsorption of rare-earth elements in oligo-grafted mesoporous carbon, Langmuir 38 (2022) 203–210.

[43] T. Glaskova-Kuzmina, L. Stankevics, S. Tarasovs, J. Sevcenko, V. Spacek, A. Sarakovskis, A. Zolotarjovs, K. Shmits, A. Aniskevich, Effect of core-shell rubber nanoparticles on the mechanical

properties of epoxy and epoxy-based CFRP, Materials 15 (2022) 7502.

[44] T. Glaskova-Kuzmina, D. Dejus, J. Jatnieks, P.-P. Kruuv, L. Lancere, S. Kobenko, A. Sarakovskis, A. Zolotarjovs, Flame-retardant and tensile properties of polyamide 12 processed by selective laser sintering, Journal of Composites Science 6 (2022) 185.

[45] M. Gorev, V. Bondarev, I. Flerov, K. Bormanis, E. Birks, T-E phase diagrams and electrocaloric effect in PNN-PT solid solutions, Journal of Alloys and Compounds 927 (2022) 167032.

[46] E. Gorokhova, O. Dymshits, I. Venevtsev, L. Basyrova, I. Alekseeva, A. Khubetsov, M. Baranov, M. Tsenter, A. Zhilin, S. Eron'ko, E. Oreschenko, F. Muktepavela, K. Kundzins, P. Loiko, ZnO–Yb_2O_3 composite optical ceramics: Synthesis, structure and spectral-luminescent properties, Journal of the European Ceramic Society 42 (2022) 616–630.

[47] D. Griesiute, E. Garskaite, A. Antuzevics, V. Klimavicius, V. Balevicius, A. Zarkov, A. Katelnikovas, D. Sandberg, A. Kareiva, Synthesis, structural and luminescent properties of Mn-doped calcium pyrophosphate ($Ca_2P_2O_7$) polymorphs, Scientific Reports 12 (2022) 7116.

[48] J. Grube, Up-conversion luminescence processes in $NaLaF_4$ doped with Tm^{3+} and Yb^{3+} and dependence on Tm^{3+} concentration and temperature, Applied Spectroscopy 76 (2022) 189–198.

[49] R. Grzibovskis, A. Ruduss, A. Polaks, The relation between photoconductivity threshold and open-circuit voltage in organic solar cells, Latvian Journal of Physics and Technical Sciences 59 (2022) 21–29.

[50] M. Iesalnieks, R. Eglıtis, T. Juhna, K.S. Šmits, A. Šutka, Photocatalytic activity of TiO_2 coatings obtained at room temperature on a polymethyl methacrylate substrate, International Journal of Molecular Sciences 23 (2022) 12936.

[51] E. Jansons, J. Lungevics, U. Kanders, A. Leitans, G. Civcisa, O. Linins, K. Kundzins, I. Boiko, Tribological and mechanical properties of the nanostructured superlattice coatings with respect to surface texture, Lubricants 10 (2022) 285.

[52] L. Jasulaneca, R. Meija, E. Kauranens, R. Sondors, J. Andzane, R. Rimsa, G. Mozolevskis, D. Erts, Cryogenic nanoelectromechanical switch enabled by Bi_2Se_3 nanoribbons, Materials Science and Engineering B: Solid-State Materials for Advanced Technology 275 (2022) 115510.

[53] I. Jogi, J. Ristkok, J. Raud, J. Butikova, K. Mizohata, P. Paris, Laser induced breakdown spectroscopy for hydrogen detection in molybdenum at atmospheric pressure mixtures of argon and nitrogen, Fusion Engineering and Design 179 (2022) 113131.

[54] N. Juneja, S. Mandati, A. Katerski, N. Spalatu, S. Daskeviciute-Geguziene, A. Vembris, S. Karazhanov, V. Getautis, M. Krunks, Oja Acik, Sb_2S_3 solar cells with a cost-effective and dopant-free fluorene-based enamine as a hole transport material, Sustainable Energy and Fuels 6 (2022) 3220–3229.

[55] M. Jurjans, L. Bikse, E. Birks, Svirskas, M. Antonova, M. Kundzins, A. Sternberg, Electromechanical properties in $CaTiO_3$ modified $Na_{0.5}Bi_{0.5}TiO_3$-$BaTiO_3$ solid solutions above morphotropic phase boundary, AIP Advances 12 (2022) 035124.

[56] K. Kadiwala, E. Butanovs, A. Ogurcovs, M. Zubkins, B. Polyakov, Comparative study of WSe_2 thin films synthesized via pre-deposited WO_3 and W precursor material selenization, Journal of Crystal Growth 593 (2022) 126764.

[57] Z. Karipbayev, K. Kumarbekov, I. Manika, A. Dauletbekova, A. Kozlovskiy, D. Sugak, S. Ubizskii, A. Akilbekov, Y. Suchikova, A. Popov, Optical, Structural, and Mechanical Properties of $Gd_3Ga_5O_{12}$ Single Crystals Irradiated with $^{84}Kr^{+}$ Ions, Physica Status Solidi (B) Basic Research 259 (2022) 2100415.

[58] V. Kavaliuke, I. Nesterova, A. Kezionis, S. Balciunas, G. Bajars, T. Salkus, G. Kucinskis, Combined conductivity and electrochemical impedance spectroscopy study of $Na_2FeP_2O_7$ cathode material for sodium ion batteries, Solid State Ionics 385 (2022) 116024.

[59] J. Kavaliauskaitė, A. Kazlauskaitė, J. Lazutka, G. Mozolevskis, A. Stirkė, Pulsed electric fields alter expression of NF-kB promoter-controlled gene, International Journal of Molecular Sciences 23 (2022) 451.

[60] Y. Kazarinov, O. Pop, I. Megela, A. Popov, effect of electron irradiation conditions on the efficiency of defect formation in $MgAl_2O_4$ spinel, Problems of Atomic Science and Technology (2022) 25–28

[61] M. Kemere, A. Antuzevics, P. Rodionovs, U. Rogulis, A. Sarakovskis, Photoluminescence and electron paramagnetic resonance studies of Mn^{2+} doped $CaAl_4O_7$, Optical Materials 127 (2022) 112352.

[62] V. Kim, I. Shuklov, A. Mardini, A. Bundulis, A. Zvyagin, R. Kholany, A. Lizunova, J. Grube, A. Sarakovskis, O. Ovchinnikov, R. Ganeev, Investigation of nonlinear optical processes in mercury sulfide quantum dots, Nanomaterials 12 (2022) 1264.

[63] V. Kim, A. Bundulis, J. Grube, R. Ganeev, Variation of the sign of nonlinear refraction of carbon disulfide in the short-wavelength region, Optical Materials Express 12 (2022) 2053–2062.

[64] V. Kim, J. Grube, J. Butikova, A. Sarakovskis, R. Ganeev, Influence of chromium plasma characteristics on high-order harmonics generation, Applied Physics B: Lasers and Optics 128 (2022) 217.

[65] V. Kim, J. Butikova, J. Grube, A. Sarakovskis, R. Ganeev, Plasma dynamics characterization for improvement of resonantly enhanced harmonics generation in indium and tin laser-produced plasmas, Photonics 9 (2022) 600.

[66] V. Kim, A. Bundulis, V. Popov, N. Lavrentyev, A. Lizunova, I. Shuklov, V. Ponomarenko, J. Grube, R. Ganeev, Third-order optical non-linearities of exfoliated Bi_2Te_3 nanoparticle films in UV, visible and near-infrared ranges measured by tunable femtosecond pulses, Optics Express 30 (2022) 6970–6980.

[67] S. Khartsev, M. Hammar, N. Nordell, A. Zolotarjovs, J. Purans, A. Hallén, Reverse-bias electroluminescence in Er-doped β-Ga_2O_3 schottky barrier diodes manufactured by pulsed laser deposition, Physica Status Solidi (A) Applications and Materials Science 219 (2022) 2100610.

[68] H. Klym, I. Hadzaman, R. Vila, A. Popov, Extended positron–positronium trapping defects in the $MgAl_2O_4$ spinel ceramics, Physica Status Solidi (B) Basic Research 259 (2022) 2100473.

[69] H. Klym, I. Karbovnyk, A. Luchechko, Y. Kostiv, A. Popov, Extended positron-trapping defects in the Eu_{3+}-doped $BaGa_2O_4$ ceramics studied by positron annihilation lifetime method, Physica Status Solidi (B) Basic Research 259 (2022) 2100485.

[70] H. Klym, L. Calvez, A. Popov, Free-volume extended defects in structurally modified Ge–Ga–S/Se glasses, Physica Status Solidi (B) Basic Research 259 (2022) 2100472.

[71] E. Kotomin, A. Kuzmin, J. Purans, J. Timoshenko, S. Piskunov, R. Merkle, J. Maier, Theoretical and experimental studies of charge ordering in $CaFeO_3$ and $SrFeO_3$ crystals, Physica Status Solidi (B) Basic Research 259 (2022) 2100238.

[72] A. Kosimov, G. Yusibova, J. Aruvali, P. Paiste, M. Kaarik, J. Leis, A. Kikas, V. Kisand, K. Šmits, N. Kongi, Liquid-assisted grinding/compression: a facile mechanosynthetic route for the production of high-performing Co–N–C electrocatalyst materials, Green Chemistry 24 (2022) 305–314.

[73] A. Kozlovskiy, D. Shlimas, M. Zdorovets, E. Popova, E. Elsts, A. Popov, Investigation of the efficiency of shielding gamma and electron radiation using glasses based on TeO_2-WO_3-Bi_2O_3-MoO_3-SiO to protect electronic circuits from the negative effects of ionizing radiation, Materials 15 (2022) 6071.

[74] A. Kozlovskiy, D. Shlimas, M. Zdorovets, A. Moskina, V. Pankratov, A. Popov, Study of the effect of two phases in Li_4SiO_4–Li_2SiO_3 ceramics on the strength and thermophysical parameters, Nanomaterials 12 (2022) 3682.

[75] V. Krasnenko, L. Rusevich, A. Platonenko, Y. Mastrikov, M. Sokolov, E. Kotomin, Water splitting on multifaceted $SrTiO_3$ nanocrystals: Calculations of Raman vibrational spectrum, Materials 15 (2022) 4233.

[76] G. Krieke, G. Doke, A. Antuzevics, I. Pudza, A. Kuzmin, E. Welter, Tuneable persistent luminescence of novel $Mg_3Y_2Ge_3O_{12}$ garnet, Journal of Alloys and Compounds 922 (2022) 166312.

[77] S. Kruchinin, R. Eglitis, V. Babak, I. Vyshyvana, S. Repetsky, Effects of electron correlation inside disordered crystals, Crystals 12 (2022) 237.

[78] G. Kucinskis, I. Nesterova, A. Sarakovskis, L. Bikse, J. Hodakovska, G. Bajars, Electrochemical performance of $Na_2FeP_2O_7$/C cathode for sodium-ion batteries in electrolyte with fluoroethylene carbonate additive, Journal of Alloys and Compounds 895 (2022) 162656.

[79] G. Kucinskis, M. Bozorgchenani, M. Feinauer, M. Kasper, M. Wohlfahrt-Mehrens, T. Waldmann, Arrhenius plots for Li-ion battery ageing as a function of temperature, C-rate, and ageing state – An experimental study, Journal of Power Sources 549 (2022) 232129.

[80] G. Kucinskis, B. Kruze, P. Korde, A. Sarakovskis, A. Viksna, J. Hodakovska, G. Bajars, Enhanced electrochemical properties of $Na_{0.67}MnO_2$ cathode for Na-Ion batteries prepared with novel tetrabutylammonium alginate binder, Batteries 8 (2022) 6.

[81] G. Kunakova, E. Kauranens, K. Niherysh, M. Bechelany, K. Smits, G. Mozolevskis, T. Bauch, F. Lombardi, D. Erts, Magnetotransport studies of encapsulated topological insulator Bi_2Se_3 nanoribbons, Nanomaterials 12 (2022) 768.

[82] A. Kuzmin, M. Dile, K. Laganovska, A. Zolotarjovs, Microwave-assisted synthesis and characterization of undoped and manganese doped zinc sulfide nanoparticles, Materials Chemistry and Physics 290 (2022) 126583.

[83] A. Kuzmin, I. Pudza, K. Klementiev, In situ study of zinc peroxide decomposition to zinc oxide by X-ray absorption spectroscopy and Reverse Monte Carlo simulations, Physica Status Solidi (B) Basic Research 259 (2022) 2200001.

[84] L. Laipniece, V. Kampars, S. Belyakov, A. Bundulis, A. Tokmakovs, M. Rutkis, Utilization of amorphous phase forming trityl groups and Ar-ArF interactions in synthesis of NLO active

azochromophores, Dyes and Pigments 204 (2022) 110395.

[85] V. Lazarenko, Y. Rublova, R. Meija, J. Andzane, V. Voikiva, A. Kons, A. Sarakovskis, A. Viksna, D. Erts, Bi_2Se_3 nanostructured thin films as perspective anodes for aqueous rechargeable lithium-ion batteries, Batteries 8 (2022) 144.

[86] E. Letko, A. Bundulis, G. Mozolevskis, Theoretical development of polymer-based integrated lossy-mode resonance sensor for photonic integrated circuits, Photonics 9 (2022) 764.

[87] F.-Y. Li, D.-C. Yang, L. Qiao, R. Eglitis, R. Jia, Z.-J. Yi, H.-X. Zhang, Novel 2D boron nitride with optimal direct band gap: A theoretical prediction, Applied Surface Science 578 (2022) 151929.

[88] Y.-P. Lin, D. Bocharov, E. Kotomin, M. Brik, S. Piskunov, Influence of Au, Ag, and Cu adatoms on optical properties of TiO_2 (110) surface: Predictions from RT-TDDFT calculations, Crystals 12 (2022) 452.

[89] Y.-P. Lin, S. Piskunov, L. Trinkler, M. Ming-Chi Chou, L. Chang, Electronic and optical properties of rocksalt $Mg_{1x}Zn_xO$ and Wurtzite $Zn_{1x}Mg_xO$ with varied concentrations of magnesium and zinc, Materials 15 (2022) 7689.

[90] Y.-P. Lin, S. Piskunov, L. Trinkler, M.-C. Chou, L. Chang, Influence of stress on electronic and optical properties of rocksalt and wurtzite MgO–ZnO nanocomposites with varying concentrations of magnesium and zinc, Nanomaterials 12 (2022) 3408.

[91] Y.-P. Lin, B. Polyakov, E. Butanovs, A. Popov, M. Sokolov, D. Bocharov, S. Piskunov, Excited states calculations of MoS_2@ZnO and WS_2@ZnO two-dimensional nanocomposites for water-splitting applications, Energies 15 (2022) 150.

[92] L. Lisitsyna, A. Popov, Z. Karipbayev, D. Mussakhanov, E. Feldbach, Luminescence of MgF_2-WO_3 ceramics synthesized in the flux of 1.5 MeV electron beam, Optical Materials 133 (2022) 112999.

[93] O. Lisovski, S. Piskunov, D. Bocharov, Y. Zhukovskii, J. Kleperis, A. Knoks, P. Lesnicenoks, CO_2 and CH_2 adsorption on copper-decorated graphene: Predictions from first principle calculations, Crystals 12 (2022) 194.

[94] Z.-Y. Liu, D.-C. Yang, R. Eglitis, R. Jia, H.-X. Zhang, Penta-silicon carbide: A theoretical investigation, Materials Science and Engineering B: Solid-State Materials for Advanced Technology 281 (2022) 115740.

[95] Z.-Y. Liu, R. Eglitis, H.-X. Zhang, R. Jia, Theoretical investigations of the heavily boron doped pentadiamond, Diamond and Related Materials 126 (2022) 109127.

[96] L.-L. Luo, P.-X. Wang, X.-Y. Geng, Y.-T. Liu, R. Eglitis, H.-Q. Xia, X.-Y. Lai, X. Wang, First-principles calculations of 0D/2D GQDs-MoS_2 mixed van der Waals heterojunctions for photocatalysis: a transition from type I to type II, Physical Chemistry Chemical Physics 24 (2022) 8529–8536.

[97] A. Lushchik, V. Seeman, E. Shablonin, E. Vasil'chenko, V. Kuzovkov, E. Kotomin, A. Popov, Detection of hidden oxygen interstitials in neutron-irradiated corundum crystals, Optical Materials: X 14 (2022) 100151.

[98] A. Lushchik, V. Kuzovkov, I. Kudryavtseva, A. Popov, V. Seeman, E. Shablonin, E. Vasil'chenko, E. Kotomin, The two types of oxygen interstitials in neutron-irradiated corundum single crystals:

Joint experimental and theoretical study, Physica Status Solidi (B) Basic Research 259 (2022) 2100317.

[99] W. Mackrodt, A. Platonenko, R. Dovesi, Self-trapped excitons in diamond: A Δ-SCF approach, Journal of Chemical Physics 157 (2022) 084707.

[100] M. Mahmoudi, J. Keruckas, D. Volyniuk, V. Andrulevičienė, R. Keruckienė, E. Narbutaitis, Y.-C. Chao, M. Rutkis, J. Grazulevicius, Bis(N-naphthyl-N-phenylamino)benzophenones as exciton-modulating materials for white TADF OLEDs with separated charge and exciton recombination zones, Dyes and Pigments 197 (2022) 109868.

[101] Y. Mastrikov, D. Gryaznov, M. Sokolov, G. Zvejnieks, A. Popov, R. Eglitis, E. Kotomin, M. Ananyev, Oxygen vacancy formation and migration within the antiphase boundaries in lanthanum scandate-based oxides: Computational study, Materials 15 (2022) 2695.

[102] Y. Mastrikov, D. Gryaznov, G. Zvejnieks, M. Sokolov, M. Putniņa, E. Kotomin, Sr doping and oxygen vacancy formation in $La_{1x}Sr_xScO_3$ solid solutions: Computational modelling, Crystals 12 (2022) 1300.

[103] M. Merisalu, L. Aarik, H.-M. Piirsoo, J. Kozlova, A. Tarre, R. Zabels, J. Wessing, A. Brieva, V. Sammelselg, Nanostructured coating for aluminum alloys used in aerospace applications, Journal of the Electrochemical Society 169 (2022) 071503.

[104] A. Mezulis, J. Kleperis, P. Lesnicenoks, L. Zemite, Prospects of decarbonizing industrial areas in the baltic states by means of alternative fuels, Journal of Ecological Engineering 23 (2022) 152–161.

[105] I. Mihailova, V. Gerbreders, M. Krasovska, E. Sledevskis, V. Mizers, A. Bulanovs, A. Ogurcovs, A non-enzymatic electrochemical hydrogen peroxide sensor based on copper oxide nanostructures, Beilstein Journal of Nanotechnology 13 (2022) 424–436.

[106] N. Mironova-Ulmane, M. Brik, J. Grube, G. Krieke, M.Kemere, A. An- tuzevics, E. Gabrusenoks, V. Skvortsova, E. Elsts, A. Sarakovskis, M. Piasecki, A. Popov, EPR, optical and thermometric studies of Cr^{3+} ions in the α-Al_2O_3 synthetic single crystal, Optical Materials 132 (2022) 112859.

[107] A. Nefedova, K. Rausalu, E. Zusinaite, A. Vanetsev, M. Rosenberg, K. Koppel, S. Lilla, M. Visnapuu, K. Smits, V. Kisand, T. T¨atte, A. Ivask, Antiviral efficacy of cerium oxide nanoparticles, Scientific Reports 12 (2022) 18746.

[108] A. Ogurcovs, K. Kadiwala, E. Sledevskis, M. Krasovska, I. Plaksen- kova, E. Butanovs, Effect of DNA Aptamer Concentration on the conductivity of a water-gated Al:ZnO thin-film transistor-based bio-sensor, Sensors 22 (2022) 3408.

[109] A. Ogurcovs, K. Kadiwala, E. Sledevskis, M. Krasovska, V. Mizers, Glyphosate sensor based on nanostructured water-gated CuO field-effect transistor, Sensors 22 (2022) 8744.

[110] A. Ozols, G. Mozolevskis, R. Zalubovskis, M. Rutkis, Development of liquid crystal layer thickness and refractive index measurement methods for scattering type liquid crystal displays, Latvian Journal of Physics and Technical Sciences 59 (2022) 25–35.

[111] E. Pajuste, I. Reinholds, G. Vaivars, A. Antuzevičs, L. Avotiņa, E. Sprūģis, R. Mikko, K. Heikki, R. Meri, R. Kaparkalējs, Evaluation of radiation stability of electron beam irradiated Nafion® and sulfonated poly(ether ether ketone) membranes, Polymer Degradation and Stability

200 (2022) 109970.

[112] F. Pascale, K. Doll, A. Platonenko, M. Rérat, R. Dovesi, The role of spin density for understanding the superexchange mechanism in transition metal ionic compounds. The case of KMF_3 (M = Mn, Fe, Co, Ni, Cu) perovskites, Physical Chemistry Chemical Physics 24 (2022) 12950–12960.

[113] H. Pauna, A. Tuomela, M. Aula, P. Turunen, V. Pankratov, M. Huttula, T. Fabritius, Toward on-line slag composition analysis: Optical emissions from laboratory electric arc, Metallurgical and Materials Transactions B: Process Metallurgy and Materials Processing Science 53 (2022) 454–465.

[114] V. Pankratov, V. Pankratova, A. Popov, Luminescence and vacuum ultraviolet excitation spectroscopy of nanophosphors under synchrotron irradiation, Physica Status Solidi (B) Basic Research 259 (2022) 2100475.

[115] V. Pankratova, E. Dunaeva, I. Voronina, A. Kozlova, R. Shendrik, V. Pankratov, Luminescence properties and time-resolved spectroscopy of rare-earth doped $SrMoO_4$ single crystals, Optical Materials: X 15 (2022) 100169.

[116] V. Pankratova, V. Skuratov, O. Buzanov, A. Mololkin, A. Kozlova, A. Kotlov, A. Popov, V. Pankratov, Radiation effects in $Gd_3(Al,Ga)_5:O_{12}:Ce^{3+}$ single crystals induced by swift heavy ions, Optical Materials: X 16 (2022) 100217.

[117] M. Petrulevičienė, J. Pilipavičius, J. Juodkazytė, D. Gryaznov, L. Vilčiauskas, Electrochemical Performance of NASICON-structured $Na_{3-x}V_{2-x}Ti_x(PO_4)_3$ ($0.0 < x < 1.0$) as aqueous Na-ion battery positive electrodes, Electrochimica Acta 424 (2022) 140580.

[118] A. Platonenko, F. Pascale, K. El-Kelany, F. Gentile, R. Dovesi, The effect of charge and spin state on the Infrared spectra and hyperfine coupling constants of point defects in Silicon, Physica B: Condensed Matter 626 (2022) 413499.

[119] B. Polyakov, E. Butanovs, A. Ogurcovs, A. Sarakovskis, M. Zubkins, L. Bikse, J. Gabrusenoks, S. Vlassov, A. Kuzmin, J. Purans, Unraveling the structure and properties of layered and mixed ReO_3-WO_3 thin films deposited by reactive DC magnetron sputtering, ACS Omega 7 (2022) 1827–1837.

[120] E. Popova, A. Popov, R. Sagdeev, Multimode representation of the magnetic field for the analysis of the nonlinear behavior of solar activity as a driver of space weather, Mathematics 10 (2022) 1655.

[121] N. Porotnikova, M. Ananyev, D. Osinkin, A. Khodimchuk, A. Fetisov, A. Farlenkov, A. Popov, Increase in the density of $Sr_2Fe_{1.5}Mo_{0.5}O_{6-}$ membranes through an excess of iron oxide: The effect of iron oxide on transport and kinetic parameters, Surfaces and Interfaces 29 (2022) 101784.

[122] I. Pudza, A. Anspoks, G. Aquilanti, A. Kuzmin, Revealing the local structure of $CuMo_{1x}W_xO_4$ solid solutions by multi-edge X-ray absorption spectroscopy, Materials Research Bulletin 153 (2022) 111910.

[123] E. Radzhabov, R. Shendrik, V. Pankratov, Emission of Tm^{2+} in alkaline-earth fluoride crystals, Journal of Luminescence 252 (2022) 119271.

[124] U. Rogulis, G. Krieke, A. Antuzevics, A. Fedotovs, D. Berzins, A. Popov, V. Pankratov, Low-temperature recombination luminescence of La-doped Ca_2SnO_4, Optical Materials 129 (2022)

112545.

[125] A. Ruduss, B. Turovska, S. Belyakov, K. Stucere, A. Vembris, K. Traskovskis, Carbene–metal complexes as molecular scaffolds for construction of through-space thermally activated delayed fluorescence emitters, Inorganic Chemistry 61 (2022) 2174–2185.

[126] A. Ruduss, B. Turovska, S. Belyakov, K. Stucere, A. Vembris, G. Baryshnikov, H. ˚Agren, J.-C. Lu, W.-H. Lin, C.-H. Chang, K. Traskovskis, Thiazoline Carbene-Cu(I)-Amide complexes: Efficient White Electroluminescence from Combined Monomer and Excimer Emission, ACS Applied Materials and Interfaces 14 (2022) 15478–15493.

[127] M. Rudysh, N. Ftomyn, P. Shchepanskyi, G. Myronchuk, A. Popov, N. Lem´ee, V. Stadnyk, M. Brik, M. Piasecki, Electronic structure, optical, and elastic properties of $AgGaS_2$ crystal: theoretical study, Advanced Theory and Simulations 5 (2022) 2200247.

[128] L. Rusevich, E. Kotomin, A. Popov, G. Aiello, T. Scherer, A. Lushchik, The vibrational and dielectric properties of diamond with N impurities: First principles study, Diamond and Related Materials 130 (2022) 109399.

[129] L. Rusevich, E. Kotomin, G. Zvejnieks, M. Kržmanc, S. Gupta, N. Daneu, J. Wu, Y.-G. Lee, W.-Y. Yu, Effects of Al doping on hydrogen production efficiency upon photostimulated water splitting on $SrTiO_3$ nanoparticles, Journal of Physical Chemistry C 126 (2022) 21223–21233.

[130] K. Saršūns, M. Kemere, A. Karziņins, I. Kļimenkovs, A. Bērziņš, A. Sarakovskis, T. Rekis, Fine-tuning solid state luminescence properties of organic crystals via solid solution formation: The example of 4-Iodothioxanthone-4-Chlorothioxanthone system, Crystal Growth and Design 22 (2022) 4838–4844.

[131] A. Sebris, I. Novosjolova, K. Traskovskis, V. Kokars, N. Tetervenoka, A. Vembris, M. Turks, Photophysical and electrical properties of highly luminescent 2/6-Triazolyl-Substituted push-pull purines, ACS Omega 7 (2022) 5242–5253.

[132] V. Seeman, A. Popov, E. Shablonin, E. Vasil'chenko, A. Lushchik, EPR-active dimer centers with S=1 in α-Al_2O_3 single crystals irradiated by fast neutrons, Journal of Nuclear Materials 569 (2022) 153933.

[133] A. Shapeev, D. Bocharov, A. Kuzmin, Validation of moment tensor potentials for fcc and bcc metals using EXAFS spectra, Computational Materials Science 210 (2022) 111028.

[134] A. Smekhova, A. Kuzmin, K. Siemensmeyer, C. Luo, K. Chen, F. Radu, E. Weschke, U. Reinholz, A. Buzanich, K. Yusenko, Al-driven peculiarities of local coordination and magnetic properties in single-phase Al_x-CrFeCoNi high-entropy alloys, Nano Research 15 (2022) 4845–4858.

[135] A. Smekhova, A. Kuzmin, K. Siemensmeyer, R. Abrudan, U. Reinholz, A. Buzanich, M. Schneider, G. Laplanche, K. Yusenko, Inner relaxations in equiatomic single-phase high-entropy cantor alloy, Journal of Alloys and Compounds 920 (2022) 165999.

[136] M. Skruodiene, R. Juodvalkyte, G. Inkrataite, A. Pakalniskis, R. Ramanauskas, A. Sarakovskis, R. Skaudzius, Sol-gel assisted molten-salt synthesis of novel single phase $Y_{3-2x}Ca_{2x}Ta_xAl_5xO_12$:1%Eu garnet structure phosphors, Journal of Alloys and Compounds 890 (2022) 161889.

[137] M. Skruodiene, R. Juodvalkyte, M. Kemere, R. Ramanauskas, A. Sarakovskis, R. Skaudzius, Enhanced optical properties of yttrium aluminum garnet with the yttrium vanadate impurity phase, Heliyon 8 (2022) e11386.

[138] L. Skuja, M. Leimane, I. Bite, D. Millers, A. Zolotarjovs, V. Vitola, K. Smits, Ultraviolet luminescence of polycyclic aromatic hydrocarbons in partially consolidated sol-gel silica glasses, Journal of Non-Crystalline Solids 577 (2022) 121325.

[139] B. Straumal, A. Korneva, A. Kuzmin, L. Klinger, G. Lopez, N. Vershinin, A. Straumal, A. Gornakova, High entropy alloys for energy conversion and storage: A review of grain boundary wetting phenomena, Energies 15 (2022) 7130.

[140] B. Straumal, L. Klinger, A. Kuzmin, G. Lopez, A. Korneva, A. Straumal, N. Vershinin, A. Gornakova, High entropy alloys coatings deposited by laser cladding: A review of grain boundary wetting phenomena, Coatings 12 (2022) 343.

[141] Y. Suchikova, I. Bohdanov, S. Kovachov, A. Lazarenko, I. Bardus, A. Dauletbekova, I. Kenzhina, A. Popov, Synthesis of porous indium phosphide with nickel oxide crystallites on the surface, Journal of Electrochemical Science and Engineering 12 (2022) 593–601.

[142] A. Šutka, L. Mežule, V. Denisova, J. Meier-Haack, A. Kulkarni, S. Bitina, K. Smits, S. Vihodceva, Straightforward approach for preparing durable antibacterial ZnO nanoparticle coatings on flexible substrates, Molecules 27 (2022) 7672.

[143] A. Šutka, L. Lapcinskis, O. Verners, L. Germane, K. Smits, A. Pludons, S. Gaidukovs, I. Jerane, M. Zubkins, K. Pudzs, P. Sherrell, J. Blums, Bio-inspired macromolecular ordering of elastomers for enhanced contact electrification and triboelectric energy harvesting, Advanced Materials Technologies 7 (2022) 2200162.

[144] A. Šutka, F.-K. Shieh, M. Kinka, L. Lapčinskis, C.-C. Chang, P. Lam, K. Pudzs, V. O., Triboelectric behaviour of selected MOFs in contact with metals, RSC Advances 13 (2022) 41–46.

[145] B. Svalbe, B. Zvejniece, G. Stelfa, K. Vilks, E. Vavers, J. Vela, M. Dambrova, L. Zvejniece, Antidepressive-like behavior-related metabolomic signatures of Sigma-1 receptor knockout mice, Biomedicines 10 (2022) 1572.

[146] Š. Svirskas, T. Kudrevičius, E. Birks, M. Dunce, A. Sternbergs, C.-H. Huang, J. Banys, Dielectric and piezoelectric properties of $0.8Na_{0.5}Bi_{0.5}TiO_3$-$0.2BaTiO_3$ modified with sodium niobate, Lithuanian Journal of Physics 62 (2022) 212–220.

[147] A. Taha, F. Casanova, P. Simonis, V. Stankevic, M. Gomaa, A. Stirke, Pulsed electric field: Fundamentals and effects on the structural and techno-functional properties of dairy and plant proteins, Foods 11 (2022) 1556.

[148] P. Talebi, A. Kistanov, E. Rani, H. Singh, V. Pankratov, V. Pankratova, G. King, M. Huttula, W. Cao, Unveiling the role of carbonate in nickel-based plasmonic core@shell hybrid nanostructure for photocatalytic water splitting, Applied Energy 322 (2022) 119461.

[149] L. Trinkler, I. Aulika, G. Krieke, D. Nilova, R. Ruska, J. Butikova, B. Berzina, M.-C. Chou, L. Chang, M.-C. Wen, T. Yan, R. Nedzinskas, Characterization of wurtzite $Zn_{1x}Mg_xO$ epilayers grown on $ScAlMgO_4$ substrate by methods of optical spectroscopy, Journal of Alloys and Compounds 912 (2022) 165178.

[150] L. Trinkler, V. Pankratov, A. Trukhin, B. Berzina, M. Chou, L. Chang, Anisotropic photoluminescence of *β*-$LiGaO_2$ crystal, Optical Materials 132 (2022) 112856.

[151] A. Trukhin, Energy transport in SiO_2 crystals: luminescence excitation spectra of stishovite and *α*-QUARTZ, Latvian Journal of Physics and Technical Sciences 59 (2022) 19–24.

[152] A. Usseinov, A. Platonenko, Z. Koishybayeva, A. Akilbekov, M. Zdorovets, A. Popov, Pair vacancy defects in *β*-Ga_2O_3 crystal: Ab initio study, Optical Materials: X 16 (2022) 100200.

[153] M. Vanags, G. Kulikovskis, J. Kostjukovs, L. Jekabsons, A. Sarakovskis, K. Smits, L. Bikse, A. Šutka, Membrane-less amphoteric decoupled water electrolysis using WO_3 and $Ni(OH)_2$ auxiliary electrodes, Energy and Environmental Science 15 (2022) 2021–2028.

[154] E. Vanags, A. Abolins, U. Cabulis, Lipase catalyzed self-epoxidation of tall oil fatty acids in batch and continuous flow conditions, Journal of Polymers and the Environment 15 (2022) 2021–2028.

[155] O. Verners, L. Lapcinskis, L. Germane, A. Kasikov, M. Timusk, K. Pudzs, A. Ellis, P. Sherrell, A. Šutka, Smooth polymers charge negatively: Controlling contact electrification polarity in polymers, Nano Energy 104 (2022) 107914.

[156] V. Vitola, K. Laganovska, I. Bite, E. Einbergs, D. Millers, The role of boric acid in optical information storage properties in Eu doped $BaSi_2O_5$, Journal of Luminescence 243 (2022) 118682.

[157] S. Vlassov, S. Oras, B. Polyakov, E. Butanovs, A. Kyritsakis, V. Zadin, Kinking in Semiconductor Nanowires: A Review, Crystal Growth and Design 22 (2022) 871–892.

[158] P. Wang, X. Geng, L. Luo, Y. Liu, R. Eglitis, X. Wang, The adsorption behavior of phenol on the surface of 1D/2D $MMoS_2$ (M = Co and Rh) for hydrodeoxidation reaction: Insights from theoretical investigations, Applied Surface Science 601 (2022) 154242.

[159] D.-C. Yang, R. Eglitis, Z.-J. Yi, C.-S. Liu, R. Jia, Overall direct photocatalytic water-splitting on *C*2*mm*-graphyne: a novel two-dimensional carbon allotrope, Journal of Materials Chemistry C 10 (2022) 10843–10852.

[160] D. Zablotsky, A. Mezulis, E. Blums, M. Maiorov, Optothermal grid activation of microflow with magnetic nanoparticle thermophoresis for microfluidics, Philosophical Transactions of the Royal Society A: Mathematical, Physical and Engineering Sciences 380 (2022) 20200310.

[161] A. Zagata, K. Traskovskis, S. Belyakov, I. Mihailovs, A. Bundulis, M. Rutkis, Dicyanomethylene-functionalized s-indacene-based D-π-A- π-D dyes exhibiting large near-infrared two-photon absorption cross-section, Dyes and Pigments 208 (2022) 110864.

[162] K. Zakis, S. Olonkins, A. Udalcovs, I. Lukosevics, D. Prigunovs, J. Grube, L. Bikse, A. Supe, O. Ozolins, S. Spolitis, V. Bobrovs, Cladding-Pumped Er/Yb-Co-Doped Fiber Amplifier for Multi-Channel Operation, Photonics 9 (2022) 457.

[163] D. Zavickis, G. Zvejnieks, A. Chesnokov, D. Gryaznov, Single oxygen vacancy in $BaCoO_3$: Hybrid DFT calculations and local site symmetry approach, Solid State Ionics 375 (2022) 115835.

[164] M. Zubkins, I. Aulika, E. Strods, V. Vibornijs, L. Bikse, A. Sarakovskis, G. Chikvaidze, J. Gabrusenoks, H. Arslan, J. Purans, Optical properties of oxygen-containing yttrium hydride thin films during and after the deposition, Vacuum 203 (2022) 111218.

[165] M. Zubkins, A. Sarakovskis, E. Strods, L. Bikse, B. Polyakov, A. Kuzmin, V. Vibornijs, J. Purans, Tailoring of rhenium oxidation state in ReO_x thin films during reactive HiPIMS deposition process and following annealing, Materials Chemistry and Physics 289 (2022) 126399.

[166] M. Zubkins, J. Timoshenko, J. Gabrusenoks, K. Pudzs, A. Azens, Q. Wang, J. Purans, Amorphous p-Type Conducting Zn–*x*Ir Oxide ($x > 0.13$) Thin Films Deposited by Reactive

Magnetron Cosputtering, Physica Status Solidi (B) Basic Research 259 (2022) 2100374.

[167] S. Artemov, E. Artemov, E. Lomonova, V. Pankratov, P. Ryabochkina, N. Sidorova, CW and Q-switch laser of ZrO_2-Y_2O_3-Ho_2O_3 crystals, Proceedings of the 2022 International Conference Laser Optics, ICLO 2022.

[168] L. Avotina, L. Bumbure, A. Goldmane, E. Vanags, M. Romanova, H. Sorokins, A. Zaslavskis, G. Kizane, Y. Dekhtyar, Thermal behaviour of magnetron sputtered tungsten and tungsten-boride thin films, Proceedings of the International Conference on Applied Electronics, 2022.

[169] I. Bohdanov, S. Kovachov, Y. Suchikova, A. Moskina, T. Tsebriienko, A. Popov, Synthesis of Diamond-Like Arsenolite Crystallites on Surface of Gallium Arsenide, Proceedings of the 2022 IEEE 12th International Conference "Nanomaterials: Applications and Properties", 2022.

[170] Z. Jansone-Langina, R. Truksa, M. Ozolins, A. Solomatin, I. Solomatins, Contrast sensitivity at different background brightness levels and objective scattering index changes in patients before and after cataract removal surgery, Proceedings of SPIE - The International Society for Optical Engineering, Vol. 12147, 2022, p. 121470B.

[171] A. Jece, A. Ruduss, K. Stucere, A. Vembris, K. Traskovskis, TADF active carbene-metal-amide complexes exhibiting through-space charge transfer: an impact of metal atom, Proceedings of SPIE - The International Society for Optical Engineering, Vol. 12149, 2022, p. 1214909.

[172] S. Kovachov, I. Bohdanov, Z. Karipbayev, Y. Suchikova, T. Tsebriienko, A. Popov, Layer-by-Layer Synthesis and Analysis of the the Phase Composition of $Cd_xTe_yO_z$/CdS/por-ZnO/ZnO Heterostructure, Proceedings of the IEEE 3rd KhPI Week on Advanced Technology, 2022.

[173] S. Kovachov, A. Lazarenko, Z. Karipbayev, Y. Suchikova, T. Tsebriienko, A. Popov, 3D $Al_xGa_{1-x}As$/por-GaAs/GaAs heterostructures for solar cells, Proceedings of the IEEE 3rd KhPI Week on Advanced Technology, 2022.

[174] E. Letko, A. Bundulis, G. Mozolevskis, V. Vibornijs, Integrated Lossy Mode Resonance Sensor Based on SU-8 Waveguides, Proceedings of SPIE - The International Society for Optical Engineering, Vol. 11998, 2022, p. 119980B.

[175] A. Maurucaite, K. Leduskrasts, E. Suna, A. Vembris, Optical properties of carbazole with pyridinium ion for light-emitting electrochemical cells, Proceedings of SPIE - The International Society for Optical Engineering, Vol. 12149, 2022, p. 121490A.

[176] J. Mikelsone, A. Vembris, Enhancement of photoluminescence properties in silver nanoparticles based organic luminophores, Proceedings of SPIE - The International Society for Optical Engineering, Vol. 12131, 2022, p. 121310A.

[177] S. Olonkins, K. Zakis, A. Udalcovs, A. Supe, O. Ozolins, J. Grube, S. Spolitis, V. Bobrovs, Experimental and Simulative Analysis of Cladding-Pumped EYDFA Gain Evolution, Proceedings of International Conference Laser Optics, ICLO, 2022.

[178] A. Ruduss, Z. Sisojevs, A. Vembris, K. Stucere, K. Traskovskis, Symmetrical versus asymmetrical molecular configuration in metal-assisted-through-space charge transfer TADF, Proceedings of SPIE - The International Society for Optical Engineering, Vol. 12149, 2022, p. 1214908.

[179] R. Silis, J. Mikelsone, A. Vembris, Amplification of organic semiconductor luminescence in thin films with silver nanoparticles, Proceedings of SPIE - The International Society for Optical

Engineering, Vol. 12131, 2022, p. 121310V.

[180] Y. Suchikova, A. Lazarenko, I. Bohdanov, A. Usseinov, Z. Karipbaev, A. Popov, The Mechanism of the Formation of Grain Boundaries Nanopores in Polycrystalline Materials, Proceedings - 16th International Conference on Advanced Trends in Radioelectronics, Telecommunications and Computer Engineering, TCSET 2022, pp. 419–422.

[181] Y. Suchikova, A. Lazarenko, S. Kovachov, A. Usseinov, Z. Karipbaev, A. Popov, Formation of porous Ga_2O_3/GaAs layers for electronic devices, Proceedings - 16th International Conference on Advanced Trends in Radioelectronics, Telecommunications and Computer Engineering 2022, pp. 410–413.

[182] Y. Suchikova, A. Lazarenko, S. Kovachov, A. Moskina, T. Tsebriienko, A. Popov, Design and Characteristics of Doughnut-Like Porous-CdO/Porous-CdS Nanostructures, Proceedings of the 2022 IEEE 12th International Conference "Nanomaterials: Applications and Properties", NAP 2022.

[183] L. Zemite, J. Kleperis, A. Mezulis, I. Bode, L. Vempere, A. Jasevics, L. Jansons, Biogas Production Support Systems for the Production and Use of Biomethane, Proceedings of the IEEE International Conference on Environment and Electrical Engineering and 2022 IEEE Industrial and Commercial Power Systems Europe, 2022.

Theses

Doctor Theses

No.	Author	Title	Supervisor	Degree
1.	I. Pudža	Impact of the local structure on the thermochromic properties of copper molybdate and its solid solutions	Dr. phys. Aleksejs Kuzmins	Ph.D.
2.	A. Ozols	Optimization of materials, design and manufacturing technology of multifocal liquid crystal diffuser used in augmented reality displays	Dr. phys. Mārtiņš Rutkis	Ph.D.
3.	J. Perveņecka	Investigation of optical properties and enhanced spontaneous emission of amorphous thin-film-forming organic compounds for possible applications in organic solid-state lasers	Asoc. prof. Dr. phys. Aivars Vembris	Ph.D.

M.Sc. Theses

No.	Author	Title	Supervisor	Study programme
1.	I. Ņesterova	Na2FeP2O7 cathode material for sodium-ion batteries: optimization of synthesis and electrochemical performance	Dr. Gints Kučinskis	Chemistry
2.	B. Krūze	The effect of binder on electrode surface and electrochemical properties of cathode material Na2/3MnO2 for sodium-ion batteries	Dr. Gints Kučinskis	Chemistry
3.	P. Paulsone	Forster resonance energy transfer in active media for organic solid state laser	Asoc. prof. Dr. phys. Aivars Vembris	Physics
4.	O. Bitmets	PEO and PEDOT:PSS polymer composite electrodes, characterization of electrical properties	Dr. phys. Kaspars Pudžs	Physics
5.	A. Kalniņa	Synthesis and optical properties of MgGeO3 material activated by Mn2+ and Cr3+ ions	MSc. Guna Doķe, Dr.Phys. Jeļena Butikova	Physics
6.	H. Ozols	The origin of photochromic effect in iron doped barium manganese silicate	Dr. phys. Andris Antuzevičs	Physics

7.	V. Pankratova	Investigation of radiation-induced defects in garnet single crystals	Dr. phys. Anatolijs Šarakovskis	Physics
8.	R. Ruska	Visible and infrared luminescence in aluminum nitride materials	Dr. habil. phys. Baiba Bērziņa	Physics
9.	Č. F. Tipaldi	Vibrational Spectroscopy of YAlO3	Dr. phys. Jevgēņijs Gabrusenoks	Physics
10.	K. Vītols	Luminescence of manganese ions in CaAl4O7	MSc. Meldra Ķemere, Dr.habil.phys Uldis Rogulis	Physics
11.	R. Kaparkalējs	Sulphonated poly (ether ether ketone) and graphene composite membranes	Dr.chem. Guntars Vaivars	Chemistry
12.	D. Bogdanovs	A study of electrical properties of sulphonated poly (ether ether ketone) using streaming potential measurem	Dr.chem. Guntars Vaivars	Chemistry
13.	E. Neilande	DFT calculations of Cu-doped titanium dioxide for antibacterial applications	Dr.phys. Dmitrijs Bočarovs	Physics
14.	A. Bendins	Light coupling into SU-8 waveguide micro-devices	Dr. sc. ing. Gatis Mozeļevskis	Physics

B.Sc. Thesis

No.	Author	Title	Supervisor	Study programme
1.	M. Kāraušs	Electrophoretically deposited transition metal and reduced graphene oxide composite films as anode for lithium- ion batteries	M.Ing. Kaspars Kaprāns, Dr. Gints Kučinskis	Physics
2.	R. Oliņš	Obtaining and application of functionalized carbon materials for energy storage	M.Ing. Pēteris Lesničenoks, M.Sc. Ainārs Knoks	Engineering sciences
3.	K. A. Štucere	Studies of the emission properties of carbene-metal-amine derivatives in thin films at different temperatures	Asoc. prof. Dr. phys. Aivars Vembris	Physics
4.	E. Strods	Automatic disinfectant overflow-filling device	Dr.sc.ing. Irīna Boiko	Engineering sciences
5.	A. Atvars	Role of mechanical activation on sintering NBT ceramics	Dr. phys. Marija Dunce, Asoc. prof. Dr. chem. Guntars Vaivars	Chemistry

6.	A. Začinskis	First-principles calculations of F-centers and iridium impurities in gallium oxide polymorphs	Dr.phys. Dmitrijs Bočarovs	Physics
7.	J. Lukaševiča	Study of NiO lattice dynamics using reverse Monte Carlo method	Dr. phys. Aleksejs Kuzmins	Chemistry
8.	V. Dimitrijevs	X-ray absorption spectroscopy of lattice dynamics in metals with cubic and hexagonal structures	Dr. phys. Aleksejs Kuzmins	Chemistry